DEUTSCHES ELEKTRONEN-SYNCHROTRON
Ein Forschungszentrum der Helmholtz-Gemeinschaft

DESY 21-149
TUM-HEP-1345-21
arXiv:2109.15085
September 2021

Electric Dipole Moments at One-Loop in the Dimension-6 SMEFT

A. Kley

Physik-Department, Technische Universität München, Garching

and

Deutsches Elektronen-Synchrotron DESY, Hamburg

and

Institut für Physik, Humboldt-Universität, Berlin

T. Theil, E. Venturini, A. Weiler

Physik-Department, Technische Universität München, Garching

ISSN 0418-9833

NOTKESTRASSE 85 - 22607 HAMBURG

To be sure that your reports and preprints are promptly included in the HEP literature database
send them to (if possible by air mail):

DESY Zentralbibliothek Notkestraße 85 22607 Hamburg Germany	DESY Bibliothek Platanenallee 6 15738 Zeuthen Germany

TUM-HEP-1345-21
DESY-21-149

Electric dipole moments at one-loop in the dimension-6 SMEFT

Jonathan Kley,[a,b,c] **Tobias Theil,**[a] **Elena Venturini,**[a] **Andreas Weiler**[a]

[a] *Physik-Department, Technische Universität München, James-Franck-Strasse 1, 85748 Garching, Germany*

[b] *Deutsches Elektronen-Synchrotron DESY, Notkestr. 85, 22607 Hamburg, Germany*

[c] *Institut für Physik, Humboldt-Universität zu Berlin, Newtonstrasse 15, 12489 Berlin, Germany*

Abstract: In this paper we present the complete expressions of the lepton and neutron electric dipole moments (EDMs) in the Standard Model Effective Field Theory (SMEFT), up to 1-loop and dimension-6 level and including both RG running contributions and finite corrections. The latter play a fundamental role in the cases of operators that do not renormalize the dipoles, but there are also classes of operators for which they provide an important fraction, $10 - 20\%$, of the total 1-loop contribution, if the new physics scale is around $\Lambda = 5$ TeV. We present the full set of bounds on each individual Wilson coefficient contributing to the EDMs using both the current experimental constraints, as well as those from future experiments, which are expected to improve by at least an order of magnitude.

Contents

1 Introduction

Electric dipole moments (EDMs) constitute a set of low energy observables which are extremely sensitive to physics beyond the Standard Model (SM). This is due to the fact that – as a consequence of their CP violating nature – EDMs are very strongly suppressed within the SM and are far below current experimental sensitivity. Contributions to the EDMs coming from new CP violating physics, however, are typically unsuppressed and expected to be within experimental reach.

The experimental sensitivity to EDMs, in particular to those of the electron and neutron, has recently improved by one order of magnitude and is going to further increase in the near future. The current bounds at 90% C.L. on lepton and neutron EDMs are

$$|d_e| < 1.1 \times 10^{-29}\ e \cdot \text{cm} \qquad [1]\,, \tag{1.1}$$
$$|d_\mu| < 1.5 \times 10^{-19}\ e \cdot \text{cm} \qquad [2]\,, \tag{1.2}$$
$$|d_\tau| < 1.6 \times 10^{-18}\ e \cdot \text{cm} \qquad [3]\,, \tag{1.3}$$
$$|d_n| < 1.8 \times 10^{-26}\ e \cdot \text{cm} \qquad [4]\,,$$

while the prospected bounds on the electron EDM[1] at the ACME III experiment and on the neutron EDM at n2EDM are

$$|d_e| < 0.3 \times 10^{-30}\ e \cdot \text{cm} \qquad [6]\,, \tag{1.4}$$
$$|d_n| < 10^{-27}\ e \cdot \text{cm} \qquad [7]\,.$$

In spite of these incredible sensitivities, the SM values for these observables are many orders of magnitude smaller than the experimental reach. In particular, the electron and neutron EDMs are estimated to be

$$d_e \sim 10^{-48}\ e \cdot \text{cm} \qquad [8]\,, \tag{1.5}$$
$$d_n \sim 10^{-32}\ e \cdot \text{cm} \qquad [9]\,.$$

How does this surprising suppression arise in the SM? And what effects are expected in a typical Beyond the SM (BSM) scenario? Let us take the electron as an example, whose EDM is found to be

$$d_e \sim e \frac{m_e}{m_W^2} \frac{g^6 g_s^2}{(16\pi^2)^4} \left(\frac{v}{m_W}\right)^{12} \frac{m_b^4 m_s^2 m_c^2}{v^8}\, J\,. \tag{1.6}$$

[1] Also the bound on the muon EDM might be improved, by three orders of magnitudes, at a future Muon Collider [5].

This result can be understood as follows. First of all, d_e originates from CP violating physics which, in the SM, has three sources: the complex CKM and PMNS matrices and the θ angle of QCD. In the case of the electron EDM, the dominant contribution comes from the CKM matrix, which must enter the observables through the Jarlskog invariant J [10]. This can be expressed in terms of CKM matrix elements as $J = \text{Im}(V_{ud}V_{cs}V_{us}^*V_{cd}^*) \sim 3 \times 10^{-5}$, showing that it is numerically small but, more importantly, proportional to *four* CKM matrix elements! This implies that diagrams contributing to the electron EDM within the SM require at least three loops as shown in Fig. 1. As one can see from the picture, a much less obvious fourth gluon loop is actually necessary to get a non vanishing contribution (we will come back to this in Sec. 2.2). This explains the 4-loop suppression factor in Eq. (1.6). But this is not the end of the story: as explained spurionicly in Sec. 2.2, a further – quite strong – quark mass suppression enters Eq. (1.6) because of the specific flavor structure of the loop in Fig. 1. Finally, another m_e/v suppression comes from the need of a chirality flip in the electron line. All in all, this makes a tiny electron EDM in the SM.

Similar considerations apply to the quark EDMs, which feed into the neutron EDM as we show in Sec. 2.3, with the important difference that they arise at 3- instead of 4-loops as shown in Fig. 1. They have also a much less severe quark mass suppression [11]. Another very important point concerns the neutron EDM, which is also sensitive to the θ angle of QCD. However we will assume in this work that this parameter is shifted away thanks to the Peccei-Quinn mechanism [12], as we will detail in Sec. 2.3.

This situation is to be contrasted with what happens in models with new physics, where new sources of CP violation can be present. Taking again the example of the electron EDM, we find in this work contributions like

$$d_e \simeq -1.1 \times 10^{-29} e \cdot \text{cm} \, \frac{\text{Im}\left[C_{\substack{eB \\ 11}}\right]}{g' y_e} \left(\frac{1350\,\text{TeV}}{\Lambda}\right)^2 , \tag{1.7}$$

which does not carry any loop suppression and comes from a tree level Feynman diagram with $O_{eB} = \left(\bar{L}_L \sigma^{\mu\nu} e_R\right) H B_{\mu\nu}$ insertion. In the above expression, we divided the Wilson coefficient by its expected size $g' y_e$ (more on this in Sec. 5 and Table 3), where g' is the $U(1)_Y$ coupling and y_e the electron yukawa coupling, and Λ is the scale of new physics. As the formula shows, if $\text{Im}\left[C_{\substack{eB \\ 11}}\right] \sim g' y_e$ the scale of the CP violating new physics contributing to the EDMs is bounded to be larger than $\sim 10^3$ TeV. One can compare this bound, which is our strongest as we will see, to constraints coming from other CP violating observables, among which some of the most stringent are associated to meson mixings. However, it turns out that the latter [13, 14], are at least one order of magnitude weaker than our bound under similar assumptions (see the last column of Table IV in [13]).

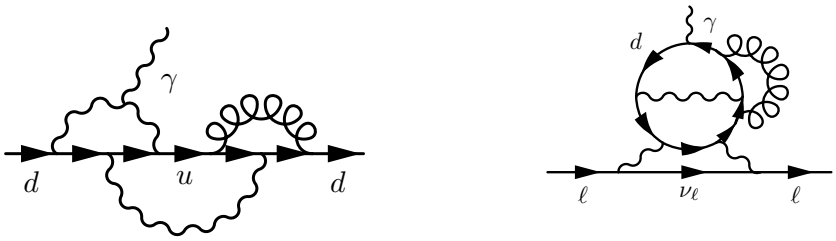

Figure 1: Representative Feynman diagrams for the leading SM contributions to the quark *(left)* and the lepton *(right)* EDMs. For the up-quark EDM the labels d and u have to be exchanged in the left diagram. Unlabeled wiggly lines correspond to W bosons.

The purpose of the present work is to study to 1-loop accuracy the EDMs in presence of new physics at some scale $\Lambda \gg v$, going to $\mathcal{O}(\Lambda^{-2})$. New physics effects are parametrized in a model independent way within the Standard Model Effective Field Theory (SMEFT), which we expand in the Warsaw basis. We will provide the complete 1-loop expressions of the low energy EDMs observables, for leptons as well as for the neutron, in terms of the Wilson coefficients of the Warsaw basis, including both RG flow effects and rational terms. In fact, while for extremely large scale separations the logarithmic contributions are expected to be larger than the corresponding finite (rational) terms, for $\Lambda \lesssim 10$ TeV we find them to be comparable. A complete 1-loop result is a step towards a higher accuracy in the theoretical predictions for EDMs observables, which will be measured with increased precision in future experiments. As a matter of fact, having accurate results would turn out crucial in the event of a non-zero measurement of a fermion EDM.

The constraining power of EDMs has stimulated a lot of different analyses in various UV completions of the SM. There are several studies of the electron and/or neutron EDMs in SUSY models [15–18], in Composite Higgs models [19–21], in Leptoquark models [22–25], in complex two-Higgs and three-Higgs doublet models [26–32], in scotogenic models [33] and in the context of dark matter [34]. On the model independent side, Ref. [35] provides an analysis of the electron EDM including some contributions that arise at 2-loop and at dimension-8 level, while Ref. [36] studies the complete 1-loop expression for the lepton EDMs. Ref. [37] studies the neutron EDM in presence of an effective CP violating Higgs-gluon interaction encoded by a dimension-6 SMEFT operator and Ref. [38] analyzes the contribution to the neutron EDM induced by chromo-dipoles of second and third generation quarks. Other studies of EDMs in presence of dimension-6 interactions involving the Higgs boson and fermion fields – in particular related to top physics – are performed in [39–44].

The paper is structured as follows. In Sec. 2 we present the EDM observables and dipole operators, both in the SM and in presence of new physics parametrized by the SMEFT. In Sec. 3 we discuss all the contributions to the dipoles generated by higher dimension-6 SMEFT operators and we furthermore study the neutron EDM in presence of $U(3)^5$ and $U(2)^5$ flavor symmetries for the SMEFT. In Sec. 4 we present some important formal and technical aspects of the calculations performed in this work and we finally show

the computed bounds in Sec. 5.

2 EDMs

2.1 Electric and magnetic dipole moments of elementary particles

The intrinsic angular momentum of a particle couples to external electric and magnetic fields, with strengths characterized by the electric and magnetic dipole moments respectively. For a spin-1/2 fermion f the non-relativistic Hamiltonian describing these interactions are given by

$$\mathcal{H}_{NR} = \frac{a_f\, eQ_f}{2m_f}\, \vec{\sigma}\cdot\vec{B} - d_f\, \vec{\sigma}\cdot\vec{E}\,, \tag{2.1}$$

where $\vec{\sigma}$ is the vector of Pauli matrices (related to the spin operator $\vec{s} = \vec{\sigma}/2$), d_f and a_f are the electric and magnetic dipole moments of the fermion and Q_f and m_f are its charge and mass. Already from this classical expression we can deduce the transformation properties of the magnetic and electric dipole moments, respectively, under CP: if the theory is invariant under CP, the only term in Eq. (2.1) which is allowed is the coupling to the magnetic field. The corresponding relativistic Lagrangian is

$$\mathcal{L} = -\frac{a_f eQ_f}{4m_f}\bar{\psi}\,\sigma^{\mu\nu}\psi\, F_{\mu\nu} - \frac{i}{2}d_f\bar{\psi}\,\sigma^{\mu\nu}\gamma_5\psi\, F_{\mu\nu}\,. \tag{2.2}$$

where the second term, barring the factor i, changes sign under a CP transformation due to the presence of the γ_5 matrix.

For the purpose of this work it is more convenient to use chiral fermions and we can rewrite the Lagrangian in Eq. (2.2) such that it becomes

$$\mathcal{L} = \frac{c_{f\gamma}}{\Lambda}\,\bar{\psi}_L\,\sigma^{\mu\nu}\psi_R\, F_{\mu\nu} + \text{h.c.}\,. \tag{2.3}$$

In the above equation we included explicitly a scale Λ for dimensional reasons, such that $c_{f\gamma}$ is dimensionless. By comparing Eqs. (2.2) and (2.3) we can relate the coefficient $c_{f\gamma}$ with the dipole moments a_f and d_f and we find

$$a_f = -\frac{4m_f}{eQ_f}\,\frac{\text{Re}\,[c_{f\gamma}]}{\Lambda}, \qquad d_f = -2\,\frac{\text{Im}\,[c_{f\gamma}]}{\Lambda}\,. \tag{2.4}$$

If not further specified, all operators of the form of Eq. (2.3), i.e. also those built from other vector fields, will be called low-energy dipole operators collectively throughout this work.

2.2 Dipole operators in the SM and in the SMEFT

Let us now further investigate the dipole operators in more detail. By dimensional counting we see immediately that the dipole operators are non-renormalizable operators of dimension $d = 5$ and the corresponding couplings are irrelevant; it follows that

$$[a_f] = [c_{f\gamma}] = 0, \qquad [d_f] = -1\,. \tag{2.5}$$

It is clear that within the Standard Model (SM) these operators cannot be generated through renormalization group (RG) effects. In fact, in the SM there are no possible counterterms that could cancel any divergence proportional to the dipole operators, in spite of the fact that a magnetic dipole moment, for massive fermions, is generated at tree level: the latter does not correspond to a contact interaction for the renormalizable SM theory. Nevertheless, they do acquire finite contributions from loop corrections to the $\bar{\psi}\psi\gamma$ vertex. While the leading contribution to a_f arises already at 1-loop, the EDM d_f receives contributions only starting at three loops, in the quark case, and at four loops, in the electron case, as mentioned in Sec. 1. In fact, in the SM, there is an accidental suppression of CP violation.

Let us briefly explain this suppression at this point. A CP odd physical amplitude, respecting the symmetries of the model, must be a combination of invariants, under (non-physical) changes of basis and field redefinitions, which should be a function of the complex phases responsible for the CP violation. We focus here on the flavor source for CP violating effects; the size of CP odd observables can therefore be estimated exploiting an analysis of the flavor structure and symmetries of the model. In the absence of Yukawa interactions, the SM, with massless neutrinos, is invariant under the global flavor symmetry [45]

$$G_F = U(3)^5 = U(3)_Q \times U(3)_u \times U(3)_d \times U(3)_L \times U(3)_e, \tag{2.6}$$

where $i = Q, u, d, L, e$ stands for the left-handed quarks, right-handed up and down quarks and left- and right-handed leptons, respectively, each of them with the corresponding gauge multiplicity. Each of these fermion species transforms as a triplet under its respective $U(3)$ and as a singlet under the remaining ones. Now, the Yukawa interactions break this symmetry explicitly, mixing different fermion species, and assuming this breaking is small due to the small Yukawas [2] we can formally reinstate G_F-invariance by promoting the Yukawa couplings to spurions in flavor space. The assumption that this is the only explicit breaking of G_F is known as *Minimal Flavor Violation* (MFV) [11, 46, 47]; MFV is exact within the SM and can be extended to the full flavor structure of the SMEFT, as we will do in Sec. 3.4. Then, in such MFV scenarios, the flavor structure, as well as any flavored CP violation effect, is completely determined by the Yukawa spurions. As we have seen, in the SM the only source of CP violation (ignoring the QCD θ term and neutrino masses) lies in the complex CKM phase in the quark sector; thus, any CP odd quantity must necessarily be built from quark Yukawas. Then, we can estimate the size of the EDMs as functions of $y_{u,d}$ in such a way that the lepton $\bar{L}\sigma_{\mu\nu}d_e y_e e F^{\mu\nu}$ and quark $\bar{Q}\sigma_{\mu\nu}d_{u(d)}y_{u(d)}u(d)F^{\mu\nu}$ dipoles are G_F invariants, where we have factored the y_f Yukawa out of the d_f dipole moments. Note, since the $\bar{L}y_e e$ term is flavor symmetric by itself, via spurionic promotion of the Yukawa coupling, the lepton dipole d_e, being a function of quark Yukawas, must be a G_F invariant; this is related to the fact that the lepton EDMs are generated through closed quark loops. Therefore, d_e must be given by the identity matrix times a traced chain of $y_{u(d)}y^\dagger_{u(d)}$ products. It turns out that the simplest such trace which is complex contains 12

[2] For now we ignore the fact that the top Yukawa is large, $y_t \sim 1$ such that it cannot be considered as a small breaking parameter. We will come back to this issue in Sec. 3.4.

quark Yukawas, with antisymmetrization under $y_u \leftrightarrow y_d$ such that it is not hermitian, and can be written as a determinant [11],

$$J_{CP} = \frac{1}{2i} \det \left\{ \left[y_u \left(y_u\right)^\dagger, y_d \left(y_d\right)^\dagger \right] \right\} . \tag{2.7}$$

The size of J_{CP} turns out to be very small, $J_{CP} \sim 10^{-22}$, due to the dependence on light quark masses, which gives the first reason for the suppression of the lepton EDMs within the SM. Actually, this determinant is related to the usual, well-known measure of CP violation in the SM, the Jarlskog invariant J shown in Sec. 1, in the following way: $J_{CP} \approx \frac{m_b^4 m_s^2 m_c^2}{v^8} J$ [11]. There is actually only a unique independent CP violating flavor invariant generated by the flavor structure of the SM: any CP odd observable in the SM can be expressed in terms of J_{CP}, or equivalently J, if we neglect the QCD θ term and PMNS matrix contributions. The flavor structure in Eq. (2.7) can be generated at least at the three-loop level, but it turns out that the three-loop diagram is symmetric under the exchange $y_u \leftrightarrow y_d$ while J_{CP} is anti-symmetric [11]. To break this symmetry an additional loop is needed, hence the suppression of lepton EDMs is evident from both the large number of (light) quark Yukawas, underlined above, as well as the high perturbative order needed to generate them. For the quarks the reasoning is similar, although $d_{u(d)}$ is not a flavor invariant, but rather transforms as an octet of $U(3)_Q$. It should therefore be a non-traced chain of $y_{u(d)} y_{u(d)}^\dagger$ products and it turns out that it needs to contain at least 8 quark Yukawas and can be generated at the three-loop level, already including the additional loop needed for amplitude to have the correct symmetries. The imaginary parts of entries of the matrix are again functions of the Jarlskog invariant, which parametrize any CP violation, but are less suppressed with respect to the lepton case: they can be 10 order of magnitudes larger than J_{CP}. For more details see e.g. [11].

Naturally, in the presence of new physics with some heavy new particles the dipole operators can potentially be generated directly together with additional effective operators after integrating out the heavy new physics. In this work we will assume that the scale of new physics lies above the electroweak (EW) scale, which can be quantified using the Higgs vacuum expectation value (VEV) v. Then the theory generated upon integrating out the heavy states is the Standard Model effective theory (SMEFT)[3], which means that the dynamical degrees of freedom are given by the SM field content. As for any effective theory there is a certain freedom of choosing a set of non-redundant operators and we can move from one basis to another by performing the appropriate field redefinitions. We will encounter the issue of non-uniqueness of the operator basis in an EFT later again. In this work we will make use of the so-called *Warsaw* basis, defined in [49], and we will explicitly give the expressions of the relevant operators in the next section. Furthermore, we will use a redundant set of operators, the so-called *Green's* basis [50, 51], for the intermediate steps

[3]Here we implicitly assume a linearly realized $SU(3)_c \times SU(2)_L \times U(1)_Y$ gauge symmetry as well as that the physical Higgs is a component of the linearly transforming Higgs doublet. An alternative to this approach is known as the Higgs effective theory (HEFT), where only the $SU(3)_c \times U(1)_{em}$ gauge symmetry is manifest and the physical Higgs is a priori not related to the components of the Goldstone Higgs doublet. For a comparison of the two approaches see for instance [48].

of the computation of the 1-loop contributions to the Warsaw basis dipole operators (see Sec. 4).

At low-energies, in particular below the EW scale, the SMEFT can be matched to a low-energy effective theory (LEFT) [52, 53], integrating out the top quark, the Higgs boson and the massive EW vectors Z and $W^{\pm}$; the LEFT, on top of the dipole operators, contains only those built from three gluons or four fermions that are not the top quark.

Going to higher orders in perturbation theory also other effective operators can contribute to the EDMs through loop effects. So one way to determine the effect on the low-energy observable EDM coming from some new physics, that is matched onto the SMEFT at some scale $\Lambda > v$, is to calculate the running of the SMEFT dipole operators, to be introduced in the next section, down to the EW scale, to match these operators onto the respective LEFT operators (providing the tree level and rational loop contributions involving virtual top, Higgs, Z and $W^{\pm}$ vector bosons) and finally calculate the loop contributions within the LEFT (generated by virtual particles that are lighter than the EW scale). Partial results of these calculations can be found scattered throughout the literature: the derivation of the renormalization group equation (RGE) within SMEFT has been performed in [54–56], both the tree level matching of the SMEFT to the LEFT as well as the LEFT RGE can be found in [52, 57] and the loop-level matching of the SMEFT to the LEFT has been calculated in [53]. Albeit these resources are useful in their own right, they cannot be used to obtain the full 1-loop correction to the EDM.

To perform the full 1-loop calculation we do not choose the multi-stage procedure described above, but instead go directly to the phase of broken EW symmetry, with all the SM fields in the (physical) basis of mass and electric charge eigenstates, and calculate all virtual effects at once, expressing our result in terms of the SMEFT coefficients in the Warsaw basis evaluated at the scale Λ above the scale of EW symmetry breaking.

We would like to stress that we are considering, in the SMEFT, tree and 1-loop level contributions to EDMs, that instead arise in the SM with much larger loop suppression: in presence of new physics, these CP odd observables can be in general largely enhanced. In fact, allowing for the presence of higher dimensional operators, CP violating effects are no more encoded only by the Jarlskog invariant, or equivalently by the J_{CP} of Eq. (2.7), and a larger variety of complex flavor invariants can be built from Wilson coefficients together with Yukawa matrices [58]. The flavor structure of the effective theory is such that these invariants can indeed be generated at lower loop level with respect to the SM case.

2.3 Dipole moments of non-elementary particles: neutron EDM

So far we have considered only fundamental particles within the SMEFT. But, as already mentioned in Sec. 1, another prominent observable other than the lepton EDMs is the electric dipole moment of the neutron. Being a composite state built from quarks and gluons we can write the neutron EDM as a function of the constituents' EDMs and chromo-electric dipole moments (cEDMs). The latter are defined as the coefficient of the CP odd operator in Eq. (2.2), but with a gluonic field strength instead of the photonic one. Putting

everything together we find [37, 59–65]

$$d_n = -(0.204 \pm 0.011)\, d_u + (0.784 \pm 0.028)\, d_d - (0.0027 \pm 0.0016)\, d_s + \tag{2.8}$$

$$+ 0.055(1 \pm 0.5)\, \hat{d}_u + 0.111(1 \pm 0.5)\, \hat{d}_d - 51.2(1 \pm 0.5)\, e \cdot \text{MeV}\, \frac{C_{\tilde{G}}}{\Lambda^2} + \tag{2.9}$$

$$- 9.22(1^{+2.33}_{-0.67})\, e \cdot \text{MeV}\, \frac{\text{Im}[C_{Hud}]_{11}}{\Lambda^2} + \tag{2.10}$$

$$- 0.615(1^{+1}_{-0.75})\, e \cdot \text{GeV} \left(\frac{\text{Im}[c^{(\text{S1,RR})}_{ud\,1111} - c^{(\text{S1,RR})}_{duud\,1111}]}{\Lambda^2} + \frac{\text{Im}[c^{(\text{S8,RR})}_{ud\,1111} - c^{(\text{S8,RR})}_{duud\,1111}]}{\Lambda^2} \right) . \tag{2.11}$$

where the "11" and "1111" subscripts of the Wilson coefficients in the last two lines indicate that the first flavor generation is taken into account.

The first three terms are contributions from the up, down and strange quark EDMs, respectively, the next two terms are the effects of the up and down quark cEDMs and the last term of the second line comes directly from the dimension-6 Weinberg operator [66] built from three gluons,

$$O_{\tilde{G}} = f^{ABC} G^{A\nu}_{\mu} G^{B\rho}_{\nu} \tilde{G}^{C\mu}_{\rho}, \tag{2.12}$$

that can be interpreted as the cEDM of the gluon. The contributions in the third and fourth lines are related to the SMEFT operators

$$O_{Hud} = (\bar{u}\gamma_\mu d)(\tilde{H}^\dagger i D^\mu H)\,, \tag{2.13}$$

$$O^{(1)}_{quqd} = (\bar{q}^r u)\epsilon_{rs}(\bar{q}^s d)\,, \tag{2.14}$$

$$O^{(8)}_{quqd} = (\bar{q}^r T^A u)\epsilon_{rs}(\bar{q}^s T^A d)\,. \tag{2.15}$$

In fact, the $c^{(\text{S1,RR})}_{ud}$ and $c^{(\text{S1,RR})}_{duud}$ are the Wilson coefficients of the following operators of the low energy effective field theory [52, 53, 57]

$$O^{(\text{S1,RR})}_{ud} = (\bar{u}_L u_R)(\bar{d}_L d_R)\,, \tag{2.16}$$

$$O^{(\text{S1,RR})}_{duud} = (\bar{d}_L u_R)(\bar{u}_L d_R)\,, \tag{2.17}$$

which are generated, below the electroweak scale, at tree level by $O^{(1)}_{quqd}$ and at 1-loop level by $O^{(8)}_{quqd}$. The tree level matching conditions are the following

$$O^{(\text{S1,RR})}_{ud\,1111} = O^{(1)}_{quqd\,1111}\,, \tag{2.18}$$

$$O^{(\text{S1,RR})}_{duud\,1111} = -O^{(1)}_{quqd\,1111}\,, \tag{2.19}$$

where the fermion fields are in the mass basis defined in Sec. 3.3. Analogously, $c^{(\text{S8,RR})}_{ud}$ and $c^{(\text{S8,RR})}_{duud}$ are the Wilson coefficients of

$$O^{(\text{S8,RR})}_{ud} = (\bar{u}_L T^A u_R)(\bar{d}_L T^A d_R)\,, \tag{2.20}$$

$$O^{(\text{S8,RR})}_{duud} = (\bar{d}_L T^A u_R)(\bar{u}_L T^A d_R)\,, \tag{2.21}$$

which are generated at tree level by $O^{(8)}_{quqd}$ and at 1-loop level by $O^{(1)}_{quqd}$, with the following tree level matching conditions

$$O^{(\mathrm{S8,RR})}_{\substack{ud\\1111}} = O^{(8)}_{\substack{quqd\\1111}}\,, \tag{2.22}$$

$$O^{(\mathrm{S8,RR})}_{\substack{duud\\1111}} = -O^{(8)}_{\substack{quqd\\1111}}\,. \tag{2.23}$$

All the terms in the third and fourth lines of Eq. (2.11) describe the contributions from CP violating low energy four-fermion interactions. In fact, below the electroweak scale, also O_{Hud} generates four-quark operators through a tree level exchange of a W boson between the right-handed fermion current of the dimension-6 operator and a left-handed current which has a SM coupling with the W. All the coefficients appearing in the above expression should be evaluated at the hadronic scale that characterizes the neutron EDM. To be more rigorous, in the case of c_{Hud} what is evaluated at such low energy scale are the coefficients of the four-quark operators generated after EW SSB by O_{Hud}, which is to say $(\bar{u}_L\gamma_\mu d_L)(\bar{d}_R\gamma^\mu u_R)$ at tree level and $(\bar{u}_L\gamma_\mu T^A d_L)(\bar{d}_R\gamma^\mu T^A u_R)$ at 1-loop level. Note that while $C_{\widetilde{G}}$, C_{Hud}, $c_{ud}^{(\mathrm{S1(8),RR})}$ and $c_{duud}^{(\mathrm{S1(8),RR})}$ are dimensionless, the fermionic dipole coefficients have the dimension of an inverse energy ($d_i, \hat{d}_i \sim v/\Lambda^2$).

As we have just discussed, the neutron EDM does not receive contributions only from quarks' EDMs and cEDMs. This allows operators to be probed, that would otherwise be only available at higher loop orders if at all. One example would be the Yukawa type operators $\psi^2 H^3$. At the 1-loop level, they cannot be accessed by EDMs of elementary particles, as they contribute only starting at the 2-loop order. However, as they give 1-loop contributions to O_{Hud}, which enters the neutron EDM also at tree level, one can probe them at a lower order as naively expected.

In this expression we implicitly assumed a Peccei-Quinn mechanism [12] to remove the contribution from the well-known QCD $\theta-$term

$$\mathcal{L}_\theta \sim \bar{\theta}\ \mathrm{Tr}\left[G^{\mu\nu}\widetilde{G}_{\mu\nu}\right], \tag{2.24}$$

which otherwise would give the dominant effect on the neutron EDM. Here $\bar{\theta}$ is a linear combination of a bare θ parameter and the argument of the determinant of the quark Yukawa couplings [67]. On top of the usual term that removes the contribution of the QCD θ-term, the Peccei-Quinn mechanism induces a shift on the axion potential due to the presence of the chromo dipole operators. In return, this shift modifies the coefficients for the light quark cEDMs and completely cancels the effect of the strange quark cEDM [61, 68, 69].

At this point we want to stress that the results presented in this paper can in principle be used for any function of the neutron EDM in terms of quark (c)EDMs, which might differ from (2.11).

3 Higher dimensional operators

3.1 1-loop effects

Within the SMEFT framework, in the phase of unbroken EW symmetry, the relevant dipole operators are the ones containing the hypercharge and weak gauge bosons B and

W^I, respectively. To ensure gauge invariance, these operators have to contain an additional Higgs doublet compared to the expression in Eq. (2.2) to compensate for the transformation of the left-handed fermion doublet. They have the form

$$O_{fB} = \left(\bar{\psi}_L \sigma^{\mu\nu} \psi_R\right) \overset{(\sim)}{H} B_{\mu\nu} \quad \text{and} \quad O_{fW} = \left(\bar{\psi}_L \sigma^{\mu\nu} \sigma^I \psi_R\right) \overset{(\sim)}{H} W^I_{\mu\nu}. \tag{3.1}$$

In these equations, $\psi_{L(R)}$ describes a left(right)-handed $SU(2)_L$ doublet (singlet) and the (conjugate) Higgs doublet has to be used if the fermion species in question sits in the (upper) lower component of the doublet. After the EW symmetry breaking and the transition from the gauge basis to the mass basis, we see that the Wilson coefficients of the EW SMEFT dipoles are related to the photonic one defined in Eq. (2.2) via the relation

$$c_{f\gamma} = \frac{v}{\Lambda} \left(c_w \; C_{fB} + 2T_f^3 s_w \; C_{fW}\right), \tag{3.2}$$

where we defined the trigonometric function of the weak mixing angle $c_w \equiv \cos\theta_w$ and $s_w \equiv \sin\theta_w$ and T_f^3 is the third component of the weak isospin for the respective fermion and is non zero only for left-handed chiralities.

Of course, for the neutron EDM also the gluonic dipole operators are relevant, as is obvious from Eq. (2.11). But since these are not affected by the EW symmetry breaking, except for effectively setting $H \to v$ and picking the relevant component from the $SU(2)_L$ quark doublet, we can see immediately that

$$c_{qg} = \frac{v}{\Lambda} C_{qG} \quad \text{and} \quad \hat{d}_q = -2\frac{v}{\Lambda^2} \text{Im}\left[C_{qG}\right]. \tag{3.3}$$

As already mentioned, if we go to the 1-loop order, various other higher-dimensional operators can enter the expression of the low-energy EDMs, be it through RG mixing, connected to the structure of divergences in the loop amplitudes, or through finite effects. Even though it is easy to see that many operators are not able to contribute to the dipoles at the 1-loop level given that one simply cannot draw any corresponding diagrams, blindly calculating all possible diagrams might not be the most efficient way. There are still a few operators that can generate a diagram that could potentially give a non-zero contribution, nevertheless it turns out to be vanishing if actually computed. Luckily, there are a few but nevertheless powerful criteria that have to be satisfied by the effective operators for them to be able to enter the EDMs at this perturbative level. This allows us to narrow down the set of operators to specifically those entering the EDMs without the need to perform a loop calculation. We summarize all the relevant effective operators in Table 1, show all the different kinds of contributions in Fig. 2 and explain our selections in the following. All the analysis is performed in the SMEFT at dimension-6 level. We do not consider in this work $O(1/\Lambda^4)$ corrections to the EDMs and we refer for a related discussion to [35], where a partial study of the contributions to the electron EDM from dimension-8 operators is presented.

1-loop contributions to the dipole operators: CP violation selection rules

The first criterion might also be the most trivial. Since we are only interested in the EDM, a CP odd observable, it makes sense to consider only those operators that can indeed

$$O_{\substack{eB\\ab}} = \left(\bar{L}_L^a \sigma^{\mu\nu} e_R^b\right) H B_{\mu\nu}$$
$$O_{\substack{eW\\ab}} = \left(\bar{L}_L^a \sigma^{\mu\nu} \sigma^I e_R^b\right) H W^I_{\mu\nu},$$
$$O_{\substack{uB\\ab}} = \left(\bar{Q}_L^a \sigma^{\mu\nu} u_R^b\right) \widetilde{H} B_{\mu\nu}$$
$$O_{\substack{uW\\ab}} = \left(\bar{Q}_L^a \sigma^{\mu\nu} \sigma^I u_R^b\right) \widetilde{H} W^I_{\mu\nu},$$
$$O_{\substack{dB\\ab}} = \left(\bar{Q}_L^a \sigma^{\mu\nu} d_R^b\right) H B_{\mu\nu}$$
$$O_{\substack{dW\\ab}} = \left(\bar{Q}_L^a \sigma^{\mu\nu} \sigma^I d_R^b\right) H W^I_{\mu\nu}$$
$$O_{\substack{uG\\ab}} = \left(\bar{Q}_L^a \sigma^{\mu\nu} T^A u_R^b\right) \widetilde{H} G^A_{\mu\nu}$$
$$O_{\substack{dG\\ab}} = \left(\bar{Q}_L^a \sigma^{\mu\nu} T^A d_R^b\right) H G^A_{\mu\nu},$$

$$O^{(3)}_{\substack{lequ\\abcd}} = \left(\bar{L}_L^{ja} \sigma_{\mu\nu} e_R^b\right) \epsilon_{jk} \left(\bar{Q}_L^{kc} \sigma_{\mu\nu} u_R^d\right)$$
$$O^{(1)}_{\substack{quqd\\abcd}} = \left(\bar{Q}_L^{ja} u_R^b\right) \epsilon_{jk} \left(\bar{Q}_L^{kc} d_R^d\right)$$
$$O^{(8)}_{\substack{quqd\\abcd}} = \left(\bar{Q}_L^{ja} T^A u_R^b\right) \epsilon_{jk} \left(\bar{Q}_L^{kc} T^A d_R^d\right)$$

$$O_{\substack{le\\abcd}} = \left(\bar{L}_L^a \gamma_\mu L_L^b\right) \left(\bar{e}_R^c \gamma_\mu e_R^d\right)$$
$$O^{(1)}_{\substack{qu\\abcd}} = \left(\bar{Q}_L^a \gamma_\mu Q_L^b\right) \left(\bar{u}_R^c \gamma_\mu u_R^d\right)$$
$$O^{(8)}_{\substack{qu\\abcd}} = \left(\bar{Q}_L^a \gamma_\mu T^A Q_L^b\right) \left(\bar{u}_R^c \gamma_\mu T^A u_R^d\right)$$
$$O^{(1)}_{\substack{qd\\abcd}} = \left(\bar{Q}_L^a \gamma_\mu Q_L^b\right) \left(\bar{d}_R^c \gamma_\mu d_R^d\right)$$
$$O^{(8)}_{\substack{qd\\abcd}} = \left(\bar{Q}_L^a \gamma_\mu T^A Q_L^b\right) \left(\bar{d}_R^c \gamma_\mu T^A d_R^d\right)$$
$$O^{(1)}_{\substack{ud\\abcd}} = \left(\bar{u}_R^a \gamma_\mu u_R^b\right) \left(\bar{d}_R^c \gamma_\mu d_R^d\right)$$
$$O^{(8)}_{\substack{ud\\abcd}} = \left(\bar{u}_R^a \gamma_\mu T^A u_R^b\right) \left(\bar{d}_R^c \gamma_\mu T^A d_R^d\right)$$

$$O_{\widetilde{W}} = \epsilon^{IJK} \widetilde{W}^{I\nu}_\mu W^{J\rho}_\nu W^{K\mu}_\rho$$
$$O_{\widetilde{G}} = f^{ABC} \widetilde{G}^{A\nu}_\mu G^{B\rho}_\nu G^{C\mu}_\rho$$

$$O_{H\widetilde{B}} = H^\dagger H B^{\mu\nu} \widetilde{B}_{\mu\nu}$$
$$O_{\widetilde{W}} = H^\dagger H W^{I\mu\nu} \widetilde{W}^I_{\mu\nu}$$
$$O_{HW\widetilde{B}} = (H^\dagger \sigma^I H) W^{I\mu\nu} \widetilde{B}_{\mu\nu}$$
$$O_{H\widetilde{G}} = H^\dagger H G^{A\mu\nu} \widetilde{G}^A_{\mu\nu}$$

$$O_{\substack{Hud\\ab}} = i \left(\tilde{H}^\dagger D_\mu H\right) \left(\bar{u}_R^a \gamma^\mu d_R^b\right)$$

$$O_{\substack{dH\\ab}} = H^\dagger H \left(\bar{Q}_L^a d_R^b H\right)$$
$$O_{\substack{uH\\ab}} = H^\dagger H \left(\bar{Q}_L^a u_R^b \tilde{H}\right)$$

Table 1: Set of dimension-6 SMEFT operators relevant in this paper, grouped in six different boxes corresponding to the different classes discussed in the main text. The operators $O^{(1,8)}_{ud}$ as well as the $\psi^2 H^3$ type operators can only be probed at the 1-loop level through the neutron EDM. The dashed line separates the 4-fermion operators of the form ψ^4 and those of the form $\psi^2 \bar{\psi}^2$. We use the usual definitions $\widetilde{H} = i\sigma^2 H^*$ and $\widetilde{F}_{\mu\nu} = \frac{1}{2}\epsilon_{\mu\nu\alpha\beta} F^{\alpha\beta}$ for F any of the gauge bosons. For the operators $O^{(3)}_{lequ}$ and $O^{(1,8)}_{quqd}$ we show SU(2) indices j, k explictly. For the vector operators in the 4-fermion class the only CP violation can arise if flavors of the fermions in each current are not identical, hence we explicitly give the generation indices a, b, c, d explicitly.

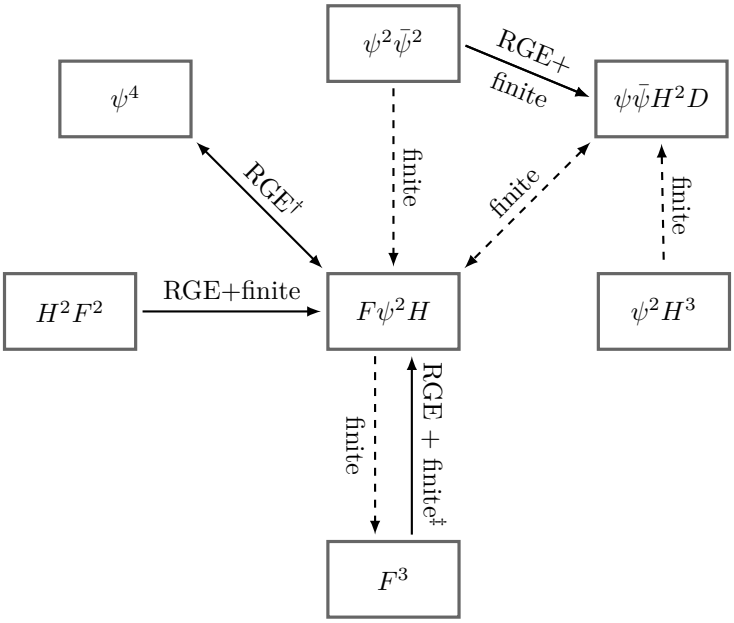

Figure 2: Contributions to the operators entering the dipoles. Operators connected with solid arrows enter the RGEs, while dashed arrows describe purely finite effects. The † indicates that the operator $O^{(1)}_{lequ}$ is not included in the ψ^4 class here. Interestingly, we find that the others operators in this class only enter via the RGE, generating no rational terms. The ‡ shows that the operator $O_{\widetilde{W}}$ gives only rational terms.

give such CP odd contributions. In other words, we are interested only in those operators that contribute to the imaginary part of the (flavor diagonal) dipole coefficient with only a single higher dimensional insertion. This significantly reduces the number of operators that we potentially need to include in our calculation, but we can go even further.

1-loop contributions to the dipole operators: helicity selection rules

In general we can use helicity [70–72] and angular momentum [73] arguments to derive selections rules, essentially making it possible to pinpoint only the relevant operators. Using the former, one finds that an operator generating a contact interaction with n external legs and total helicity $\sum h$ can only be renormalized by another operator with $(n', \sum h')$ if the relations

$$n' \leq n \quad \text{and} \quad \left|\sum h - \sum h'\right| \leq n - n' \tag{3.4}$$

hold [70, 72]. The dipole operators are of the form $F\psi^2H$, where F and ψ are positive helicity field strength tensor and fermion respectively, so we can characterize them by $(n, \sum h) = (4, 2)$. Using the above relations we see that the only operators able to renormalize the dipoles within the Warsaw basis of the SMEFT are:

- Operators with $(n, \sum h) = (3, 3)$, i.e. operators of the class F^3;
- Operators with $(n, \sum h) = (4, 2)$. This includes operators of the form F^2H^2, ψ^4 and of course the dipole operators $F\psi^2H$ themselves.

Although there is an exception to Eq. (3.4), we can show that it does not change the set of renormalizing operators given above. It is related to the existence of the so-called exceptional, four-dimensional ψ^4 amplitude with $(n, \sum h) = (4, 2)$.[4] [70–72]. It can be shown that an insertion of this exceptional amplitude could potentially lead to the renormalization of the dipoles from higher-dimensional operators with $(n, \sum h) = (4, 0)$. Operators with this number of legs and total helicity in the Warsaw basis are of the form $\psi^2\bar{\psi}^2$, $\psi\bar{\psi}H^2D$ and H^4D^2. Hence we see that we can not build a loop amplitude with the particle content of the dipole in the external states by combining these higher-dimensional contact amplitudes with the four-dimensional exceptional amplitude.

While these helicity selection rules provide a helpful tool when aiming to calculate the RGEs of various operators there, they have one major shortcoming if one is interested in a full 1-loop calculation. This is related to the fact that helicity arguments deal only with the renormalization of operators and are not able to tell if there are operators that contribute only through rational terms[5].

Interestingly, although the operator $O_{\widetilde{W}}$ belongs to the F^3 class, hence could renormalize the dipole operators, it instead gives only a finite, rational contribution. This was computed using both Feynman diagrams [35, 77, 78] as well as on-shell methods [79]. Its gluonic counterpart on the other hand does also enter the dipole operator RGE.

1-loop contributions to the dipole operators: angular momentum selection rules

We can alleviate the problem of rational terms by augmenting the helicity selection rules with angular momentum considerations [73]. So far these were used as an alternate way to derive the pattern of renormalization among operators using the conservation of angular momentum of external states, instead of employing the cut-based factorization of loop amplitudes that is used to arrive at the above helicity selection rules. At the core of the argument lies the fact that for every amplitude (at least) one well-defined scattering channel can be defined, where the angular momentum has to be conserved in the sense that the total angular momentum j of the initial states, as well as the projection m along an axis, has to equal the one of the final states. Then, for an operator to be able to renormalize another operator there has to be at least one pair of channels of these operators with matching angular momentum; angular momentum arguments show directly not only which renormalizations are allowed, but also in which channels they can arise. Note that this approach is complementary to the helicity selection rules in the sense that operators allowed by the former can be forbidden if we additionally use the latter and vice versa. Let us illustrate this with an example relevant for this paper, the renormalization of the lepton dipole operators by 4-fermion operators. We find two possible scattering channels for the dipoles, namely

- the $VH \to \psi\psi$ channel, with $j = 1$;

[4] This amplitude is proportional to the product of up and down quark Yukawa couplings and is the only SM 4-point amplitude having total helicity different from zero

[5] While there are no helicity selection rules for rational terms, they can still be calculated using helicity amplitudes. However, this would require to perform all possible multi-particle cuts either in D dimensions, see e.g. [74], or using massive loop propagators [75, 76]

- and the $V\psi \to H\psi$ channel, with $j = 1/2$.

On the other hand, using helicity selection rules, we already know that the only possible 4-fermion operators that can renormalize the dipoles necessarily have to take the form ψ^4, with total helicity $\sum h = 2$. It turns out that in this class of operators, some have $j = 0$ and others $j = 1$ in the $\psi\psi$ scattering channel, while for the dipole operators only the latter is allowed. In the Warsaw basis, the only two operators that could potentially be relevant, concerning the lepton dipole operators, are the semileptonic operator

$$O_{lequ}^{(1)} = \left(\bar{L}_L^j e_R\right)\epsilon_{jk}\left(\bar{Q}_L^k u_R\right) \tag{3.5}$$

and its tensorial cousin $O_{lequ}^{(3)}$ defined in Table 1. We see that the former could contribute to the dipole only through a $j = 0$ two-lepton channel, while the latter contributes through a $j = 1$ channel. Since the dipole operators have $j = 1$ in the two-fermion channels, only the tensor operator can in fact renormalize the dipole. We want to stress here, that, without actually performing the loop calculation, we were not able to see this by using only helicity selection rules without the angular momentum conservation. Among the operators mixing with the dipoles through RG flow, the one with $O_{lequ}^{(1)}$ is the only one which would have been allowed by helicity selection rules but is forbidden by angular momentum conservation.

As an example for the opposite relation we want to mention operators in the class $\psi\bar{\psi}H^2D$, with zero total helicity. By angular momentum arguments these would be allowed to renormalize the dipole, via the ψH channel [73], but they do not satisfy the conditions in Eq. (3.4) and therefore do in fact not enter the dipole operators' RGE. Note that these operators can not give a CP odd contribution with only a single insertion, apart from O_{Hud}. Hence, the latter enters indeed in the 1-loop corrections to (chromo-)dipoles of the quarks, while we can remove the remaining operators of this class from the set of relevant operators with only the condition of CP violation.

Because the angular momentum argument does not rely on performing cuts in the loop integral but only on the angular momentum of external states it should be possible to extend the procedure to rational terms. While we are not aware of a rigorous proof for this and leave any detailed investigation for later work, we checked a few cases and the procedure worked for all of them. For example, the $\psi\bar{\psi}H^2D$ operators discussed above, whose renormalization to the dipoles is forbidden by helicity selection rules, can generate dipole operators at 1-loop level according to angular momentum arguments and it turns out that they indeed give rational contributions to the $F\psi^2H$ operators. There is, however, a caveat that might be worth investigating in a future work and is related to the existence of so-called evanescent operators. These are operators that generate non-vanishing amplitudes in $d \neq 4$ space-time dimensions that then vanish in the limit $d \to 4$ and often arise in the context of 4-fermion operators and Fierz identities that change for $d \neq 4$. In particular, let us look at the operator O_{le} in the Warsaw basis and its counterparts with quarks defined in Table 1; the connection of evanescent operators to the dipole through this particular operator was already mentioned in [35]. It lives in the operator class $\psi^2\bar{\psi}^2$, having $j = 0$ in the $\psi\psi$ channel, so by angular momentum conservation it neither can renormalize the dipole nor give only rational contributions. On the other hand, it is straightforward to

compute the loop diagram with a single insertion of this operator and see that it, against all odds, does in fact give a rational contribution. This apparent contradiction with angular momentum conservation can be resolved by realizing that we can apply a Fierz identity to rewrite this operator as

$$O_{le} = \big(\bar{L}_L\gamma_\mu L_L\big)\big(\bar{e}_R\gamma_\mu e_R\big) \propto \big(\bar{L}_L e_R\big)\big(\bar{e}_R L_L\big). \tag{3.6}$$

Again, we can calculate the corresponding diagram with an insertion of this operator after the Fierzing and we indeed find a vanishing result, in accordance with angular momentum conservation. At this point, we have to stress that the above Fierzing does only hold in $d = 4$, in a general number of space-time dimensions the identity reads [53]

$$O_{le} = \big(\bar{L}_L\gamma_\mu L_L\big)\big(\bar{e}_R\gamma_\mu e_R\big) = 2\big(\bar{L}_L e_R\big)\big(\bar{e}_R L_L\big) + E^{(2)}_{LR}, \tag{3.7}$$

where $E^{(2)}_{LR}$ is an evanescent operator that vanishes in 4 dimensions. This additional operator then gives a rational term when inserted into the loop integral.

In this paper we use the Warsaw basis without any Fierzing, so the contribution from this kind of operators appears explicitly in the final result, however, keeping in mind that it is related to the presence of an evanescent operator.

1-loop contributions to the Weinberg operator

So far we considered only the effects on the dipole operators, but also the Weinberg operator enters the neutron EDM directly as a measure of the gluon cEDM. Because it is the only operator with $n < 4$ legs in the Warsaw basis, apart from the W^3 operators, it can only be renormalized by itself, following the first condition in Eq. (3.4). In terms of rational terms, the only other class of operators are the dipole operators[6]. This pattern of contributions is summarized in Fig. 2. Therein, we show all the 1-loop contributions, allowed by the discussed selection rules, to the dipole $F\psi^2 H$ operators and to the F^3 operators. However, as we mentioned, only the imaginary parts of the flavor diagonal elements in the dipole WCs enter in the CP odd EDMs; therefore, for us the $\psi\bar{\psi}H^2D$ class is not relevant and among the H^2F^2 and F^3 operators we are interested only in those that are CP odd.

1-loop contributions to the O_{Hud} operator

Using both the CP and helicity selections rules from above shows that the only the flavor off-diagonal pieces of $\psi^2\bar{\psi}^2$ class operators can renormalize O_{Hud}, apart from O_{Hud} itself. To be more precise, the only possible operators are $O^{(1)}_{ud}$ and its color-octet counterpart, as these are the only ones that contain both a right-handed up and down quark. On top of that, we can use angular momentum selection rules to find purely rational effects. In perfect analogy to the discussion of the dipole operators above, where we saw that such selection

[6] In fact, deriving this using angular momentum conservation is not as straightforward as before, due to the 3-point nature of the F^3 amplitude, and was not performed here. But because the gluon couples only to quarks and itself in the SM and requiring only single higher dimensional insertions, there are only these two possibilities for particles running in the loop. Then one can check that the latter is already covered by insertions of the Weinberg operator itself while the only fermionic operator that can maybe generate the CP odd operators are the dipole operators.

rules tell us that O_{Hud} gives rational contributions to those, we find opposite relation here, namely that the dipole operators give rational contributions to O_{Hud}. Further, we find also non vanishing finite contributions from $\psi^2 H^3$ operators, allowed by angular momentum selection rules.

1-loop contributions to the $O_{quqd}^{(1,8)}$ operators

It is easy to see that these operators can get 1-loop contributions only from operators containing at least two fermions, otherwise it is simply not possible to draw corresponding diagrams. Apart from self-renormalization, this leaves only a few viable classes, $F\psi^2 H$, $\psi^2\bar{\psi}^2$, $\psi\bar{\psi}H^2 D$ and $\psi^2 H^3$. Remembering that we only care for the first generation quarks in the direct contributions of these operators to the nEDM, the latter three classes don't give any non-negligible CP violating 1-loop corrections. In fact, $\psi^2 H^3$ operators have too many legs to effectively close a single loop. On the other hand, the contributions form the $\psi\bar{\psi}H^2 D$ and $\psi^2\bar{\psi}^2$ operators are either CP even or suppressed by two powers of a light quark Yukawa, so we neglect them compared to their respective contribution to the dipole operators. Consequently, the only operators contributing to $O_{quqd}^{(1,8)}$, apart from themselves, are the dipole operators which give both logarithmic and rational effects. As for the RG effects, this can also be explained through helicity selection rules, since $O_{quqd}^{(1,8)}$ are $(n, \sum h) = (4, +2)$ operators, while $\psi^2\bar{\psi}^2$, $\psi\bar{\psi}H^2 D$ and $\psi^2 H^3$ have total helicity equal to zero or one.

3.2 2-loop effects

Although the main focus of this paper lies on the full 1-loop calculation we want to briefly discuss possible higher order effects. Formally, these are suppressed by additional loop factors and more powers of some coupling, so naively these higher order processes are always suppressed compared to the leading order term. In a realistic theory like the SM and extensions thereof with many different couplings and likely a large hierarchy among them, this does not hold in general. A prominent example is the Barr-Zee diagram for fermion EDMs in the presence of additional Higgs doublets [80]. Here, the leading oder diagram is suppressed by two powers of the fermion Yukawa, y_f^2, due to two couplings of a Higgs to the fermion line. However, by going to the next order in perturbation theory one of these Yukawas can be traded for a factor of $\frac{g^2}{16\pi^2}$, by adding e.g. an additional top quark loop. In this case, for light external fermions, this factor is still larger than a potentially tiny Yukawa, hence the formally subleading 2-loop effects can actually dominate over the leading order contribution.

We mention the Barr-Zee type diagrams because a similar effect may be important for the results in this paper. In particular, we want to look at the terms in the expression of the EDMs proportional to the coefficients of operators in the class H^2F^2. By anticipating the final result we note that these terms are proportional to the external fermion mass leading to a strong suppression of these terms compared to other operators. A representative diagram for these contributions is shown in Fig. 3, all other diagrams generated by this class of operators can be found in App. A.

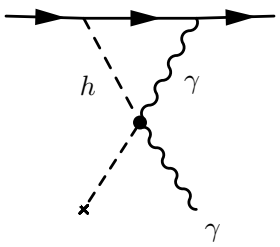

Figure 3: Representative diagram giving a contribution of the H^2F^2 class of operators to the dipole operators.

Now, in the light of the Barr-Zee diagram we might think there is a higher-order diagram in which the direct coupling of the scalar to the fermion is replaced by an additional loop in such a way that it overcompensates the severe suppression from the light Yukawa. It turns out that this is not the case and there is no 2-loop diagram generated by this class of operators where this Higgs-external fermion coupling is not present and still a contribution to the EDM is generated; so the 1-loop contribution is indeed the leading one and in comparison all 2-loop effects remain suppressed. Note that the same happens for the F^3 class operators, where the proportionality to the fermion mass or equivalently the Yukawa is more evident in the phase of unbroken symmetry. On the other hand, this shows that there is in fact no higher-order, formally subleading effect that dominates over the 1-loop ones calculated in this work, for a given class of operators, justifying the truncation of the perturbation series at this order, in setting bounds on a certain Wilson coefficient.

Nonetheless, there are effects that become important and have to be included at higher perturbative order, for instance operators that can not enter at the 1-loop level but do so at the 2-loop level. This can happen in two ways. Either such operators give a direct 2-loop contribution, like for example the Yukawa-type operator $O_{eH} = |H|^2 \bar{L}_L e_R H$ [35], or they mix at the 1-loop level with operators that themselves mix with the dipoles at the 1-loop level. Two interesting examples are the scalar 4-fermion operator $O^{(1)}_{lequ}$, which we excluded at the 1-loop level by using angular momentum arguments but renormalizes its tensorial counterpart [56], effectively using it as a portal to enter the EDM, and the operator $O_{\widetilde{W}}$, which gives only rational effects at 1-loop but also renormalizes the operators in the class H^2F^2 [56], so it can contribute to the dipole RGE via these. For a more in-depth look at these 2-loop effects see [35].

3.3 Transition from the gauge to the mass basis

As already explained, all calculations in this paper were performed directly in the phase of spontaneously broken electroweak symmetry and it is convenient to go from the gauge to the mass basis for fermions. This basis transformation is, in any case, eventually necessary, in order to take into account the propagating degrees of freedom. Now that we have defined all relevant operators, we want to briefly discuss the effect this basis change has on the

coefficient of each of the operators before we go into more detail about the calculation itself and the results thereof.

We diagonalize the fermion mass matrices by rotating each chiral fermion, which are triplets in generation space, using unitary transformations in flavor space,

$$\psi'^{\,i}_{L/R} = U^i_{L/R}\,\psi^i_{L/R} \tag{3.8}$$

with (un)primed fields in the (mass) gauge basis and i denotes any of the fermion flavors. Note, that in a general SMEFT the matrices $U^i_{L/R}$ are modified by Yukawa-type dimension-6 operators with respect to the SM transformations. For our purposes, however, it is sufficient to use the SM transformations, because these modifications would enter only at $\mathcal{O}(1/\Lambda^4)$ once we take into account fermions involved in dimension-6 operators. These flavor rotations introduce the transformation matrices for higher dimensional operators including fermions and can be reabsorbed by redefining the respective Wilson coefficients, as shown in Table 2, where the C coefficients in the mass basis are obtained as bi-unitary transformations of the C' coefficients defined in the gauge basis. Because the components of electroweak quark doublets are transformed differently, in order to simultaneously diagonalize all the Yukawa matrices, one can not redefine, in the phase of unbroken gauge symmetry, all Wilson coefficients in such a way that the corresponding gauge invariant operators are in the mass basis for all the involved fermions. In fact, before electroweak breaking, a flavor redefinition of the operators can be performed only through a $U(3)^5$ transformation (see Eq. 2.6), where a unique $U(3)_Q$ acts on the full $SU(2)_L$ quark doublet. Possible choices, for the gauge basis in which the SMEFT Wilson coefficients are defined in the unbroken phase, are the absorption either of the up-type or of the down-type rotation: we denote them in the following as up- and down-quark bases, in which the up- and down-quark Yukawa matrices are diagonal respectively. Then, after EW spontaneous symmetry breaking and full rotation to the mass basis, in the quark sector this generates the CKM matrix, defined as

$$V \equiv V_{CKM} = (U^u_L)^\dagger\, U^d_L, \tag{3.9}$$

and the precise terms where it appears are given by the choice of the definition of the Wilson coefficients in the gauge basis[7]. We choose, in our work, to present the final expressions for the EDMs in terms of the Wilson coefficients in the mass basis, defined in Table 2, in such a way that the least amount of CKM matrices appear explicitly. Furthermore, also the bounds are set here on the mass basis Wilson coefficients, even if in presenting these constraints in Table 8 and 11, the C' coefficients in the gauge basis are shown explicitly, choosing the up-quark basis and consequently $U^d_L = V$ and $U^u_{L/R} = \mathbf{1}$.

3.4 Neutron EDM Bounds under the Light of Flavor Symmetries

Since a lot of different flavor components of the fermionic Wilson coefficients enter through the various quark EDMs in the expression of the neutron EDM in Eq. (2.11), in particular in the gauge basis, due to the misalignement with the mass basis in the quark sector, as

[7] If we would relax our assumption of massless neutrinos the PMNS matrix would be generated accordingly in the lepton sector.

$$C_{dW} = \left(U_L^d\right)^\dagger C'_{dW} U_R^d$$

$$C_{dB} = \left(U_L^d\right)^\dagger C'_{dW} U_R^d$$

$$C_{dG} = \left(U_L^d\right)^\dagger C'_{dW} U_R^d$$

$$C_{dH} = \left(U_L^d\right)^\dagger C'_{dH} U_R^d$$

$$C_{uW} = \left(U_L^u\right)^\dagger C'_{uW} U_R^u$$

$$C_{uB} = \left(U_L^u\right)^\dagger C'_{uW} U_R^u$$

$$C_{uG} = \left(U_L^u\right)^\dagger C'_{uW} U_R^u$$

$$C_{uH} = \left(U_L^u\right)^\dagger C'_{uH} U_R^u$$

$$C_{Hud} = \left(U_R^u\right)^\dagger C'_{Hud} U_R^d$$

$$C^{(3)}_{\substack{lequ\\abcd}} = \delta_{ia}\delta_{jb}\left(U_L^u\right)^\dagger_{ck}\left(U_R^u\right)_{ld} C'^{(3)}_{\substack{lequ\\ijkl}}$$

$$C^{(1,8)}_{\substack{quqd\\abcd}} = \left(U_L^d\right)^\dagger_{ai}\left(U_R^u\right)_{jb}\left(U_L^u\right)^\dagger_{ck}\left(U_R^d\right)_{ld} C'^{(1,8)}_{\substack{quqd\\ijkl}}$$

$$C^{(1,8)}_{\substack{qu\\abcd}} = \left(U_L^u\right)^\dagger_{ai}\left(U_L^u\right)_{jb}\left(U_R^u\right)^\dagger_{ck}\left(U_R^u\right)_{ld} C'^{(1,8)}_{\substack{qu\\ijkl}}$$

$$C^{(1,8)}_{\substack{qd\\abcd}} = \left(U_L^d\right)^\dagger_{ai}\left(U_L^d\right)_{jb}\left(U_R^d\right)^\dagger_{ck}\left(U_R^d\right)_{ld} C'^{(1,8)}_{\substack{qd\\ijkl}}$$

$$C^{(1,8)}_{\substack{ud\\abcd}} = \left(U_R^u\right)^\dagger_{ai}\left(U_R^u\right)_{jb}\left(U_R^d\right)^\dagger_{ck}\left(U_R^d\right)_{ld} C'^{(1,8)}_{\substack{ud\\ijkl}}$$

Table 2: Definitions of Wilson coefficients of fermionic operators used in this work. We suppress flavor indices for the dipole operators because their contraction is non-ambiguous. (Un)primed coefficients denote the ones in the (mass) gauge basis. The specific form of the U unitary matrices, needed to the transformation to the mass basis, depends on the specific choice for the gauge basis in which the C' coefficients are defined: for example, $U^u_{L/R} = 1$, $U^d_L = V$ ($U^d_{L/R} = 1$, $U^u_L = V^\dagger$) in the up (down) - quark basis. Here we already assumed a diagonal lepton Yukawa, hence $U^e_{L/R} = 1$ and $C_{eV} = C'_{eV}$.

shown in the previous section, it is interesting to study the effects of flavor symmetries that relate the components of the flavor tensors. We have already discussed the simplest such symmetry in Sec. 2.2 that usually goes under the name of minimal flavor violation and assumes a $U(3)$ symmetry for each of the five different types of fermions in the Standard Model, broken only by the Yukawa couplings.

By enforcing this symmetry on the SMEFT and promoting the Wilson coefficients to spurions, we can completely determine the flavor tensors of the fermionic Wilson coefficients in terms of Standard Model parameters and a reduced number of flavor indipendent coefficients, one for each term in the spurionic Yukawa expansion of the SMEFT operators [81]. Notice, that this expansion is performed for Wilson coefficients in the gauge basis, where the latter can be rotated applying a transformation of the flavor symmetry group. By only including terms up to $\mathcal{O}(y^2_{u,d,e})$, we can reduce the Wilson coefficient of most fermionic operators to one complex coefficient while the operators $O^{(1,8)}_{qu}, O^{(1,8)}_{qd}$, combining two chirality-conserving currents, are forbidden at the considered order. E.g. for the dipole

operator we find

$$C'_{\substack{uB\\pr}} O'_{\substack{uB\\pr}} = C'_{\substack{uB\\pr}} \left(\bar{Q}'_p \sigma^{\mu\nu} u'_r\right) \widetilde{H} B_{\mu\nu} \longrightarrow F_{uB} \left(\bar{Q}'_p \sigma^{\mu\nu} u'_r\right) \widetilde{H} B_{\mu\nu} \left((y_u)_{pr} + \mathcal{O}(y^3_{u,d,e})\right) , \quad (3.10)$$

where C'_{uB} is in the same basis as y_u (for C'_{uB} in the up-quark gauge basis, $C_{uB} = C'_{uB}$). For $U(3)^5$ to be a good symmetry of the Standard Model we would expect it to be softly broken by the Yukawa couplings. However, with the top Yukawa being of $\mathcal{O}(1)$, this is not the case and we lose consistency of the power counting in our expansion. In addition, there are many BSM models where the third generation plays a special role motivating the complete removal of the third generation from the flavor group [82, 83]. The simplest smaller allowed symmetry group is then

$$H_F = U(2)^5 = U(2)_Q \times U(2)_L \times U(2)_u \times U(2)_d \times U(2)_e \,. \quad (3.11)$$

In order to make the full flavor structure of the Yukawa interactions invariant under the new symmetry group we have to introduce additional spurions with respect to MFV to make the Yukawa interactions of the first two and third generation – which is now invariant under the flavor group – formally invariant. We can parametrize the Yukawa matrices in terms of these spurions as follows [82]

$$y_u = \lambda_t \begin{pmatrix} \Delta_u & x_t V_q \\ 0 & 1 \end{pmatrix} \qquad y_d = \lambda_b \begin{pmatrix} \Delta_d & x_b V_q \\ 0 & 1 \end{pmatrix} \qquad y_e = \lambda_\tau \begin{pmatrix} \Delta_e & x_\tau V_l \\ 0 & 1 \end{pmatrix} . \quad (3.12)$$

where the Δ_i are in general 2×2 complex matrices, the V_i are complex 2-vectors and the λ_i are complex parameters expected to be of $\mathcal{O}(1)$. The spurions have the following transformation properties under H_F

$$\begin{gathered} \Delta_u \sim (2,1,\bar{2},1,1) \qquad \Delta_d \sim (2,1,1,\bar{2},1) \qquad \Delta_e \sim (1,2,1,1,\bar{2}) \\ V_q \sim (2,1,1,1,1) \qquad V_l \sim (1,2,1,1,1) \,. \end{gathered} \quad (3.13)$$

In the case of MFV it was easy to relate the spurions to parameters of the Standard Model. For the $U(2)^5$ flavor symmetry, we first apply the H_F transformations to go to a basis in which two of the three 2×2 Δ matrices in Eq. (3.12) are diagonal and then express most of the parameters in terms of Standard Model masses and CKM matrix elements (see App. C). However, there are some left-over $U(2)^5$ parameters that can in general not be related to measurable objects. Ignoring the leptonic parameters which are irrelevant to us, the phase of V_q for example can only be fixed in the limit where $x_t \to 0$ [82].

The key assumption is, also in this case, that all the flavor tensors in the Wilson coefficients can be expressed in terms of the spurions contained in the Yukawa matrices which are the unique source of H_F symmetry breaking in the SM as well as in the SMEFT. If we construct the flavor tensor of the dipole operator again, now assuming $U(2)^5$, we get [81]

$$C'_{\substack{uB\\pr}} O'_{\substack{uB\\pr}} \supset f_{uB} \left[\alpha_1 \bar{q}'_3 \sigma^{\mu\nu} u'_3 \widetilde{H} B_{\mu\nu} + \beta_1 \bar{Q}'^p V_q^p \sigma^{\mu\nu} u'_3 \widetilde{H} B_{\mu\nu} + \rho_1 \bar{Q}_p \sigma^{\mu\nu} (\Delta_u)_{pr} U_r \widetilde{H} B_{\mu\nu}\right] \quad (3.14)$$

where the fields in capitals denote fields from the first two generations and the field with the subscript 3 a field from the third generation. For convenience we introduced the notation $C_X(Y) = f_X Y$ in analogy to Ref. [81]. We will work at an accuracy of $\mathcal{O}(10^{-2})$ which means that we have to keep terms up to $\mathcal{O}(\Delta_{u,d,e}, V_{q,l}^2)$. We have listed an exemplary set of expansions of all relevant Wilson coefficients in App. C.

It is also worth noting is that upon going to the mass basis there will be additional CKM matrix elements in front of all fermionic operators including left-handed down quarks. We perform the sum over these CKM elements and the respective flavor components of the Wilson coefficients in order to relate the Wilson coefficients in the mass basis to those in the gauge basis. We subsequently replace the flavor tensors of the Wilson coefficients in the gauge basis by their spurionic expansions dictated by the flavor symmetries. Since more fermionic operators appear in the expression of the up-type quark dipoles we choose the up-quark basis for the SMEFT operators in the unbroken phase. Then, e.g. the β_1 component in Eq. (3.14) can be ignored for the dipole Wilson coefficients in the mass basis but is generated for the down-type dipole after relating the Wilson coefficient in the mass basis to the one in the gauge basis. Since the Wilson coefficient of the up-type dipole is the same in the gauge and in the mass basis, we can ignore this term there.

4 Loop calculation

4.1 Scheme definitions

By performing a simple power counting we can easily verify the expectation that most of the diagrams we encounter, see App. A, are UV divergent. We regularize these by using dimensional regularization and evaluate all loop diagrams in $D = 4 - 2\epsilon$ space-time dimensions performing the limit $\epsilon \to 0$ at the end of the calculation. In this regularization scheme 1-loop UV divergences manifest themselves as simple poles in the expansion for small ϵ and we subtract these poles with appropriate counterterms in the $\overline{\text{MS}}$ scheme. The only exception to this procedure are the scalar tadpoles, loop contributions to the Higgs one-point function, that renormalize the Higgs VEV and are present only in the broken phase of the SMEFT. To deal with this type of diagrams, we chose the tadpole counterterm such that it cancels the tadpole diagrams completely, analogously to what was done in [84]. The result is that no such diagrams have to be calculated and the loop contributions to the Higgs VEV are given by the loops in the physical Higgs 2-point function. In addtion, due to the photon and gluon being massless, we encounter a few IR divergent diagrams. We regularize these by assigning both these bosons an infinitesimally small mass m and keeping only terms that are regular in the limit $m \to 0$.

While dimensional regularization has its well-known advantages, like being a mass-independent regulator and preserving gauge invariance and other symmetries, certain theories have to be treated with special care. The SMEFT is one of these theories, since due to its chiral structure and the presence of CP violating, purely bosonic operators both the fifth Dirac matrix γ_5 as well as the Levi-Civita symbol $\epsilon^{\mu\nu\alpha\beta}$ ($\epsilon^{0123} = +1$) appear explicitly. It is well-known that these two objects are intrinsically defined as four-dimensional and there exists no generally accepted procedure to consistently extend them to D dimension.

Considering first γ_5, there exist various schemes on how to treat γ_5 in $D \neq 4$ space-time dimensions [85] that all have advantages and disadvantages compared to respective other schemes. For simplicity, will use the *naive dimensional regularization* (NDR) scheme [86–88]. In this scheme, the anti-commutation property of γ_5,

$$\{\gamma_\mu, \gamma_5\} = 0 \quad \text{for any } \mu\,, \tag{4.1}$$

is retained for an arbitrary number of space-time dimensions and in particular we use the definition

$$\gamma_5 = -\frac{i}{4!}\epsilon^{\mu\nu\alpha\beta}\gamma_\mu\gamma_\nu\gamma_\alpha\gamma_\beta\,, \tag{4.2}$$

making the connection between γ_5 and the Levi-Civita symbol evident.

This leads to obvious inconsistencies in four dimensions by recalling that for $D = 4$ the relation

$$\mathrm{Tr}\left\{\gamma^\mu\gamma^\nu\gamma^\alpha\gamma^\beta\gamma_5\right\} = 4i\epsilon^{\mu\nu\alpha\beta} \tag{4.3}$$

holds. Because of the appearance of the Levi-Civita symbol we can expect this relation to hold strictly only in $D = 4$ dimensions and in fact, preserving the anti-commutation relation of Eq. (4.1), we find

$$\mathrm{Tr}\left\{\gamma^\mu\gamma^\nu\gamma^\alpha\gamma^\beta\gamma_5\right\} = 0 \tag{4.4}$$

in $D \neq 4$ dimensions, which obviously is not smoothly connected to Eq. (4.3) in the limit $D \to 4$. Nevertheless, we will use this scheme for its simplicity and implementation in various computer programs used for evaluating loop integrals, keeping in mind that the finite terms arising in our calculation depend explicitly on this scheme choice and paying attention to possible inconsistencies that could arise in diagrams including traces with an odd number of γ_5 matrices.

The NDR scheme as we use it in this paper also fixes the treatment of the Levi-Civita symbol in an arbitrary number of space-time dimensions, namely, we treat its properties the usual way, pretending as we would be working in four dimensions. This can lead to possible issues for diagrams containing the CP odd operators from the H^2F^2 and F^3 classes. These would arise mainly from contractions of two or more Levi-Civita symbols, but they can be avoided by performing the loop integral before contracting any of the indices of the Levi-Civita symbol, leaving only four four-dimensional indices to be contracted and hence no source of any inconsistencies remain [53]. In fact, we explicitly checked that for the H^2F^2 operators the result does not change if the indices are contracted from the beginning.

Additional care has to be taken when calculating the contributions of the CP odd F^3 operators to the dipoles, independently of the gauge bosons they are built from. By investigating the respective diagram and performing a power counting we note that its most singular piece is linearly divergent and from the treatment of axial anomalies it is known that such diagrams are not necessarily independent of the choice of momentum routing in the loop. Together with the NDR scheme this leads to the result for e.g. the W^3 operator,

$$\frac{d_\psi}{e} \times \Lambda^2 \supset \frac{3 - A}{32\pi^2}\frac{e\, m_\psi}{s_w}\, C_{\widetilde{W}}. \tag{4.5}$$

Here A is a constant, arbitrary shift of the loop momentum in the convention where the fermion in the loop carries the momentum $q + A\ p_1$, where q is the loop momentum and p_1 the incoming fermion momentum. In this calculation the choice $A = 0$ corresponds to the known result found in the literature [35, 77, 78]. The same dependence on A appears in the rational part of the gluonic diagram if it is calculated in this naive way, while the divergent structure is independent of the loop momentum routing. To circumvent this issue, we proceed as mentioned above and explained in [53] and keep the Levi-Civita symbol external to the loop integral and contract its indices only after evaluating said integral. However, contrary to [53], we extract the $W^+W^-\gamma$ vertex by treating all the legs of the operator $O_{\widetilde{W}}$ to be on-shell and in $D = 4$, such that we can use properties of the the Levi-Civita symbol to simplify the vertex rule. This procedure reproduces the results in [35, 77, 78], where the authors start from a $W^+W^-\gamma$ operator, but does not capture the the contribution of an evanescent operator, see [53].

4.2 Gauge invariance and redundant operators

4.2.1 Gauge invariance and BFM

Being built upon the SM, the SMEFT is imbued with the same gauge symmetry, hence our results respect this gauge invariance as well.

However, it is a long and well known fact of QFT that in order to quantize gauge theories it is necessary to introduce a gauge fixing term to the Lagrangian to cure the issues arising from the integration over all gauge-related field configurations in the path integral. This explicitly breaks gauge invariance leaving the theory invariant under the more general BRST transformations [89–91]. For loop calculations, this implies the necessity of gauge-variant, but BRST-invariant, operator structures to account for all the ones appearing in the loops. Allowing for non-renormalizable operators, the usual gauge fixing procedure makes any calculation more tedious because of the large number of such gauge-variant structures needed that did not appear in the original operator basis and hence have to be removed by using field redefinitions. For a calculation of the dipole renormalization using R_ξ gauges with gauge-variant operators see e.g. [92].

An alternate way to fix the gauge of a gauge theory lies in the background field method (BFM) [93–96], which greatly simplifies the calculation and was used for any calculation performed in this paper. The key point is that all the fields are split into a classical background field as well as a quantum field, where the path integral is performed only over field configurations of the latter. By doing so, gauge invariance for the classical fields can be made manifest, such that only gauge-invariant operators have to be considered, greatly simplifying any calculation and the gauge for the quantum fields can fixed independently off the classical fields. We choose a linear R_ξ gauge and in particular the Feynman gauge ($\xi = 1$) for quantum and unitary gauge ($\xi \to \infty$) for classical fields. We will not go into further detail about the BFM and refer the reader to [93–96] for a more rigorous treatment in general and to [97–99] for the BFM in the context of gauge fixing the SMEFT.

In practice, the classical fields correspond to external fields and tree level propagators while the quantum fields describe fields running in loops and differences to the conven-

tional gauge fixing procedure can arise only in Feynman rules containing both classical and quantum fields. In fact, because we are dealing only with CP odd dimension-6 operators that are not directly affected by gauge fixing, the only modifications we encounter involve only the gauge boson self-interactions, Goldstone-gauge and ghost-gauge vertices within the SM.

4.2.2 Redundant operators and choice of basis

As already mentioned, for loop calculations within effective theories one can also use a complete set of operators which are independent under integration by parts (IBP), but possibly redundant under the SM renormalizable equations of motion (EOMs). By applying the latter, this set should then be reduced to an operator basis; this procedure is related to the fact for theories with non-renormalizable operators there is no unique basis and all different basis choices are related by field redefinitions. In particular, we consider as redundant set the so-called *Green's* basis [50, 51], which is given by all the operators, independent under IBP, which are directly generated by 1PI Green's functions. In such a way one can avoid the calculation of reducible diagrams: they correspond indeed, among all the contributions to the operators in the non-redundant basis, to the ones that arise through field redefinitions. So the procedure is the following:

I. Calculate all the relevant, irreducible loop diagrams (see App. A).

II. Extend the original, non-redundant operator basis to a redundant set as an intermediate step, such that all operator structures from the previous step can be accounted for. As mentioned, we temporarily extend the *Warsaw* basis [49] to the *Green's* basis, both taken to be in phase of broken EW symmetry.

III. Once all operator structures from step I are taken care of, remove the redundant operators by performing the appropriate field redefinitions. This induces shifts of the coefficients of the operators in the non-redundant set as well as those of higher dimensional operators, in terms of the redundant ones, which in turn are fixed by the result of step I. For our purposes, we can neglect the latter, as they would correspond to dimension-8 effects.

Let us note that an alternative to this approach, which avoids the introduction of redundant operators, is to directly compute all reducible diagrams with the desired final states. For our purposes this would correspond to attaching e.g. the 1-loop fermion 2-point function to the tree level dipole vertex. But since we are working in the phase of broken EW symmetry with massive particles a cancellation between the 2-point function and the on-shell propagator connecting the loop to the tree level vertex is not obvious and spurious kinematic divergences appear if not treated with care.

4.2.3 Contributions related by gauge invariance

It is well known that due to gauge invariance certain terms in diagrams with differing numbers of external fields can correspond to the same operator if it contains covariant

derivatives or non-Abelian field strength tensors. This allows us to relate terms in different n-point functions coming from the same gauge-invariant operator through the common corresponding Wilson coefficient.

We will explicitly demonstrate this with a situation appearing during our calculations. Consider the loop contributions to the fermion 2-point function, especially the middle and right diagram in Fig. 8. The left diagram does not matter for the discussion to follow as it is a purely SM diagram, therefore giving contributions only to the fermion wave function and the fermion masses. On the other hand, exchanging one of the SM vertices in this diagram with the electron dipole operator (diagrams on the right) we find that, not only the usual SM structures appear but also one that is proportional to the fermion momentum squared, p^2. Clearly, no operator either within the SM or the Warsaw basis is able to give rise to such a structure, but there is one in the Green's basis and in the phase of broken EW symmetry it has the form

$$O_{D^2} \sim \bar{\psi} D^2 \psi \,, \tag{4.6}$$

where $D^2 = D_\mu D^\mu$ and the covariant derivative is defined as $D_\mu = \partial_\mu + ieQA_\mu$, in which Q is the electromagnetic charge generator. Note that we could have chosen an operator with $\not{D}\not{D}$ instead of D^2, since these are related by

$$\not{D}\not{D} = D^2 + \frac{1}{2} e Q_e \sigma_{\mu\nu} F^{\mu\nu} \,, \tag{4.7}$$

and both operators have the same p^2 matrix element. However, we chose the former, as it is easier to relate it to matrix elements with additional gauge bosons, which will be important shortly. Note also that Eq. (4.7) is a purely algebraic identity, as it uses only the anti-commutation relation of the Dirac matrices and the definition of the field strength tensor as the commutator of two covariant derivatives: the two operators are indeed equivalent even in the Green's basis, since the above relation does not rely on redefitions via EOMs.

In the following, we will use the electron field below the weak scale for illustrative purpose, such that the covariant derivative only contains the photon. The reasoning holds for all of the other gauge bosons in exactly the same way. The coefficient c_{D^2} of the redundant operator is then given by precisely the 1-loop sized term in the 2-point function proportional to p^2 and, as explained above, we now need to find a field redefinition that removes the D^2 operator at the cost of redefining the coefficients of the other operators appearing in our Warsaw basis. To do so we summarize the relavant operators for this little exercise,

$$\mathcal{L} \supset i\bar{e}\not{D}e + \frac{c_{D^2} v}{\sqrt{2}} \bar{e} D^2 e + \frac{c_{e\gamma} v}{\sqrt{2}} \bar{e}\sigma_{\mu\nu} e F^{\mu\nu} \,. \tag{4.8}$$

The appropriate field redefiniton to remove the O_{D^2} operator is

$$e \to e + i \frac{c_{D^2} v}{\sqrt{2}} \not{D} e \tag{4.9}$$

and we find that it also induces a shift of the dipole coefficient

$$c_{e\gamma} \to c_{e\gamma} - \frac{1}{2} c_{D^2}, \tag{4.10}$$

which is straightforward to see by plugging the above field redefinition into Eq. (4.8) and neglecting higher dimensional terms.

Accounting for the p^2 term in the 2-point function concerns only the derivative part in the covariant derivatives of the redundant operator. Therefore, investigating the other terms in the covariant derivatives, by gauge invariance, we expect an operator structure in the $ee\gamma$ vertex function that can not be accounted for by any SM or Warsaw basis operator but instead by the one-photon part of O_{D^2} and is numerically related to the p^2 structure we found above. And we find this exact 1-loop contribution, which serves as another check of our calculations. Taking this reasoning even further, we deduce that there have to be a term in the $ee\gamma\gamma$ 4-point function corresponding to the two-photon part of O_{D^2}, whose coefficient we can predict by gauge invariance from the ones in the 2- or 3-point function, but we have not performed this check explicitly.

A similar situation could appear when calculating terms in C_{Hud} proportional to the dipole operators, where one needs the following operators from the Green's basis, here expressed in the unbroken phase,

$$O_{D^2}^{(2)} = \left(\bar{\psi}_L D_\mu \psi_R\right) D^\mu H \,, \tag{4.11}$$

$$O_{D^2}^{(3)} = \left(\bar{\psi}_L i\sigma_{\mu\nu} D^\mu \psi_R\right) D^\nu H \,, \tag{4.12}$$

$$O_{D^3} = \frac{i}{2}\bar{\psi}_L \{D_\mu D^\mu, \not{D}\}\psi_L \,. \tag{4.13}$$

We refer to [51] for the coefficients in Warsaw basis in terms of the ones in the Green's basis. However, in the considered case, only the contributions from the redundant operators in Eq. (4.11) turn out to be non-vanishing and non-quadratic in the light quark Yukawa couplings.

4.3 Additional cross-checks

Before moving on to the results of our calculations we want to briefly comment on all the checks performed that give us confidence in their correctness. During the course of arriving at the final results we checked various different aspects of our results.

First of all we used two different computer programs, the two Mathematica packages Package-X [100] and the FeynRules/FeynArts/FormCalc [101–103] pipeline, finding the same results in both cases. We use the former to obtain explicit analytic expressions of the Passarino-Veltman (PV) loop integrals.

Further, although Feynman gauge is used for the quantum fields in our calculations we explicitly checked gauge invariance by leaving the gauge parameter ξ generic in various subsets of diagrams and confirming analytically that every dependence on ξ drops out. Further, as illustrated in the last section, we used the cancellation of various divergences related by gauge symmetry by the same redundant operator as a further check related to gauge invariance.

By performing a full 1-loop calculation we automatically rederived the RGEs in both the SMEFT [54–56] and LEFT [52, 57] and we explicitly verified that our RGEs coincide with the ones in the literature, after performing the respective weak rotations in the case of the SMEFT RGEs.

Finally, the full calculation of all diagrams was performed with two independent implementations, again yielding the same result.

All these aspects collectively give us the confidence to believe that the results presented here are correct and can be reproduced if the the same regularization and schemes are employed.

5 Results and bounds

Now that we have established all the technical details of our calculation, we will present the results and bounds derived from them in this section. Because the full expressions for all the EDMs are quite long we will not report them here but instead refer the reader to App. B. The results shown there are taken to be at leading order in the external m/v, where m is the mass of the external fermion. While this is a good approximation even for the third-generation leptons, this is not applicable for the third generation quarks. Further, due to the sheer amount of Wilson coefficients appearing we also do not present all the bounds we obtained here, rather we quote them in App. D. Nevertheless, we will discuss the most interesting points in the following. In particular one of the main focuses in this work lies on the inclusion of finite terms, so we are also interested in quantifying the impact these terms have on the final result. To extract the bounds on various Wilson coefficients from any of the experimental EDM bounds, we neglect the SM contributions, that are many orders of magnitude smaller than the experimental constraints, and turn on only one coefficient at a time, rescaling them by the appropriate combination of SM couplings, reflecting the naturally expected to be carried by the corresponding coefficient, see also Table 3. Using this factorization, we expect, in most of the BSM theories, order one rescaled Wilson coefficients, if the parameters of the UV completion have natural $O(1)$ size. For the new physics scale we assume $\Lambda = 5$ TeV. Furthermore, we will also set lower bounds on the new physics scale Λ, assuming that the Wilson coefficients have the naturally expected size; we will see that EDMs push Λ to be very large, of the order of 10^3 TeV.

5.1 Non-rational functions

In this section we want to discuss the presence, in the EDMs expressions, of *finite* but *non-rational* terms, where finite contributions are meant to be the ones that do not contain a logarithmic function of the SMEFT cut-off Λ. Thus, these terms cannot be directly derived from the RGE of the Wilson coefficients in the unbroken phase of the SMEFT and, as we will explain here, they are intrinsically related to the multi-scale nature of the SM in the phase of broken EW symmetry.

We see that in App. B, in particular in Eqs. (B.3) and (B.8a)-(B.8c), non-rational functions on only SM scales appear. For such functions to appear at least two massive particles have to take part in one Feynman diagram and because we are working at leading order in m/v, this effectively means that at least two particles with masses of the order of the electroweak scale need to be present. In fact, the equations that we are discussing are the only places in which multiple heavy scales can arise and even though the analytic

$$C_{\underset{ii}{\psi B}} \to (y_\psi)_{ii}\, g'\; C_{\underset{ii}{\psi B}}$$

$$C_{\underset{ii}{\psi W}} \to (y_\psi)_{ii}\, g\; C_{\underset{ii}{\psi W}}$$

$$C_{\underset{ii}{qG}} \to (y_q)_{ii}\, g_s\; C_{\underset{ii}{qG}}$$

$$C_{\underset{ii}{qH}} \to (y_q)_{ii}\; C_{\underset{ii}{qH}}$$

$$C^{(3)}_{\underset{iijj}{lequ}} \to (y_\ell)_{ii}\,(y_u)_{jj}\; C^{(3)}_{\underset{iijj}{lequ}}$$

$$C^{(1,8)}_{\underset{ijji}{quqd}} \to (y_d)_{ii}\,(y_u)_{jj}\; C^{(1,8)}_{\underset{ijji}{quqd}}$$

$$C_{H\widetilde{B}} \to g'^2\; C_{H\widetilde{B}}$$

$$C_{H\widetilde{W}} \to g^2\; C_{H\widetilde{W}}$$

$$C_{HW\widetilde{B}} \to g g'\; C_{HW\widetilde{B}}$$

$$C_{H\widetilde{G}} \to g_s^2\; C_{H\widetilde{G}}$$

$$\mathcal{C} \equiv \left\{C_{Hud}, C^{(1,8)}_{ud}, C^{(1,8)}_{qu}, C^{(1,8)}_{qd}, C_{le}\right\} \to g'^2\; \mathcal{C}$$

Table 3: Rescalings of the Wilson coefficients performed throughout this work to reflect the natural size we expect them to carry. We assume the operators which are built from vector currents and therefore do not involve a chirality flip to be generated by a heavy vector boson exchange and choose the SM $U(1)_Y$ gauge coupling as a representative.

form of these functions looks very different in (B.3) and (B.8a)-(B.8c) have a very similar origin.

To illustrate this, let us first focus on Eq. (B.3), specifically the arctan functions. By looking closely at these expressions it is not too hard to reconstruct the origin. They come from loop corrections to the scalar 2-point functions, hence the two heavy scales involved in this amplitude are the external Higgs mass and m_i, with m_i any of the W, Z or top mass from the particles in the loop. As is well-known, this kind of diagrams exhibit a branch cut in the complex s plane starting at $(2\,m_i)^2$, corresponding to the production of a 2-particle state with arbitrary momenta. Then, by setting the external fields to be on-shell and rewriting the complex logarithms appearing in the analytic expression of the discontinuity across this branch cut, we arrive at the arctan functions appearing in (B.3).

The non-rational terms in the contributions of the H^2F^2 operators are a bit more involved as they are 4- instead of 2-point functions with three internal propagators. After the PV decomposition of the loop integrals again two-propagator bubble integrals are generated with branch cuts, corresponding to either the production of a lepton-Z or lepton-Higgs system, plus additional non-rational functions from three-propagator triangle integrals. Then, keeping leading terms in m/v only the logarithms of ratios of heavy scales survive. And even though they are not related to the divergences of the diagram they are not completely disconnected from the RG running. In fact, they can be interpreted as the part of the running between the Higgs and the Z boson, that could also be obtained after integrating out only the Higgs boson.

5.2 Lepton EDMs

We will start by investigating the lepton EDMs, where less operators appear, compared to the neutron case. In the following, we illustrate the impact of different terms in the contributions to EDMs coming from various class of operators. For the H^2F^2 class, we

illustrate the impact of finite terms, showing, in the upper panel of Fig. 4, the relative change when using only the RGE versus the full 1-loop result. For illustrative purposes we use the electron EDM, and while the numerics change due to differing masses, the overall pattern is the same for the other lepton flavors.

In fact, these, together with the dipole operators themselves, are the only operators that give both RGE and finite contributions, while operators of the ψ^4 class give vanishing rational terms and both the F^3 and $\psi^2\bar{\psi}^2$ class operators enter only through purely rational terms. We want to note that, on the other hand, for the dipole operators finite terms play a negligible role affecting the result by $\lesssim 1\%$, but this is simply because they enter the EDMs also at tree level, completely dominating over corrections to higher order terms. This is why, in this case, we do not show the impact of the 1-loop finite terms but rather of the full 1-loop result compared to the tree level term for these operators only, in Fig. 4. We see that these higher order effects add to the destructively to the tree level piece, therefore actually lowering the bound on the scale Λ.

On the contrary, for the H^2F^2 class operators any tree level contribution is obviously absent, which presents a great opportunity to study the size of finite terms. Indeed, we find that the finite terms change the bound by $\sim 10-20\%$, however, due to positive relative signs they interfere constructively and consequently increase the bound compared to when using the RG running only. By looking at the corresponding expression we can also easily explain why the effects of the two operators with only one kind of gauge field appearing are very similar but on the other hand quite different from the mixed one. The operators $O_{H\widetilde{B}}$ and $O_{H\widetilde{W}}$ do only get contributions from the photon and Z components of the weak bosons, meaning apart from numerical prefactors coming from different couplings they give the same contributions. On top of that the mixed operator, $O_{HW\widetilde{B}}$, also receives contributions from its W component and it turns out that this piece has the opposite sign of the neutral ones, again reducing the total impact on the lepton EDMs.

Of course, these statements are depend on the scale Λ, as this changes the energy regime that needs to be swept by the RGE logs. This implies that for new physics sectors well above the TeV the finite terms will be completely subdominant compared to the huge logarithms appearing. On the other hand, the closer the new sector lies to EW scale the smaller the logs and therefore finite terms can have an increasingly big effect. We illustrate this in the lower panel of Fig. 4, where we show the dependence on Λ of the relative shift in the electron EDM for the H^2F^2-class operators. We see that, due to the slow logarithmic growth, the effect of finite terms does not deteriorate tremendously for e.g. $\Lambda \sim 10$ TeV, while it almost doubles for Λ approaching ~ 1 TeV.

Finally, let us briefly discuss the bounds on the Wilson coefficients from the electron, muon and tau EDM, summarized in Fig. 5 and computed assuming $\Lambda = 5$ TeV and applying the rescalings shown in Table 3. Here we show the full tree plus loop level result, i.e. including both the RG running and finite terms; in the case of the electron EDM the prospected future bounds are shown as well. Note that for the 4-fermion operators, we chose to show only the component with the most stringent bound for each of the operators. The bounds on other components can easily be obtained from the ones shown in Fig. 5 by rescaling them with the appropriate ratio of fermion masses. The most obvious conclusion

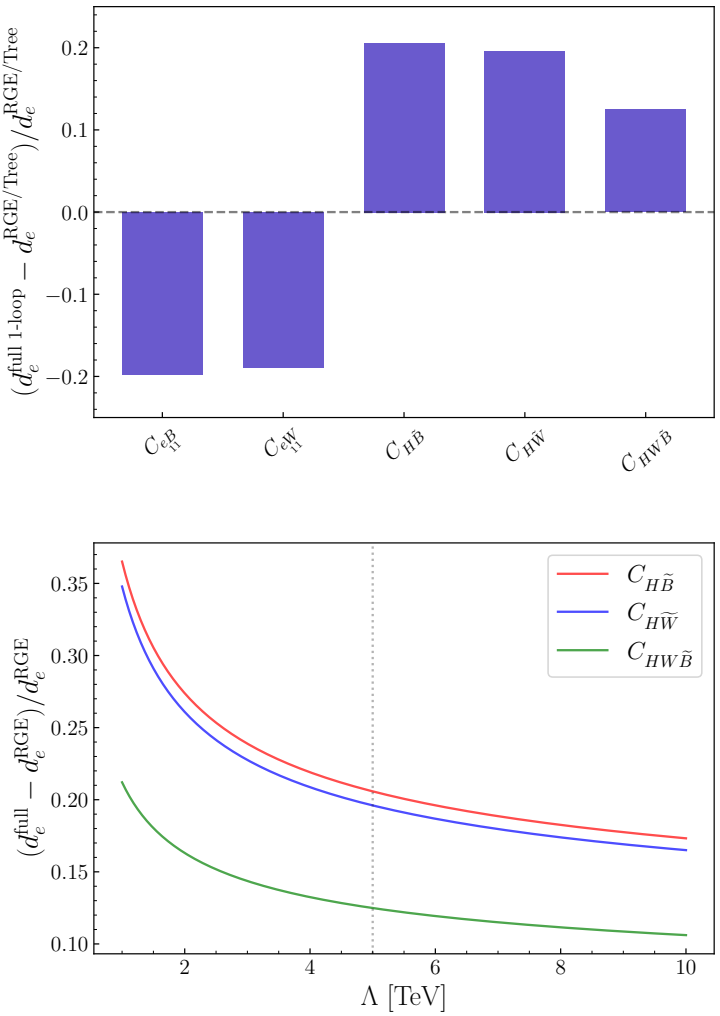

Figure 4: *Upper panel:* Relative change of the electron EDM when using the full 1-loop result compared to only the RG running (H^2F^2 operators) and impact of the full 1-loop effects compared to the tree level term ($F\psi^2H$ operators). *Lower panel:* Dependence of the relative shift in the EDMs as a function of the scale Λ. Here the dotted line shows the benchmark value of $\Lambda = 5$ TeV used in this paper.

that can be drawn from this figure, by comparing the upper panel with the lower one (and with the values in Table 4) is that the supreme precision of the eEDM measurement gives by far the most stringent bounds from any of the lepton flavors. One can notice that, for $\Lambda = 5$ TeV, the constraints from the electron EDM can set bounds of order 10^{-5} on the Wilson coefficients of operators with fermions and of $10^{-3} \div 10^{-2}$ in the case of purely bosonic operators. These bounds will further improve of one or two orders of magnitude at ACME III.

Nevertheless, we can make another interesting observation. Even though the experimental sensitivity to the muon EDM is roughly one order of magnitude higher than for the

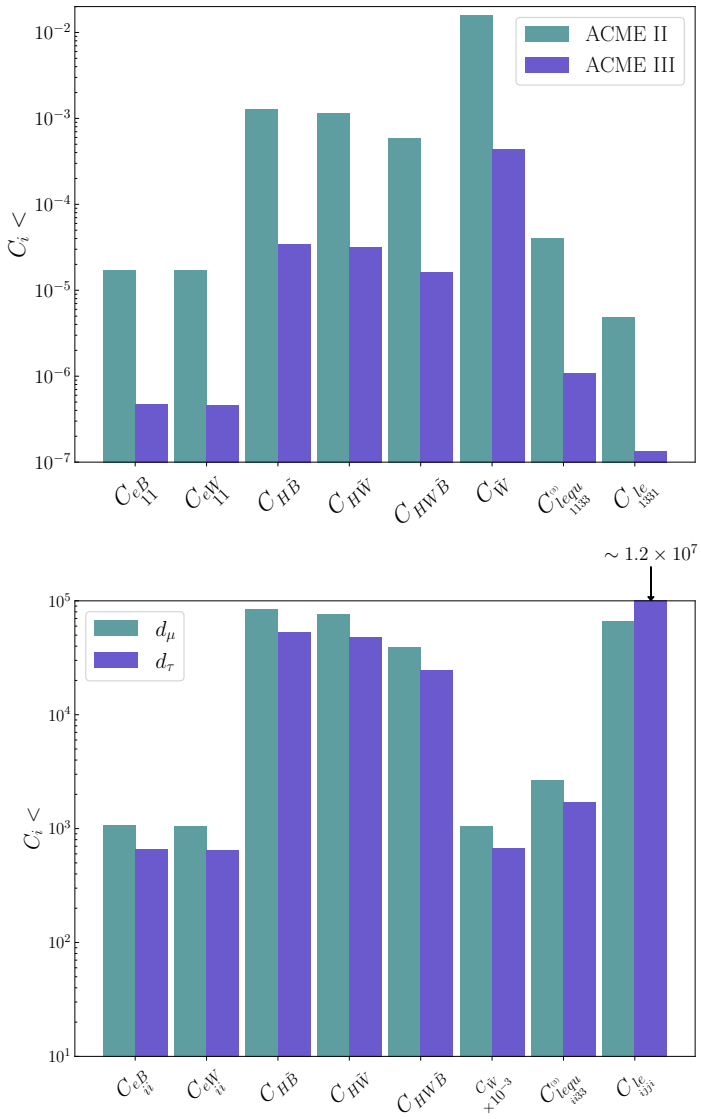

Figure 5: Upper bounds on the Wilson coefficients, assuming $\Lambda = 5$ TeV and applying the rescalings shown in Table 3, obtained including the full 1-loop expressions, from the experimental bounds on the different lepton EDMs. *Upper panel:* The current constraints (ACME II) coming from the best bounds on the electron EDM, compared to the ones from the projected future bounds (ACME III). *Lower panel:* We compare the bounds from the two heavy lepton flavors with each other. Here $i = 2(3)$ stands for the muon (tau) EDM and j denotes the heavier of the two lepton flavors different from i in the operator O_{le}.

tau EDM, it still happens to be the case that the tau lepton is slightly more constraining than its lighter cousin. Speaking of the different masses of these leptons, this is exactly the reason why this happens. For every operator the contribution is proportional to the lepton Yukawa, either through our rescaling of the Wilson coefficients to their natural size

or because the contribution itself is directly proportional to the lepton mass. So it turns out that with the current sensitivites the mass difference between the muon and tau lepton barely overcompensates the lower experimental reach for the latter such that the tau EDM is indeed more constraining than its muonic counterpart. This argument, however, does not hold for the operator O_{le}. For this operator we see the inverted situation, where the tau EDM is less constraining that the muon EDM. But this is readily explained by closer examining the corresponding expression in Eq. (B.11). Here we see that it is in fact not proportional to mass of the external lepton but of the lepton inside the loop instead. Because we chose the most constraining component of each Wilson coefficient, this mass is the tau mass for the muon EDM and vice versa, such that the reasoning here is exactly inverted with respect to all the other operators and on top of the weaker experimental bound, the constraint from the tau EDM is further suppressed by the muon mass, contrary to the tau mass in the muon EDM. From this point of view, the phenomenal constraining power of the electron EDM is even more impressive, as the mass gap between the electron mass and the other lepton masses spans multiple orders of magnitude, but still the electron bounds by far overshadow the other ones.

As mentioned before, we also set lower bounds on the new physics scale Λ, assuming that the Wilson coefficients have values corresponding to the natural size indicated in Table 3. Turning on one operator at a time, the strongest constraints come from the dipole and the $O^{(3)}_{\substack{lequ \\ 1133}}$ and $O_{\substack{le \\ 1331}}$ contributions and are of the order of 10^3 TeV.

5.3 Neutron EDM

We proceed with the neutron EDM which is composed of the (chromo-)EDMs of the quarks and gluons as well as the operators $O_{\substack{Hud \\ 11}}$ and $O^{(1,8)}_{\substack{quqd \\ 1111}}$ which can be matched to operators which have a non-vanishing matrix element on the neutron EDM. There are several differences with respect to the lepton EDMs as we can now have cancellations between the 1-loop contributions of the EDMs and chromo-EDMs of the light quarks, more flavor components of the Wilson coefficients are contributing to the dipole amplitudes (this is all the more true in the gauge basis, due to the non-trivial rotation between gauge and mass basis, see Sec. 3.3) and in general more operators due to the presence of QCD degrees of freedom. We show a selection of bounds in Fig. 6 where we have also included a conservative estimate of the influence of the uncertainties in the determination of the matrix elements of all contributing effective operators in the expression of the neutron EDM and a projection for the expected accuracy of the n2EDM experiment [7]. The full set of bounds can be found in App.s D.2.1 and D.2.2.

Starting with the dipole operators, in addition to the electroweak dipole operators also the gluonic dipole operators contribute to the neutron EDM. There, the effects of including finite terms are much larger than for the electroweak dipoles. This is due to the large rational terms in the wave function renormalization of the gluon. In addition, we can also probe more flavor components of the dipole operators through the appearance of the strange quark dipole in the neutron EDM as well as the appearance of all flavor components of the quark dipole Wilson coefficients in the 3-gluon 1-loop amplitudes. The bounds on

these flavor components are suppressed with respect to the dominant up and down quark chromo-dipole operators, since the matrix elements in the expression for the neutron EDM are smaller and some of the flavor elements only enter through loop corrections. Note also, that the contribution of the dipole operators through effective operators other than dipole operators in the expression of the neutron EDM is negligible, since these contributions are suppressed by the much smaller matrix elements of the effective operators and the common loop factor that all dipole contributions receive that are sourced by these additional effective operators. One exception to this is the contribution through the Weinberg operator as those loop contributions are enhanced by an inverse quark mass. This can be seen in particular in the bounds on the coefficients in the spurionic expansion of the different flavor symmetries as we will see later.

For the H^2F^2 type operators we also have to differentiate between the operators with field strengths of electroweak and strong gauge bosons. The bounds on the electroweak operators are less stringent, by around three orders of magnitude, than the ones obtained from the electron EDM, as is expected due to the experimental bound on the neutron EDM being so much weaker. Interestingly, for all three electroweak operators there is a

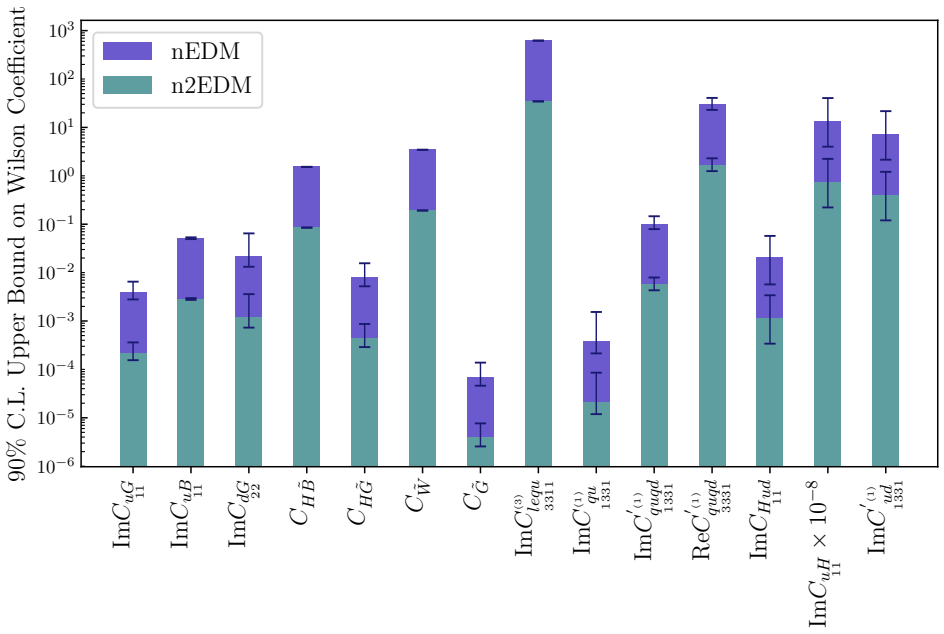

Figure 6: Selected upper bounds on the Wilson coefficients, assuming $\Lambda = 5$ TeV and applying the rescalings shown in Table 3, obtained including the full 1-loop expressions, from the experimental bounds on the neutron EDM. In addition to the bounds from the central values, we also show the influence of the uncertainties in the determination of the chromo-dipole and Weinberg operator matrix elements. We also show bounds on the Wilson coefficients for the projected accuracy of the n2EDM experiment. Notice that the last two Wilson coefficients are in the up-quark gauge basis, while the others in the mass basis.

constructive interference between the terms from the different quark EDMs, enhancing the contribution to the neutron EDM, together with the enhancement from the quark Yukawas with respect to the electron case. Therefore with an experimental bound on the neutron EDM with the same constraining power as the current electron EDM sensitivity, the bounds on the Wilson coefficients would actually be stronger than those obtained from the electron EDM. The neutron EDM receives, through the quark chromo-EDMs, contributions also from the gluonic H^2G^2 operator. Such terms are additionally enhanced by the strong coupling and for this reason the bound on the corresponding Wilson coefficient is stronger than the constraints obtained for the Wilson coefficients of the electroweak bosonic operators by more than two orders of magnitude, as shown in Fig. 6.

For the 4-fermion operators we have the same situation as for the lepton EDMs, only now there are more operators including quarks contributing to the EDM. As for the lepton EDMs, the 4-fermion operators either enter only via RG running or only via rational terms to the dominant contributions that are given by the (chromo-)dipole operators. They can also enter directly with a small hadronic matrix element in the neutron EDM. What is interesting for these 4-fermion operators made from quarks is that the change of basis from the gauge to the mass basis is non-trivial, as discussed in Sec. 3.3. Starting, for example, from an up- or down-quark gauge basis, in the rotation to the mass basis a CKM matrix appears for the down or up component of the operators, respectively. As mentioned above, whenever we use expressions in terms of Wilson coefficients in the gauge basis, we choose the up-basis since more operators with up quarks appear in the final expression of the neutron EDM. In fact, with this choice, a larger number of operators is left unchanged by the basis transformation; for example, this is the case for the $O^{(3)}_{lequ}$ operator already considered in the previous section in the discussion of the lepton EDMs. However, since both the up and down type dipole appear in the neutron EDM it is inevitable that CKM matrix elements appear somewhere. Since the CKM matrix contains a CP violating phase this also enables us to probe the real part of some of the Wilson coefficients in the gauge basis, in particular of some of the flavor off-diagonal ones (see the rightmost column in Fig. 6). In fact, these real parts contribute to the imaginary parts of the Wilson coefficients in the mass basis, that enter the EDMs expressions. Those constraints are of the same order as the bounds on the corresponding imaginary parts, since the imaginary part of the very off-diagonal part of the CKM matrix is of the same order as its real part.

Another interesting contribution appears through the Weinberg operator. Unlike $O_{\tilde{W}}$, it can also contribute with RG running and in addition to its appearance through the quark chromo-dipoles, it also enters directly in the expression of the neutron EDM, interpreted as the chromo-dipole of the gluon. As can be seen in the analytical expressions of the dipoles in combination with how they enter in the neutron EDM, the interference between the different chromo-EDMs is constructive and all effects proportional to the Weinberg Wilson coefficient add up to the comparably strong bound. This, together with the strong coupling enhancement for this contributions, leads to the most stringent among the constraints imposed by the neutron EDM experimental bound, being of order 10^{-4} for $\Lambda = 5$ TeV and for a $C_{\tilde{G}}$ rescaled as in Table 3. In addition, there are large finite terms in the self 1-loop contributions of the Weinberg operator which give corrections of $\sim 45\%$ with respect to

only including RG running at the considered scale.

Furthermore, there can be direct contributions of the 4-fermion operators $O_{quqd}^{(1,8)}$ which are however largely suppressed by their small matrix element in the neutron EDM. This leads to an interesting interference where loop suppressed contributions of these 4-fermion operators to the dipole operators, which are further suppressed by small Yukawa couplings, are of the same order as the direct tree level contributions of those operators (see App.B and Eq. (2.11)). The dipole contributions to those 4-fermion operators are suppressed by small matrix elements and loop factors as discussed before.

Finally, there is a small direct contribution to the neutron EDM of the operator O_{Hud} which also contributes with a finite term to the dipole operators. As can be seen in Fig. 6, the Wilson coefficient of this operators gets a significant bound from the neutron EDM mostly due to the tree level contribution to the neutron EDM. The Yukawa-like operators $O_{uH,dH}$ which appear in the 1-loop contribution to this operator on the other hand are largely suppressed by a loop-factor and small Yukawas and therefore only get bounds beyond the perturbative unitarity limit. As mentioned previously, the dipole contributions which also enter in this 1-loop expression are negligible when compared to the dominant direct contributions to the neutron EDM. Lastly, there is another 4-fermion operator which enters in the 1-loop expression of the operator O_{Hud}, $O_{ud}^{(1,8)}$, which also only receives a bound around the perturbative unitarity limit.

We also show in Fig. 6 the error bars associated to the 50% uncertainties of the matrix elements of the quark and gluon chromo-EDMs. Wherever the Wilson coefficients of the chromo-dipole operators enter at tree level, the uncertainties translate direcly to the bound. In the case of the electroweak operators, which can only enter at loop level in the chromo-EDMs, the dependence on the uncertainties is much smaller.

Furthermore, we also estimate the bounds on all Wilson coefficients with the projected experimental bound of the n2EDM experiment [7]. With the projected experimental bound of $\sim 10^{-27} e$ cm, we expect an improvement of about one order of magnitude for all Wilson coefficients.

As mentioned before, see Sec. 3.4, it is also interesting to consider the expression of the neutron EDM under flavor symmetries relating the different flavor components that appear in the neutron EDM with some minimal assumptions (for the notation we refer to App. C). The bounds on the coefficients in the spurionic expansion of the Wilson coefficients, as discussed above, can be found in Fig. 7 (notice that this expansion is performed for the Wilson coefficients in the up-quark gauge basis). The key feature of the different flavor symmetric scenarios, namely the correlation among components of flavor tensors, leads to the combination in a single bound of various contributions, that would have been separated for a generic flavor structure. Then, the constraints on flavor blind coefficients of the spurionic expansion are dominated by the strongest among the bounds on the various flavor components. For example, the up-quark dipole receives contributions from all the $\mathrm{Im}[C_{lequ}^{(3)}]_{ii11}$ components, which, if taken as independent among each others, have very different constraints: $\mathrm{Im}[C_{lequ}^{(3)}]_{1111} < 7.54 \cdot 10^9 \lambda_e \lambda_u$ and $\mathrm{Im}[C_{lequ}^{(3)}]_{3311} < 6.21 \cdot 10^2 \lambda_\tau \lambda_u$, where the λs are entries of the diagonalized Yukawa matrices. On the other hand, if

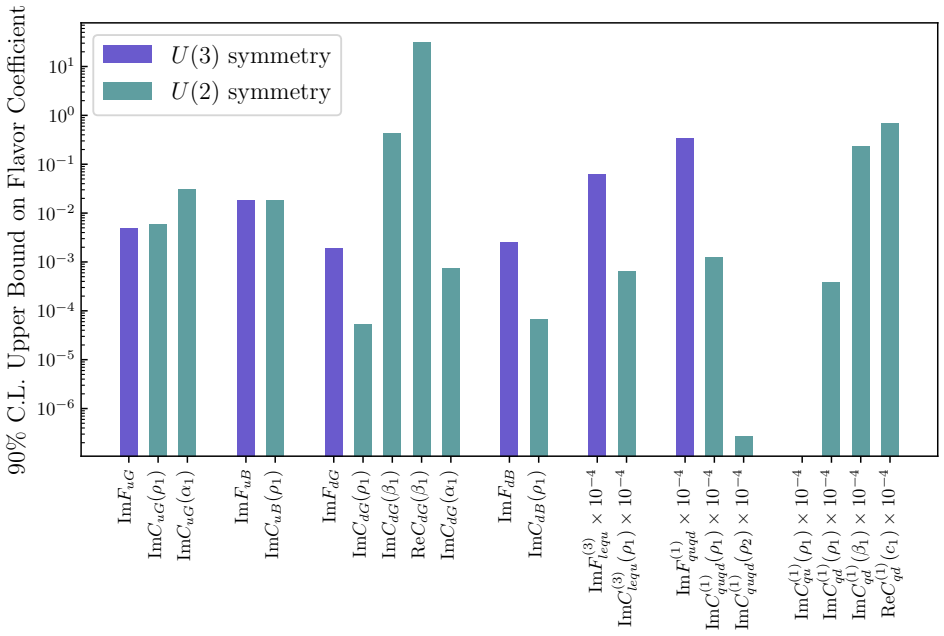

Figure 7: Selected bounds on coefficients in spurionic expansion assuming the different flavor symmetries and for $\Lambda = 5$ TeV.

a $U(3)^5$ flavor symmetry is imposed, exactly the same Yukawa dependence as above is assigned to each component, but with a unique coefficient in front, whose bound reads $\mathrm{Im}F^{(3)}_{lequ} < 6.19 \cdot 10^2$: it is of the same order, but even slightly stronger, as the previous bound on the τ matrix element, which was the most severe. Similarly, the limit on the down-type flavor coefficients is particularly interesting because it combines the contributions of the down and strange quark dipoles into one bound. In addition, the $U(2)$ flavor symmetry disentangles the contributions from the third and first two generations which is visible in the bounds on $\mathrm{Im}C_{uG}(\rho_1)$ and $\mathrm{Im}C_{uG}(\alpha_1)$, where the α_1 component only receives contributions from the contributions of the top dipole operator to the three-gluon amplitude and, thus, has weaker constraints.

Most of the bounds on the flavor coefficients of the 4-fermion operators are just around or beyond the perturbative unitarity limit, still allowing the flavor symmetries as a valid symmetry of UV physics, but not setting any significant constraint on the parameter space. As for the dipole operators, the difference between the $U(2)$ and $U(3)$ flavor symmetry is apparent in the expansion of the Wilson coefficient $C^{(3)}_{lequ}$. In the $U(3)$ spurionic expansion all lepton flavors contribute in the loop but they are all suppressed with the respective small lepton Yukawa. For the $U(2)$ symmetry on the other hand, only the third generation of the leptons is allowed at the considered accuracy. However, since the third generation is excluded from the flavor group, it is completely unsuppressed apart from the small up-quark Yukawa that is also present in the $U(3)$ spurionic expansion.

What is also worth noting are the Wilson coefficients $C^{(1)}_{qu,qd}$ which are completely forbidden by the $U(3)$ flavor symmetry at the considered order. Some elements of the

flavor tensor are allowed in the $U(2)$ expansion, giving however fairly lose bounds. As we saw earlier in the discussion of the neutron bounds without flavor symmetries, we can also probe the real parts of flavor coefficient, if other phases are present. This is the case here, where the CKM phase can also appear through the V_q spurion in the expansion of these Wilson coefficients.

One should notice that, in the $U(2)$ case, the different independent terms in the spurionic expansion of a certain Wilson coefficient have to be of the same order, in order to allow the parameters $\rho_{1,2}$, α_1, β_1 and c_1 (see App. C) to be of order 1, such that the flavor symmetry breaking pattern is respected. However, as we can see from Table 14, this is usually not the case.

Importantly, we notice that, assuming the Wilson coefficients are of the natural size shown in Table 3, the experimental constraint on the neutron EDM sets a lower bound on the new physics scale of order 10^3 TeV, coming from the Weinberg operator G^3 contributions. All the bounds imposed when any of the other operators is instead turned on are at least one order of magnitude weaker.

6 Conclusions

In this paper, we perform the analysis at 1-loop level of the lepton and neutron electric dipole moments, using the model independent EFT approach. We provide, at this accuracy, the complete expressions of these CP violating low energy observables as a function of the dimension-6 SMEFT Wilson coefficients in the Warsaw basis, including the RG running effects as well as finite terms. The latter play a fundamental role in the cases of operators that do not renormalize the dipoles, but there are also classes of operators for which they provide an important fraction, $10 - 20\%$, of the total 1-loop contribution, if the NP scale is around $\Lambda = 5$ TeV. In presenting these results, we also discuss the various loop contributions to the EDMs under the light of selection rules, based on helicity, angular momentum and CP arguments.

Furthermore, we compute the full set of bounds that the current and prospected experimental constraints impose on the Wilson coefficients, with one single operator turned on at a time, for a fixed SMEFT cut-off scale. On the other hand, we provide also the lower bounds on the scale of new physics, obtained assuming that the Wilson coefficients values are given by the natural sizes that we expect them to carry. The analysis of the neutron EDM is performed both in scenarios with generic flavor structure and in presence of $U(3)^5$ and $U(2)^5$ flavor symmetries for the SMEFT. One can see that EDMs provide a very powerful probe for deviations from the SM, since the computed bounds are very strong and can push the scale of new physics above 10^3 TeV, with the mentioned natural values for the Wilson coefficients. This means that any UV completion of the SM, for which the operators responsible for these strong bounds are generated, should accidentally have a very suppressed CP violation, similar to the SM one, unless some fine-tuning mechanism is present.

Acknowledgments

The authors thank Emanuele Mereghetti for helpful exchanges and discussions. E.V. would like to thank Pietro Baratella for useful discussions and comments on the draft. This work has been partially funded by the Deutsche Forschungs-gemeinschaft (DFG, German Research Foundation) under Germany's Excellence Strategy- EXC-2094 - 390783311, by the Collaborative Research Center SFB1258, and the BMBF grant 05H18WOCA1. We warmly thank the Munich Institute for Astro- and Particle Physics (MIAPP) for hospitality, which is also funded under Germany's Excellence Strategy - EXC-2094 - 390783311.

A Relevant diagrams

In this appendix we present all the relevant diagrams needed to calculate all the 1-loop contributions to the (c)EDMs. Since the diagrams contributing to the EDMs are the same for any fermion species and flavor we collectively denote them as f. Additionally, because of possible W bosons in the loop the fermion running in the loop is not necessarily of the same flavor as the external ones, hence they are denoted by f'

In all diagrams the black dot denotes the insertion of any of the dimension-6 operators possible at any given position. Since we are performing all calculations in the phase of broken EW symmetry we denote Higgs fields that are set to their VEV by scalar legs ending in a cross.

Notice that we do not show diagrams that could in principle contribute but vanish due to scaleless integrals or antisymmetry. Additionally, we do not show diagrams of 3-point functions with only scalars in the loop, as these would contribute only at higher orders in the fermion masses.

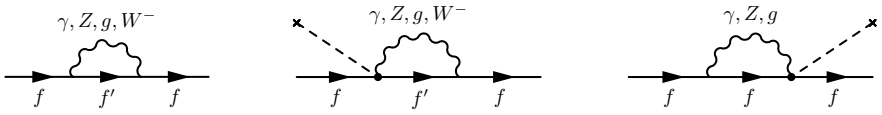

Figure 8: Diagrams contributing to the fermion 2-point function.

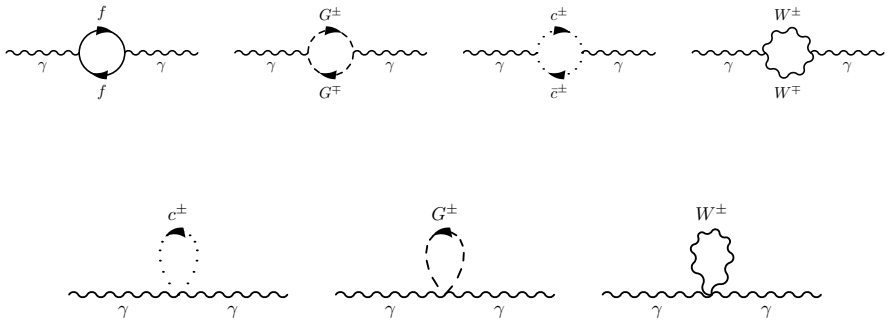

Figure 9: Diagrams contributing to the photon 2-point function.

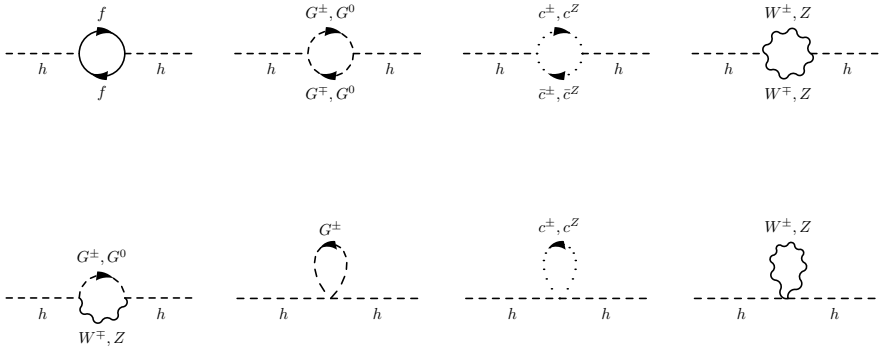

Figure 10: Diagrams contributing to the Higgs 2-point function.

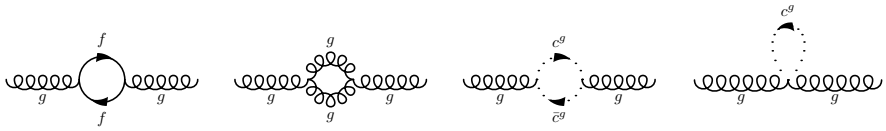

Figure 11: Diagrams contributing to the gluon 2-point function.

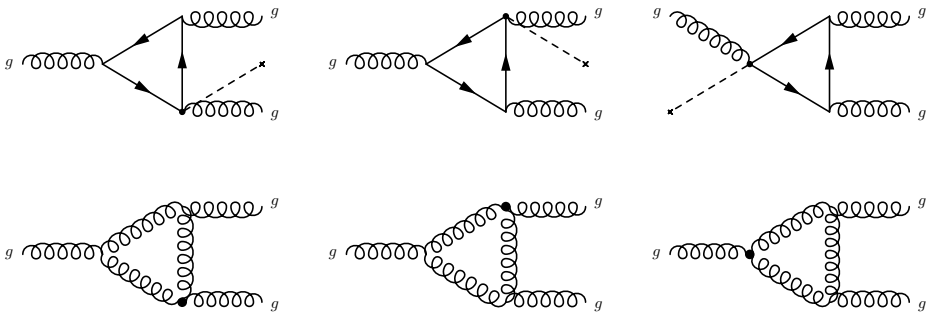

Figure 12: 1PI diagrams contributing to the ggg 3-point function. Of course, there are also diagrams with only two propagators for both the insertion of the Weinberg and the dipole operator, but we find that these vanish, so we do not display them here. We also do not show diagrams with the external gluons attached to an SM vertex crossed.

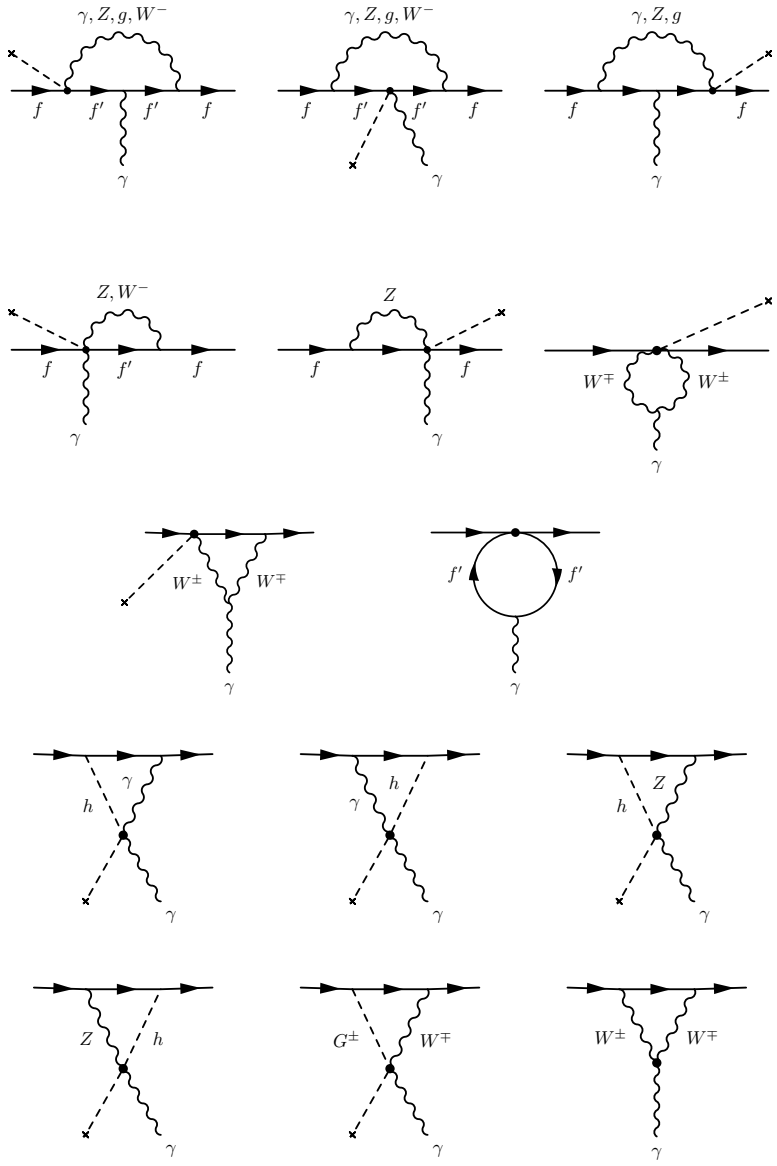

Figure 13: 1PI diagrams contributing to the $\bar{\psi}\psi\gamma$ 3-point function. Notice that the diagram with the lepton loop exists only for external up-type quarks and leptons.

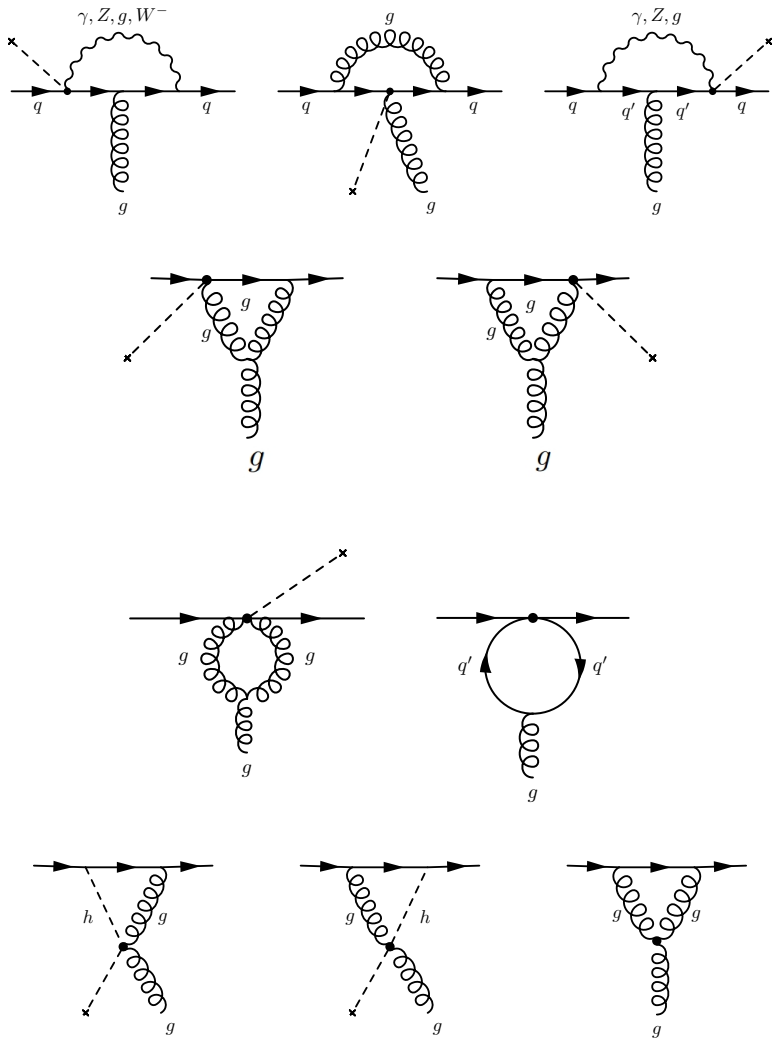

Figure 14: 1PI diagrams contributing to the $\bar{q}qg$ 3-point function.

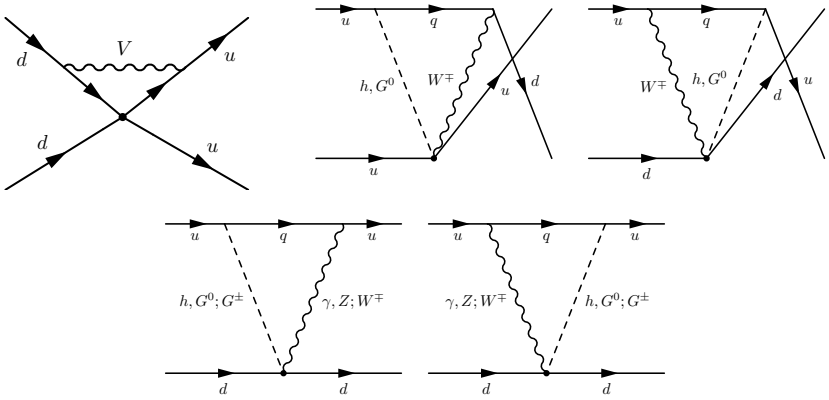

Figure 15: 1PI diagrams contributing to the *udud* 4-point function. For diagrams contributing to the self-renormalization, we show only one representative diagram, all the others can be obtained by connecting all possible pairs of external fermions with the internal vector. The other diagrams show the contribution of the down-type dipole operators. The corresponding up-dipole diagrams can be obtained by just exchanging up and down quarks.

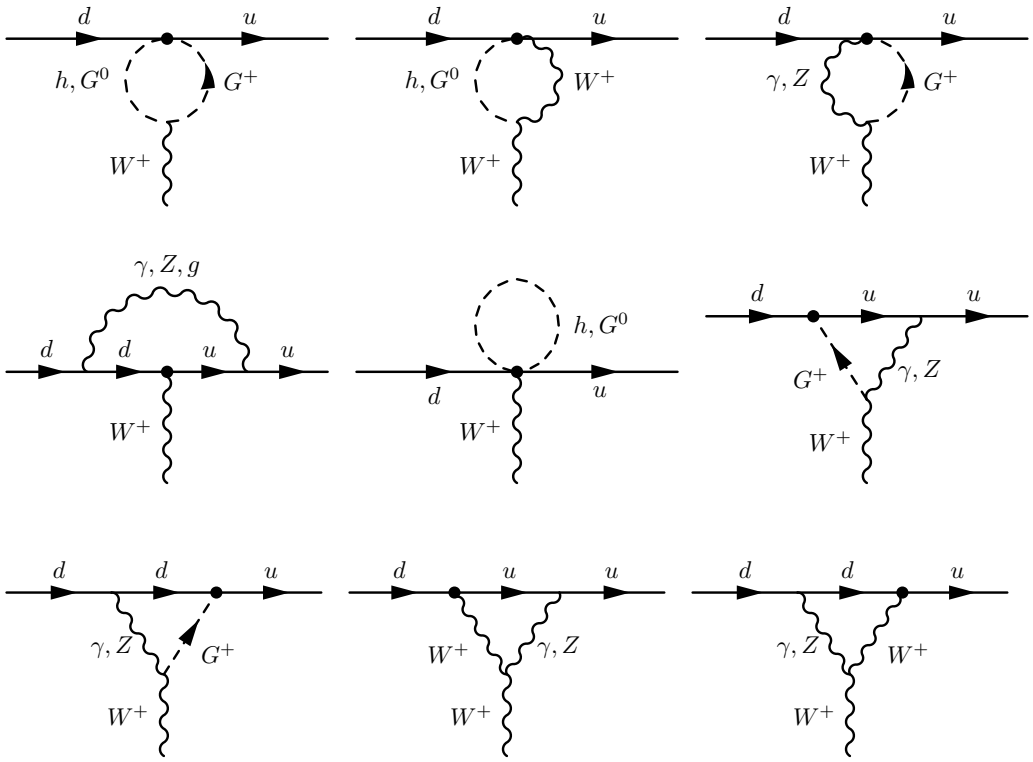

Figure 16: 1PI diagrams contributing to the udW^+ 4-point function which were used to calculate the self-renormalization of O_{Hud}.

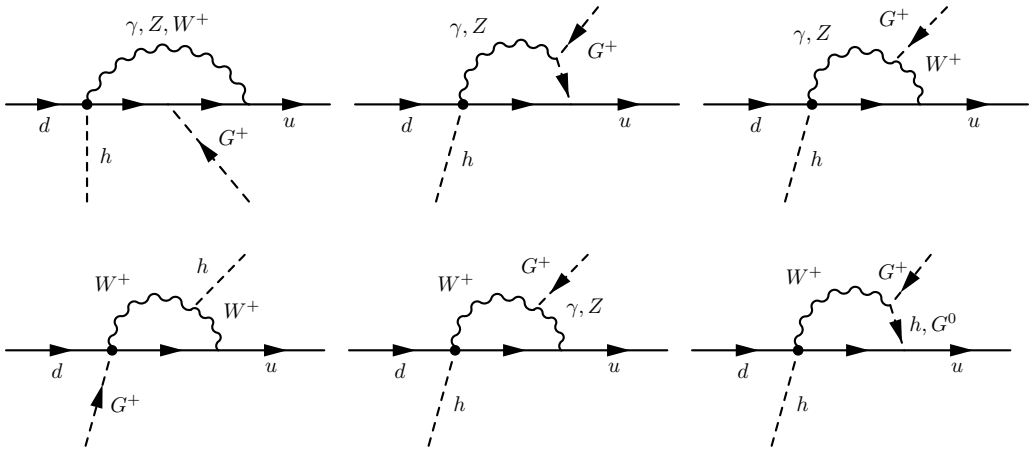

Figure 17: 1PI diagrams contributing to the $udhG^+$ 4-point function. We only show the contribution of the down-type dipole. Furthermore, additional diagrams can be generated by exchanging $h \leftrightarrow G^+$.

B Analytic expressions of various EDMs

In this appendix we report the analytic expressions computed in this work. To improve readability we divide the full expressions into categories defined by the field content of the operators contributing to the dipole. Because we give the expression of the observable EDM we repeat here its relation to the Wilson coefficient $c_{f\gamma}$, of the operator $\bar{f}_L \sigma^{\mu\nu} f_R F_{\mu\nu}$,

$$d_f = -\frac{2}{\Lambda^2} \mathrm{Im}\, c_{f\gamma}, \tag{B.1}$$

and similar for the chromo-dipoles.

B.1 Universal contributions

Since the full expression of the fermion (c)EDMs is rather long, we will start by providing their universal parts first. Apart from the term proportional to g_s, Eq. (B.2b), which is present only for quark dipoles, these are universal in the sense that they correspond to pure SM loops on the external particle 2-point functions and are independent of the fermion species and therefore enter all dipoles in the same way. This includes both the renormalization of the Higgs VEV, which in this work is given by just the loops in the physical Higgs 2-point function, as well as the mixing of the neutral gauge bosons at 1-loop.

All these contributions are:

- Loops on external fermions:

$$16\pi^2 \times \text{Fermion 2-pt.} = 2\sqrt{2}\, e Q_f^2 v - \frac{ev}{4\sqrt{2}s_w^2} - \frac{ev}{2\sqrt{2}s_w^2 c_w^2}\left[(T_f^3 + Q_f s_w^2)^2 + Q_f^2 s_w^2\right] \tag{B.2a}$$

$$+ 2\sqrt{2}\, e Q_f^2 v \log\left(\frac{\Lambda}{m_f}\right) + \frac{ev}{\sqrt{2}s_w^2}\log\left(\frac{\Lambda}{m_W}\right)$$

$$+ \frac{\sqrt{2}\, ev}{s_w^2 c_w^2}\left[(T_f^3 + Q_f s_w^2)^2 + Q_f^2 s_w^2\right]\log\left(\frac{\Lambda}{m_Z}\right)$$

$$+ 2\sqrt{2}\, v\, c_{F,3} + 4\sqrt{2}\, v\, c_{F,3}\log\left(\frac{\Lambda}{m_f}\right) \tag{B.2b}$$

- Loop contributions to the Higgs VEV:

$$
\begin{aligned}
16\pi^2 \times \text{Scalar 2-pt.} = & \frac{2\sqrt{2}\,N_c m_t^2}{ev} - \frac{2\sqrt{2}\,ev}{\pi^2 s_w^2} - \frac{\sqrt{2}\,ev}{s_w^2 c_w^2} \\
& + \frac{2\sqrt{2}\,N_c m_t^2}{ev}\log\left(\frac{\Lambda}{m_t}\right) - \frac{2\sqrt{2}\,ev}{s_w^2}\log\left(\frac{\Lambda}{m_W}\right) \\
& - \frac{\sqrt{2}\,ev}{s_w^2 c_w^2}\log\left(\frac{\Lambda}{m_Z}\right) \\
& - \frac{\sqrt{2}\,m_t^2}{ev}\sqrt{\frac{4m_t^2 - m_h^2}{m_h^2}}\arctan\left(m_h\sqrt{\frac{4m_t^2 - m_h^2}{\left(2m_t^2 - m_h^2\right)^2}}\right) \\
& + \frac{\sqrt{2}\,ev}{s_w^2}\sqrt{\frac{4m_W^2 - m_h^2}{m_h^2}}\left[\arctan\left(m_h\sqrt{\frac{4m_W^2 - m_h^2}{\left(2m_W^2 - m_h^2\right)^2}}\right) + \pi\right] \\
& + \frac{ev}{\sqrt{2}s_w^2 c_w^2}\sqrt{\frac{4m_Z^2 - m_h^2}{m_h^2}}\arctan\left(m_h\sqrt{\frac{4m_Z^2 - m_h^2}{\left(2m_Z^2 - m_h^2\right)^2}}\right)\Bigg\}
\end{aligned}
\tag{B.3}
$$

- Loops on external photons:

$$
\begin{aligned}
16\pi^2 \times \text{Photon 2-pt.} = & -\frac{\sqrt{2}\,ev}{3} - 7\sqrt{2}\,ev\log\left(\frac{\Lambda}{m_W}\right) \\
& + \frac{4\sqrt{2}}{3}\sum_{\text{fermions}}\left(\delta_{i\ell} + N_c\delta_{iq}\right)eQ_i^2 v\log\left(\frac{\Lambda}{m_i}\right)
\end{aligned}
\tag{B.4}
$$

- Photon-Z mixing:

$$
\begin{aligned}
16\pi^2 \times \text{Photon-Z Mixing} = & \frac{\sqrt{2}ev}{3t_w} + \frac{ev}{6\sqrt{2}}\frac{1 + 42c_w^2}{s_w c_w}\log\left(\frac{\Lambda}{m_Z}\right) \\
& - \frac{2\sqrt{2}}{3}\frac{ev}{s_w c_w}\sum_{i\neq t}\left(\delta_{i\ell} + N_c\delta_{iq}\right)Q_i(T_i^3 - 2Q_i s_w^2)\log\left(\frac{\Lambda}{m_Z}\right) \\
& - \frac{2\sqrt{2}}{3}\frac{N_c ev}{s_w c_w}Q_t(T_t^3 - 2Q_t s_w^2)\log\left(\frac{\Lambda}{m_t}\right)
\end{aligned}
\tag{B.5}
$$

- Loops on external gluons:

$$
\begin{aligned}
16\pi^2 \times \text{Gluon 2-pt.} = & -\frac{67N_c v}{9\sqrt{2}}\frac{g_s^2}{e} - \frac{8\sqrt{2}}{3}\left[\frac{11N_c v}{6}\frac{g_s^2}{e} - v\frac{g_s^2}{e}\right]\log\left(\frac{\Lambda}{m_n}\right) \\
& + \frac{2\sqrt{2}\,v}{3}\frac{g_s^2}{e}\log\left(\frac{\Lambda}{m_b}\right) + \frac{2\sqrt{2}\,v}{3}\frac{g_s^2}{e}\log\left(\frac{\Lambda}{m_t}\right)\Bigg\}
\end{aligned}
\tag{B.6}
$$

B.2 Lepton EDMs

We start with showing the results for lepton EDMs. Note that the logs arising from the divergent terms of the photon wave function renormalization do not necessarily run down to the mass of the fermion running in the loop but only to the mass of the external lepton if the latter is heavier than the former.

Contributions from $\psi^2 HF$ operators

$$\frac{d_\ell}{e}\times(4\pi\Lambda)^2 \supset \mathrm{Im}\left[c_w C_{\underset{11}{eB}} + 2\,T^3_\ell s_w C_{\underset{11}{eW}}\right]\left\{-\frac{16\sqrt{2}\,\pi^2\,v}{e}+\frac{4\sqrt{2}\,eQ_\ell^2 v}{v}+\frac{8\sqrt{2}\,eQ_\ell^2 v}{v}\log\left(\frac{\Lambda}{m_\ell}\right)\right. \tag{B.7a}$$

$$\left. + \text{Eq. (B.2a)} + \text{Eq. (B.3)} + \text{Eq. (B.4)}\right\}$$

$$-\mathrm{Im}\left[s_w C_{\underset{11}{eB}} - 2\,T^3_\ell c_w C_{\underset{11}{eW}}\right]\left\{\sqrt{2}\,eQ_\ell\,v\frac{T^3_\ell - 2Q_\ell s_w^2}{s_w c_w}\left[\frac{1}{2}+\log\left(\frac{\Lambda}{m_Z}\right)\right]\right. \tag{B.7b}$$

$$\left. + \text{Eq. (B.5)}\right\}$$

$$-\mathrm{Im}\left[C_{\underset{11}{eW}}\right]\left\{\frac{ev(5+Q_\ell)}{2\sqrt{2}s_w}-\frac{\sqrt{2}\,ev(3Q_\ell-1)}{s_w}\log\left(\frac{\Lambda}{m_W}\right)\right\}. \tag{B.7c}$$

Contributions from H^2F^2 operators

$$\frac{d_\ell}{e}\times(4\pi\Lambda)^2 \supset -m_\ell\left\{3\,(2\,Q_\ell - T^3_\ell)+(8\,Q_\ell - 4T^3_\ell)\log\left(\frac{\Lambda}{m_h}\right)\right. \tag{B.8a}$$

$$\left.+(2s_w^2 Q_\ell - T^3_\ell)\frac{4m_Z^2}{m_Z^2-m_h^2}\log\left(\frac{m_h}{m_Z}\right)\right\} C_{H\widetilde{B}}$$

$$-m_\ell\left\{3\;T^3_\ell + 4T^3_\ell\log\left(\frac{\Lambda}{m_h}\right)\right. \tag{B.8b}$$

$$\left.-(2s_w^2 Q_\ell - T^3_\ell)\frac{4m_Z^2}{m_Z^2-m_h^2}\log\left(\frac{m_h}{m_Z}\right)\right\} C_{H\widetilde{W}}$$

$$+m_\ell\left\{\frac{12\;Q_\ell s_w^2 - 2\;c_w^2 + 6\;T^3_\ell c_{2w}}{(4\pi)^2 c_w s_w}\right. \tag{B.8c}$$

$$+\frac{4s_w^2 Q_\ell + 2T^3_\ell c_{2w}}{c_w s_w}\log\left(\frac{\Lambda}{m_h}\right)-\frac{2}{t_w}\log\left(\frac{\Lambda}{m_W}\right)$$

$$\left.-(2s_w^2 Q_\ell - T^3_\ell)\frac{c_{2w}}{c_w s_w}\frac{2m_Z^2}{m_Z^2-m_h^2}\log\left(\frac{m_h}{m_Z}\right)\right\} C_{HW\widetilde{B}}$$

Contributions from F^3 operators

$$\frac{d_\ell}{e}\times(4\pi\Lambda)^2 \supset \frac{3}{2}\frac{e\,m_\ell}{s_w}C_{\widetilde{W}} \tag{B.9}$$

Contributions from ψ^4 operators

$$\frac{d_\ell}{e} \times (4\pi\Lambda)^2 \supset 16N_c \sum_{i\in\{1,2,3\}} m_i Q_i \log\left(\frac{\Lambda}{m_i}\right) \mathrm{Im}\left[C^{(3)}_{lequ}{}_{\ell\ell ii}\right] \tag{B.10}$$

Contributions from $\psi^2\bar{\psi}^2$ operators

$$\frac{d_\ell}{e} \times (4\pi\Lambda)^2 \supset -2Q_e \sum_{i\neq 1} m_i \,\mathrm{Im}\left[C_{le}{}_{1ii1}\right] \tag{B.11}$$

B.3 Quark EDMs

We show here the results for the quark EDMs; for the scale in the logs of the photon 2-point function, the same discussion as in the case of the lepton EDMs applies.

Contributions from $\psi^2 HF$ operators

$$\frac{d_q}{e} \times (4\pi\Lambda)^2 \supset \mathrm{Im}\left[c_w C_{qW}{}_{11} + 2\, T_q^3 s_w C_{qW}{}_{11}\right] \left\{ -\frac{16\sqrt{2}\,\pi^2\, v}{e} + \frac{4\sqrt{2}\, eQ_\ell^2 v}{v} + \frac{8\sqrt{2}\, eQ_\ell^2 v}{v} \log\left(\frac{\Lambda}{m_n}\right) \right. \tag{B.12a}$$

$$+ \text{Eq. (B.2a)} + \text{Eq. (B.2b)}$$

$$+ \text{Eq. (B.3)} + \text{Eq. (B.4)}$$

$$-\mathrm{Im}\left[s_w C_{qB}{}_{11} - 2\, T_q^3 c_w C_{qW}{}_{11}\right] \left\{ \sqrt{2} eQ_q v \,\frac{T_q^3 - 2Q_q s_w^2}{s_w c_w} \left[\frac{1}{2} + \log\left(\frac{\Lambda}{m_Z}\right)\right] \right. \tag{B.12b}$$

$$+ \text{Eq. (B.5)}$$

$$+2T_q^3 \mathrm{Im}\left[C_{qW}{}_{11}\right] \left\{ \frac{ev(5+Q_q)}{2s_w} - \frac{\sqrt{2}\, ev(3Q_q - 1)}{s_w} \log\left(\frac{\Lambda}{m_W}\right) \right\} \tag{B.12c}$$

$$+\mathrm{Im}\left[C_{qG}{}_{11}\right] \left\{ 2\sqrt{2} v\, c_{F,3} g_s + 4\sqrt{2} v\, c_{F,3} g_s \log\left(\frac{\Lambda}{m_n}\right) \right\}. \tag{B.12d}$$

Contributions from H^2F^2 operators

$$\frac{d_q}{e}\times(4\pi\Lambda)^2 \supset -m_q\left\{(6\,Q_q-3T_q^3)+(8\,Q_q-4T_q^3)\log\left(\frac{\Lambda}{m_h}\right)\right. \tag{B.13a}$$

$$\left.+(2s_w^2Q_q-T_q^3)\frac{2m_Z^2}{m_Z^2-m_h^2}\log\left(\frac{m_h}{m_Z}\right)\right\}C_{H\widetilde{B}}$$

$$-m_q\left\{3\,T_q^3+4\,T_q^3\log\left(\frac{\Lambda}{m_h}\right)\right. \tag{B.13b}$$

$$\left.-(2s_w^2Q_q-T_q^3)\frac{2m_Z^2}{m_Z^2-m_h^2}\log\left(\frac{m_h}{m_Z}\right)\right\}C_{H\widetilde{W}}$$

$$+m_q\left\{\frac{12\;Q_qs_w^2-2\;c_w^2+6\;T_q^3c_{2w}}{4c_ws_w}\right. \tag{B.13c}$$

$$+\frac{4s_w^2Q_q+2T_q^3c_{2w}}{c_ws_w}\log\left(\frac{\Lambda}{m_h}\right)-\frac{2}{t_w}\log\left(\frac{\Lambda}{m_W}\right)$$

$$\left.-(2s_w^2Q_q-T_q^3)\frac{c_{2w}}{c_ws_w}\frac{m_Z^2}{m_Z^2-m_h^2}\log\left(\frac{m_h}{m_Z}\right)\right\}C_{HW\widetilde{B}}$$

Contributions from F^3 operators

$$\frac{d_q}{e}\times(4\pi\Lambda)^2 \supset \frac{3}{2}\frac{e\,m_q}{s_w}\;C_{\widetilde{W}} \tag{B.14}$$

Contributions from ψ^4 operators

$$\frac{d_d}{e}\times(4\pi\Lambda)^2 \supset 2\sum_{i\in\{1,2,3\}} m_iQ_i\;\log\left(\frac{\Lambda}{m_i}\right)\mathrm{Im}\left[C^{(1)}_{\substack{quqd\\1ii1}}+c_{F,3}\,C^{(8)}_{\substack{quqd\\1ii1}}\right] \tag{B.15}$$

$$\frac{d_u}{e}\times(4\pi\Lambda)^2 \supset 8\sum_{i\in\{1,2,3\}} m_iQ_i\;\log\left(\frac{\Lambda}{m_i}\right)\mathrm{Im}\left[C^{(3)}_{\substack{lequ\\ii11}}\right] \tag{B.16}$$

$$+2\sum_{i\in\{1,2,3\}} m_iQ_i\;\log\left(\frac{\Lambda}{m_i}\right)\mathrm{Im}\left[C^{(1)}_{\substack{quqd\\i11i}}+c_{F,3}\,C^{(8)}_{\substack{quqd\\i11i}}\right]$$

Contributions from $\psi\bar{\psi}H^2D$ operators

$$\frac{d_d}{e}\times(4\pi\Lambda)^2 \supset \sum_{i\in\{1,2\}}\frac{4m_i}{\sqrt{2}v}(1+Q_u)\mathrm{Im}\left[C_{\substack{Hud\\i1}}\right] \tag{B.17}$$

$$+\frac{m_t}{\sqrt{2}v}\left[\frac{m_t^4-11m_t^2m_W^2+4m_W^4}{(m_t^2-m_W^2)^2}\right.$$

$$+Q_u\frac{m_t^4+m_t^2m_W^2+4m_W^4}{(m_t^2-m_W^2)^2}$$

$$\left.+\,6m_t^2m_W^2\frac{m_t^2-Q_um_W^2}{(m_t^2-m_W^2)^3}\log\left(\frac{m_t^2}{m_W^2}\right)\right]\mathrm{Im}\left[C_{\substack{Hud\\31}}\right] \tag{B.18}$$

$$\frac{d_u}{e}\times(4\pi\Lambda)^2 \supset -\frac{2\sqrt{2}}{v}\sum_{i\in\{1,2,3\}}m_i\,\mathrm{Im}\left[C^\dagger_{\substack{Hud\\1i}}\right] \tag{B.19}$$

Contributions from $\psi^2\bar{\psi}^2$ operators

$$\frac{d_d}{e}\times(4\pi\Lambda)^2 \supset -2\sum_{i\in\{2,3\}}m_iQ_i\,\mathrm{Im}\left[C^{(1)}_{\substack{qd\\1ii1}}+c_{F,3}\,C^{(8)}_{\substack{qd\\1ii1}}\right] \tag{B.20}$$

$$\frac{d_u}{e}\times(4\pi\Lambda)^2 \supset -2\sum_{i\in\{2,3\}}m_iQ_i\,\mathrm{Im}\left[C^{(1)}_{\substack{qu\\1ii1}}+c_{F,3}\,C^{(8)}_{\substack{qu\\1ii1}}\right] \tag{B.21}$$

B.4 Quark cEDM

Contributions from ψ^2HF operators

$$\frac{\hat{d}_q}{e}\times(4\pi\Lambda)^2 \supset \mathrm{Im}\left[c_wC_{\substack{qB\\11}}+2T_q^3s_wC_{\substack{qW\\11}}\right]\left\{6\sqrt{2}\,g_sQ_qv+8\sqrt{2}\,g_sQ_qv\log\left(\frac{\Lambda}{m_n}\right)\right\} \tag{B.22a}$$

$$+\mathrm{Im}\left[s_wC_{\substack{qB\\11}}-2T_q^3c_wC_{\substack{qW\\11}}\right]\left\{\sqrt{2}(2Q_qs_w^2-T_q^3)g_sv+4\sqrt{2}\,(2Q_qs_w^2-T_q^3)g_sv\log\left(\frac{\Lambda}{m_Z}\right)\right\} \tag{B.22b}$$

$$-2T_q^3\mathrm{Im}\left[C_{\substack{qW\\11}}\right]\left\{\frac{\sqrt{2}\,g_sv}{s_w}+\frac{4\sqrt{2}\,g_sv}{s_w}\log\left(\frac{\Lambda}{m_W}\right)\right\} \tag{B.22c}$$

$$+\mathrm{Im}\left[C_{\substack{qG\\11}}\right]\left\{-\frac{16\sqrt{2}\pi^2v}{e}-2\sqrt{2}eQ_d^2v-\frac{v}{\sqrt{2}}\frac{4+3N_c^2}{N_c}\frac{g_s^2}{e}\right. \tag{B.22d}$$

$$-\frac{4\sqrt{2}\,v}{N_c}\frac{g_s^2}{e}\log\left(\frac{\Lambda}{m_n}\right)$$

$$\left.+\text{Eq. (B.2a)}+\text{Eq. (B.2b)}+\text{Eq. (B.3)}+\text{Eq. (B.6)}\right\} \tag{B.22e}$$

Contributions from H^2F^2 operators

$$\frac{\hat{d}_q}{e} \times (4\pi\Lambda)^2 \supset -C_{H\widetilde{G}} \left\{ \frac{6m_q g_s}{e} + \frac{8m_q g_s}{e} \log\left(\frac{\Lambda}{m_n}\right) \right\} \tag{B.23}$$

Contributions from F^3 operators

$$\frac{\hat{d}_q}{e} \times (4\pi\Lambda)^2 \supset C_{\widetilde{G}} \left\{ 8N_c m_q \frac{g_s^2}{e} + 6N_c m_q \frac{g_s^2}{e} \log\left(\frac{\Lambda}{m_n}\right) \right\} \tag{B.24}$$

Contributions from ψ^4 operators

$$\frac{\hat{d}_d}{e} \times (4\pi\Lambda)^2 \supset -2 \sum_{i\in\{1,2,3\}} \frac{m_i g_s}{e} \log\left(\frac{\Lambda}{m_n}\right) \mathrm{Im}\left[C^{(1)}_{\substack{quqd \\ 1ii1}} - \frac{1}{2N_c} C^{(8)}_{\substack{quqd \\ 1ii1}} \right] \tag{B.25}$$

$$- \frac{2m_t g_s}{e} \log\left(\frac{\Lambda}{m_t}\right) \mathrm{Im}\left[C^{(1)}_{\substack{quqd \\ 1331}} - \frac{1}{2N_c} C^{(8)}_{\substack{quqd \\ 1331}} \right]$$

$$\frac{\hat{d}_u}{e} \times (4\pi\Lambda)^2 \supset -2 \sum_{i\in\{1,2\}} \frac{m_i g_s}{e} \log\left(\frac{\Lambda}{m_n}\right) \mathrm{Im}\left[C^{(1)}_{\substack{quqd \\ i11i}} - \frac{1}{2N_c} C^{(8)}_{\substack{quqd \\ i11i}} \right] \tag{B.26}$$

$$- \frac{2m_b g_s}{e} \log\left(\frac{\Lambda}{m_b}\right) \mathrm{Im}\left[C^{(1)}_{\substack{quqd \\ 3113}} - \frac{1}{2N_c} C^{(8)}_{\substack{quqd \\ 3113}} \right]$$

Contributions from $\psi\bar{\psi}H^2D$ operators

$$\frac{\hat{d}_d}{e} \times (4\pi\Lambda)^2 \supset \frac{g_s}{e} \sum_{i\in\{1,2\}} \frac{4m_i}{\sqrt{2}v} \mathrm{Im}\left[C_{\substack{Hud \\ i1}} \right] + \frac{g_s m_t}{e\sqrt{2}v} \left[\frac{m_t^4 + m_t^2 m_W^2 + 4m_W^4}{(m_t^2 - m_W^2)^2} \right.$$

$$\left. - \frac{6m_t^2 m_W^4}{(m_t^2 - m_W^2)^3} \log\left(\frac{m_t^2}{m_W^2}\right) \right] \mathrm{Im}\left[C_{\substack{Hud \\ 31}} \right] \tag{B.27}$$

$$\frac{\hat{d}_u}{e} \times (4\pi\Lambda)^2 \supset 0 \times \mathrm{Im}\left[C^{\dagger}_{\substack{Hud \\ ij}} \right] \tag{B.28}$$

Contributions from $\psi^2\bar{\psi}^2$ operators

$$\frac{\hat{d}_d}{e} \times (4\pi\Lambda)^2 \supset -2 \sum_{i\in\{2,3\}} \frac{m_i g_s}{e} \mathrm{Im}\left[C^{(1)}_{\substack{qd \\ 1ii1}} - \frac{1}{2N_c} C^{(8)}_{\substack{qd \\ 1ii1}} \right] \tag{B.29}$$

$$\frac{\hat{d}_u}{e} \times (4\pi\Lambda)^2 \supset -2 \sum_{i\in\{2,3\}} \frac{m_i g_s}{e} \mathrm{Im}\left[C^{(1)}_{\substack{qu \\ 1ii1}} - \frac{1}{2N_c} C^{(8)}_{\substack{qu \\ 1ii1}} \right] \tag{B.30}$$

B.5 Gluon cEDM

Contributions from F^3 operators

$$C_{\widetilde{G}} \times (4\pi\Lambda)^2 \supset \left\{ 2\sqrt{3}\pi^2 N_c - \frac{7N_c}{2} - [8+N_c]\log\left(\frac{\Lambda}{m_n}\right) \right. \tag{B.31}$$

$$\left. -2\log\left(\frac{\Lambda}{m_b}\right) - 2\log\left(\frac{\Lambda}{m_t}\right) \right\} g_s^2 C_{\widetilde{G}} \tag{B.32}$$

Contributions from $\psi^2 HF$ operators

$$C_{\widetilde{G}} \times (4\pi\Lambda)^2 \supset \frac{\sqrt{2}\, g_s^2 v}{3} \sum_{\substack{q\in\{u,d\} \\ i\in\{1,2,3\}}} \frac{\mathrm{Im}\left[C_{\substack{qG \\ ii}}\right]}{m_i} \tag{B.33}$$

B.6 $O_{ud}^{(\mathrm{S1/8,\ RR})}$

Contributions from ψ^4 operators

$$\mathrm{Im}\left[c^{(\mathrm{S1,RR})}_{\substack{ud\\1111}}\right]\times(4\pi\Lambda)^2 \supset -\frac{c_{F,3}g_s^2}{N_c}\left\{3+4\log\left(\frac{\Lambda}{m_n}\right)\right\}\mathrm{Im}\left[C^{(8)}_{\substack{quqd\\1111}}\right] \tag{B.34}$$

$$+\Big\{(4\pi)^2+2\times(\text{B.2a})+2\times(\text{B.2b}) \tag{B.35}$$

$$+4c_{F,3}g_s^2+2e^2(Q_d^2-3Q_dQ_u+Q_u^2)+\frac{5e^2}{4s_w^2}$$

$$+2e^2t_w(Q_d^2-3Q_dQ_u+Q_u^2)-\frac{5}{2}\frac{T_d^3T_u^3}{c_w^2s_w^2}-\frac{5e^2}{c_w^2}$$

$$+8\left[2c_{F,3}g_s^2+e^2(Q_d^2-Q_dQ_u+Q_u^2)\right]\log\left(\frac{\Lambda}{m_n}\right)+2\frac{e^2}{s_w^2}\log\left(\frac{\Lambda}{m_W}\right)$$

$$+\frac{4e^2}{s_w^2c_w^2}\left[2(Q_d^2-Q_dQ_u+Q_u^2)s_w^4-3T_u^3s_w^2-T_d^3T_u^3\right]\Big\}\mathrm{Im}\left[C^{(1)}_{\substack{quqd\\1111}}\right]$$

$$+c_{F,3}\left\{3\,g_s^2\,\frac{N_c^2-2}{N_c^2}+3\,\frac{e^2(Q_d+Q_u)^2}{N_c}-\frac{3\,e^2}{2N_cs_w^2}\right. \tag{B.36}$$

$$+\frac{3\,e^2}{N_cs_w^2c_w^2}\left[(Q_d+Q_u)s_w^2-T_d^3\right]\left[(Q_d+Q_u)s_w^2-T_u^3\right]$$

$$+\left[4\,g_s^2\,\frac{N_c^2-2}{N_c^2}-4\,\frac{e^2(Q_d+Q_u)^2}{N_c}\right]\log\left(\frac{\Lambda}{m_n}\right)-\frac{2\,e^2}{N_cs_w^2}\log\left(\frac{\Lambda}{m_W}\right)$$

$$\left.+\frac{4e^2}{N_cs_w^2c_w^2}\left[(Q_d+Q_u)s_w^2-T_d^3\right]\left[(Q_d+Q_u)s_w^2-T_u^3\right]\log\left(\frac{\Lambda}{m_Z}\right)\right\}\mathrm{Im}\left[C^{(8)}_{\substack{quqd\\1111}}\right]$$

$$+\left\{\frac{12c_{F,3}g_s^2}{N_c}+3\frac{e^2(Q_d+Q_u)^2}{N_c}-\frac{3e^2}{2N_c\,s_w^2}\right. \tag{B.37}$$

$$+3\frac{e^2}{N_c\,s_w^2c_w^2}\left[(Q_d+Q_u)s_w^2-T_d^3\right]\left[(Q_d+Q_u)s_w^2-T_u^3\right]$$

$$+\frac{4}{N_c}\left[4c_{F,3}g_s^2+e^2(Q_d+Q_u)^2\right]\log\left(\frac{\Lambda}{m_n}\right)-\frac{2e^2}{s_w^2}\log\left(\frac{\Lambda}{m_W}\right)$$

$$\left.+\frac{4e^2}{N_c\,s_w^2c_w^2}\left[(Q_d+Q_u)s_w^2-T_d^3\right]\left[(Q_d+Q_u)s_w^2-T_u^3\right]\log\left(\frac{\Lambda}{m_Z}\right)\right\}\mathrm{Im}\left[C^{(1)}_{\substack{quqd\\1111}}\right]$$

$$\mathrm{Im}\left[c^{(\mathrm{S8,RR})}_{ud\,1111}\right]\times(4\pi\Lambda)^2 \supset \Big\{(4\pi)^2 + 2\times(\text{B.2a}) + 2\times(\text{B.2b}) \tag{B.38}$$

$$+\frac{g_s^2(8-N_c^2)}{2N_c} + 2e^2(Q_d^2 - 3Q_dQ_u + Q_u^2) + \frac{5e^2}{4s_w^2}$$

$$+ 2e^2 t_w(Q_d^2 - 3Q_dQ_u + Q_u^2) - \frac{5}{2}\frac{T_d^3T_u^3}{c_w^2s_w^2} - \frac{5e^2}{c_w^2}$$

$$+ 8e^2(Q_d^2 - Q_dQ_u + Q_u^2)\log\left(\frac{\Lambda}{m_n}\right) + 2\frac{e^2}{s_w^2}\log\left(\frac{\Lambda}{m_W}\right)$$

$$+\frac{4e^2}{s_w^2c_w^2}\left[2(Q_d^2 - Q_dQ_u + Q_u^2)s_w^4 - 3T_u^3s_w^2 - T_d^3T_u^3\right]\Big\}\,\mathrm{Im}\left[C^{(8)}_{quqd\,1111}\right]$$

$$-\left\{6g_s^2 + 8g_s^2\log\left(\frac{\Lambda}{m_n}\right)\right\}\mathrm{Im}\left[C^{(1)}_{quqd\,1111}\right] \tag{B.39}$$

$$+\left\{3g_s^2\frac{2+N_c^2}{N_c^2} - 3\frac{e^2(Q_d+Q_u)^2}{N_c} + \frac{3\,e^2}{2N_cs_w^2}\right. \tag{B.40}$$

$$-\frac{3e^2}{N_cs_w^2c_w^2}\left[(Q_d+Q_u)s_w^2 - T_d^3\right]\left[(Q_d+Q_u)s_w^2 - T_u^3\right]$$

$$+\left[4g_s^2\frac{2+N_c^2}{N_c^2} - 4\frac{e^2(Q_d+Q_u)^2}{N_c}\right]\log\left(\frac{\Lambda}{m_n}\right) + \frac{2e^2}{N_cs_w^2}\log\left(\frac{\Lambda}{m_W}\right)$$

$$\left.-\frac{4e^2}{N_cs_w^2c_w^2}\left[(Q_d+Q_u)s_w^2 - T_d^3\right]\left[(Q_d+Q_u)s_w^2 - T_u^3\right]\log\left(\frac{\Lambda}{m_Z}\right)\right\}\mathrm{Im}\left[C^{(8)}_{quqd\,1111}\right]$$

$$+\left\{-\frac{12g_s^2}{N_c} + 6e^2(Q_d+Q_u)^2 - \frac{3e^2}{s_w^2}\right. \tag{B.41}$$

$$+6\frac{e^2}{s_w^2c_w^2}\left[(Q_d+Q_u)s_w^2 - T_d^3\right]\left[(Q_d+Q_u)s_w^2 - T_u^3\right]$$

$$-8\left[\frac{2g_s^2}{N_c} - e^2(Q_d+Q_u)^2\right]\log\left(\frac{\Lambda}{m_n}\right) - \frac{4e^2}{s_w^2}\log\left(\frac{\Lambda}{m_W}\right)$$

$$\left.+8\frac{e^2}{s_w^2c_w^2}\left[(Q_d+Q_u)s_w^2 - T_d^3\right]\left[(Q_d+Q_u)s_w^2 - T_u^3\right]\log\left(\frac{\Lambda}{m_Z}\right)\right\}\mathrm{Im}\left[C^{(1)}_{quqd\,1111}\right]$$

Contributions from $\psi^2 HF$ operators

$$\mathrm{Im}\left[c^{(\mathrm{S1,RR})}_{ud\,1111}\right]\times(4\pi\Lambda)^2 \supset \frac{\sqrt{2}e\,m_u}{v}\,\mathrm{Im}\left[c_w C_{\underset{11}{dB}} - s_w C_{\underset{11}{dW}}\right]\left\{\frac{6}{N_c}[Q_d+Q_u-N_cQ_u]\right. \tag{B.42}$$

$$\left. -\frac{8(Q_d+Q_u)}{N_c}\log\left(\frac{\Lambda}{m_W}\right) - 4Q_u\left[\log\left(\frac{\Lambda}{m_Z}\right)+\log\left(\frac{\Lambda}{m_h}\right)\right]\right\}$$

$$+\frac{\sqrt{2}e\,m_u}{v\,c_w s_w}\,\mathrm{Im}\left[s_w C_{\underset{11}{dB}} + c_w C_{\underset{11}{dW}}\right]\left\{\frac{2}{N_c}(N_cT_u^3-3T_d^3)\right. \tag{B.43}$$

$$+\frac{2s_w^2}{N_c}(3Q_d+3Q_u-2N_cQ_u)+\frac{2}{N_c}(N_cT_u^3-4T_d^3)\log\left(\frac{\Lambda}{m_Z}\right)$$

$$+\frac{2s_w^2}{N_c}(4Q_d+4Q_u-2N_cQ_u)\log\left(\frac{\Lambda}{m_Z}\right)+2(T_u^3-2Q_us_w^2)\log\left(\frac{\Lambda}{m_h}\right)$$

$$-2(T_u^3-2Q_us_w^2)\frac{m_Z^2}{m_h^2-m_Z^2}\log\left(\frac{m_h}{m_Z}\right)+$$

$$\left.+8(T_d^3-(Q_u+Q_d)s_w^2)\frac{m_W^2}{m_Z^2-m_W^2}\log\left(\frac{m_Z}{m_W}\right)\right\}$$

$$+\frac{\sqrt{2}e\,m_u}{v\,s_w}\,\mathrm{Im}\left[C_{\underset{11}{dW}}\right]\left\{1-6\frac{1-2T_d^3}{N_c}\right. \tag{B.44}$$

$$-\frac{16s_w^2\,(Q_d+Q_u)}{N_c}\frac{m_Z^2}{m_Z^2-m_W^2}$$

$$+4\left[1+\frac{4(Q_d+Q_u)s_w^2}{N_c}\right]\log\left(\frac{\Lambda}{m_W}\right)$$

$$-4\left[\frac{1-4T_d^3}{N_c}+\frac{4(Q_d+Q_u)s_w^2}{N_c}\right]\log\left(\frac{\Lambda}{m_Z}\right)-\frac{4}{N_c}\log\left(\frac{\Lambda}{m_h}\right)$$

$$+4\left[1-4T_d^3+4(Q_d+Q_u)s_w^2\right]\frac{m_W^2}{m_Z^2-m_W^2}\log\left(\frac{m_Z}{m_W}\right)$$

$$+\frac{32\,s_w^2\,m_W^2}{N_c(m_Z^2-m_W^2)}\left[\frac{T_u^3}{s_w^4}+Q_u+(Q_d+Q_u)\frac{m_Z^2}{m_Z^2-m_W^2}\right]\log\left(\frac{m_Z}{m_W}\right)$$

$$\left.+\frac{4}{N_c}\frac{m_W^2}{m_h^2-m_W^2}\log\left(\frac{m_h}{m_W}\right)\right\}$$

$$+\frac{4\sqrt{2}g_s m_u}{v}\frac{c_{F,3}}{N_c}\,\mathrm{Im}\left[C_{\underset{11}{dG}}\right]\left\{3+4\log\left(\frac{\Lambda}{m_W}\right)\right\} \tag{B.45}$$

$$+\left(C_{\underset{11}{dW}}\to -C_{\underset{11}{uW}}, d\leftrightarrow u\right) \tag{B.46}$$

$$\mathrm{Im}\left[c^{(\mathrm{S8,RR})}_{ud\,1111}\right]\times(4\pi\Lambda)^2 \supset \frac{\sqrt{2}e\,m_u}{v}\,\mathrm{Im}\left[c_w C_{\underset{11}{dB}} - s_w C_{\underset{11}{dW}}\right]\left\{4(Q_d+Q_u)\left[3+4\log\left(\frac{\Lambda}{m_W}\right)\right]\right\} \tag{B.47}$$

$$+\frac{\sqrt{2}e\,m_u}{v\,c_w s_w}\,\mathrm{Im}\left[s_w C_{\underset{11}{dB}} + c_w C_{\underset{11}{dW}}\right] \tag{B.48}$$

$$\times\left\{4\left[(Q_d+Q_u)s_w^2 - T_d^3\right]\left[3-\frac{4m_W^2}{m_Z^2-m_W^2}\log\left(\frac{m_Z}{m_W}\right)+4\log\left(\frac{\Lambda}{m_W}\right)\right]\right\}$$

$$+\frac{\sqrt{2}e\,m_u}{v\,s_w}\,\mathrm{Im}\left[C_{\underset{11}{dW}}\right]\left\{12(2T_d^3-1)\right. \tag{B.49}$$

$$-32s_w^2\,(Q_d+Q_u)\frac{m_Z^2}{m_Z^2-m_W^2}$$

$$+32(Q_d+Q_u)s_w^2\log\left(\frac{\Lambda}{m_W}\right)-8\log\left(\frac{\Lambda}{m_h}\right)$$

$$-8\left[1-4T_d^3+4(Q_d+Q_u)s_w^2\right]\log\left(\frac{\Lambda}{m_Z}\right)+\frac{8m_W^2}{m_h^2-m_W^2}\log\left(\frac{m_h}{m_W}\right)$$

$$+\left[1-4T_d^3+4(Q_d+Q_u)s_w^2\right]\frac{8m_W^2}{m_Z^2-m_W^2}\log\left(\frac{m_Z}{m_W}\right)$$

$$\left.+\frac{64\,s_w^2\,m_W^2}{m_Z^2-m_W^2}\left[\frac{T_u^3}{s_w^2}+Q_u+(Q_d+Q_u)\frac{m_Z^2}{m_Z^2-m_W^2}\right]\log\left(\frac{m_Z}{m_W}\right)\right\}$$

$$+\frac{2\sqrt{2}g_s m_u}{v}\,\mathrm{Im}\left[C_{\underset{11}{dG}}\right]\left\{-\frac{3(2+N_c)}{N_c}-\frac{8}{N_c}\log\left(\frac{\Lambda}{m_W}\right)\right. \tag{B.50}$$

$$\left.-2\log\left(\frac{\Lambda}{m_Z}\right)-2\log\left(\frac{\Lambda}{m_h}\right)\right\}$$

$$+\left(C_{\underset{11}{dW}}\to -C_{\underset{11}{uW}}, d\leftrightarrow u\right) \tag{B.51}$$

B.7 $O_{duud}^{(\mathbf{S1/8,\ RR})}$

Contributions from ψ^4 operators

$$\mathrm{Im}\left[c^{(\mathrm{S1,RR})}_{\substack{duud\\1111}}\right]\times(4\pi\Lambda)^2 \supset \left\{3g_s^2\frac{2+N_c^2}{N_c^2}-\frac{12e^2Q_dQ_u}{N_c}+\frac{3e^2}{2s_w^2}\right. \tag{B.52}$$

$$-\frac{3e^2}{N_c\,s_w^2c_w^2}(2Q_ds_w^2-T_d^3)(2Q_us_w^2-T_u^3)$$

$$+\frac{4}{N_c^2}\left[g_s^2(2+N_c^2)-4e^2N_cQ_dQ_u\right]\log\left(\frac{\Lambda}{m_n}\right)+\frac{2e^2}{N_c\,s_w^2}\log\left(\frac{\Lambda}{m_W}\right)$$

$$\left.-\frac{4e^2}{N_c\,s_w^2c_w^2}(2Q_ds_w^2-T_d^3)(2Q_us_w^2-T_u^3)\log\left(\frac{\Lambda}{m_Z}\right)\right\}\mathrm{Im}\left[C^{(8)}_{\substack{quqd\\1111}}\right]$$

$$+\left\{-\frac{12g_s^2}{N_c}+24e^2Q_dQ_u-\frac{3e^2}{s_w^2}\right. \tag{B.53}$$

$$+\frac{6e^2}{s_w^2c_w^2}(2Q_ds_w^2-T_d^3)(2Q_us_w^2-T_u^3)$$

$$-\frac{16g_s^2}{N_c}+32e^2Q_dQ_u\log\left(\frac{\Lambda}{m_n}\right)-\frac{4e^2}{s_w^2}\log\left(\frac{\Lambda}{m_W}\right) \tag{B.54}$$

$$\left.+\frac{8e^2}{s_w^2\,c_w^2}(2Q_ds_w^2-T_d^3)(2Q_us_w^2-T_u^3)\log\left(\frac{\Lambda}{m_Z}\right)\right\}\mathrm{Im}\left[C^{(1)}_{\substack{quqd\\1111}}\right]$$

$$+(4\pi)^2+\Big\{2\times(\text{B.2a})+2\times(\text{B.2b}) \tag{B.55}$$

$$+\frac{g_s^2(8-N_c^2)}{2N_c}-\frac{e^2(Q_d+Q_u)^2}{2}+\frac{5e^2}{4s_w^2}$$

$$-\frac{e^2}{2c_w^2s_w}\left[5T_d^3T_u^3+(Q_d+Q_u)^2s_w^4\right]$$

$$+8e^2Q_dQ_u\log\left(\frac{\Lambda}{m_n}\right)+\frac{2e^2}{s_w^2}\log\left(\frac{\Lambda}{m_W}\right)$$

$$+\left[8Q_dQ_ut_w^2+\frac{4T_u^3}{c_w^2}-\frac{4T_u^3T_d^3}{s_w^2c_w^2}\right]\log\left(\frac{\Lambda}{m_Z}\right)\Big\}\mathrm{Im}\left[C^{(8)}_{\substack{quqd\\1111}}\right]$$

$$-2g_s^2\left\{3+4\log\left(\frac{\Lambda}{m_n}\right)\right\}\mathrm{Im}\left[C^{(1)}_{\substack{quqd\\1111}}\right] \tag{B.56}$$

$$\mathrm{Im}\left[c^{(\mathrm{S8,RR})}_{\substack{duud\\1111}}\right]\times(4\pi\Lambda)^2 \supset c_{F,3}\left\{3g_s^2\frac{N_c^2-2}{N_c^2}+\frac{12e^2Q_dQ_u}{N_c}-\frac{3e^2}{2s_w^2}\right. \tag{B.57}$$

$$+\frac{3e^2}{N_c\,s_w^2c_w^2}(2Q_ds_w^2-T_d^3)(2Q_us_w^2-T_u^3)$$

$$+\frac{4}{N_c^2}\left[g_s^2(N_c^2-2)+4e^2N_cQ_dQ_u\right]\log\left(\frac{\Lambda}{m_n}\right)-\frac{2e^2}{N_c\,s_w^2}\log\left(\frac{\Lambda}{m_W}\right)$$

$$\left.+\frac{4e^2}{N_c\,s_w^2c_w^2}(2Q_ds_w^2-T_d^3)(2Q_us_w^2-T_u^3)\log\left(\frac{\Lambda}{m_Z}\right)\right\}\mathrm{Im}\left[C^{(8)}_{\substack{quqd\\1111}}\right]$$

$$+\left\{\frac{12c_{F,3}g_s^2}{N_c}+12\frac{e^2Q_dQ_u}{N_c}-\frac{3e^2}{2N_c\,s_w^2}\right. \tag{B.58}$$

$$+\frac{3e^2}{N_c\,s_w^2c_w^2}(2Q_ds_w^2-T_d^3)(2Q_us_w^2-T_u^3)$$

$$+\frac{16}{N_c}\left[g_s^2c_{F,3}+e^2Q_dQ_u\right]\log\left(\frac{\Lambda}{m_n}\right)-\frac{2e^2}{N_c\,s_w^2}\log\left(\frac{\Lambda}{m_W}\right) \tag{B.59}$$

$$\left.+\frac{4e^2}{N_c\,s_w^2c_w^2}(2Q_ds_w^2-T_d^3)(2Q_us_w^2-T_u^3)\log\left(\frac{\Lambda}{m_Z}\right)\right\}\mathrm{Im}\left[C^{(1)}_{\substack{quqd\\1111}}\right]$$

$$-\frac{c_{F,3}g_s^2}{N_c}\left\{3+4\log\left(\frac{\Lambda}{m_n}\right)\right\}C^{(8)}_{\substack{quqd\\1111}} \tag{B.60}$$

$$+(4\pi)^2+\Big\{2\times\text{(B.2a)}+2\times\text{(B.2b)} \tag{B.61}$$

$$+4c_{F,3}g_s^2-\frac{e^2(Q_d+Q_u)^2}{2}+\frac{5e^2}{4s_w^2}$$

$$-\frac{e^2}{2c_w^2s_w^2}\left[5T_d^3T_u^3+(Q_d+Q_u)^2s_w^4\right]$$

$$+8\left[2c_{F,3}g_s^2+e^2Q_dQ_u\right]\log\left(\frac{\Lambda}{m_n}\right)+\frac{2e^2}{s_w^2}\log\left(\frac{\Lambda}{m_W}\right)$$

$$\left.+\left[8Q_dQ_ut_w^2+\frac{4T_u^3}{c_w^2}-\frac{4T_u^3T_d^3}{s_w^2c_w^2}\right]\log\left(\frac{\Lambda}{m_Z}\right)\right\}\mathrm{Im}\left[C^{(1)}_{\substack{quqd\\1111}}\right]$$

Contributions from $\psi^2 HF$ operators

$$\mathrm{Im}\left[c^{(\mathrm{S1,RR})}_{duud\,1111}\right]\times(4\pi\Lambda)^2 \supset \frac{\sqrt{2}e\,m_u}{v}\,\mathrm{Im}\left[c_w C_{\underset{11}{dB}} - s_w C_{\underset{11}{dW}}\right]\left\{\frac{12Q_u}{N_c} - 3(Q_d+Q_u)\right. \tag{B.62}$$

$$+ 2(Q_d+Q_u)\log\left(\frac{\Lambda}{m_W}\right) - \frac{4Q_u}{N_c}\left[\log\left(\frac{\Lambda}{m_Z}\right) + \log\left(\frac{\Lambda}{m_h}\right)\right]$$

$$+ \frac{\sqrt{2}e\,m_u}{v\,c_w s_w}\,\mathrm{Im}\left[s_w C_{\underset{11}{dB}} + c_w C_{\underset{11}{dW}}\right]\left\{3T_d^3 - \frac{4T_u^3}{N_c}\right. \tag{B.63}$$

$$+ \frac{8Q_u - 3N_c(Q_d+Q_u)}{N_c}s_w^2$$

$$- 2\left[T_d^3 - \frac{T_u^3}{N_c} - \frac{N_c(Q_d+Q_u)-2Q_u}{N_c}s_w\right]\log\left(\frac{\Lambda}{m_Z}\right)$$

$$+ \frac{2}{N_c}(T_u^3 - 2Q_u s_w^2)\log\left(\frac{\Lambda}{m_h}\right)$$

$$- (T_u^3 - 2Q_u s_w^2)\frac{4m_Z^2}{m_Z^2 - m_H^2}\log\left(\frac{m_h}{m_Z}\right)$$

$$\left. - ((Q_d+Qu)s_w^2 - T_d^3)\frac{4m_W^2}{m_Z^2-m_W^2}\log\left(\frac{m_Z}{m_W}\right)\right\}$$

$$+ \frac{\sqrt{2}e\,m_u}{v\,s_w}\,\mathrm{Im}\left[C_{\underset{11}{dW}}\right]\left\{3 - 6T_d^3 - \frac{2}{N_c}\right. \tag{B.64}$$

$$+ 8s_w^2\,(Q_d+Q_u)\frac{m_Z^2}{m_Z^2-m_W^2}$$

$$- 8\left[\frac{1}{N_c} + (Q_d+Q_u)s_w^2\right]\log\left(\frac{\Lambda}{m_W}\right)$$

$$- 2\left[4T_d^3 - 1 - 4(Q_d+Q_u)s_w^2\right]\log\left(\frac{\Lambda}{m_Z}\right) + 2\log\left(\frac{\Lambda}{m_h}\right)$$

$$+ \left[4T_d^3 - 1 - 4(Q_d+Q_u)s_w^2\right]\frac{2m_W^2}{m_Z^2-m_W^2}\log\left(\frac{m_Z}{m_W}\right)$$

$$- \frac{16\,s_w^2\,m_W^2}{m_Z^2-m_W^2}\left[\frac{T_u^3}{s_w^2} + Q_u + (Q_d+Q_u)\frac{m_Z^2}{m_Z^2-m_W^2}\right]\log\left(\frac{m_Z}{m_W}\right)$$

$$- \frac{2m_W^2}{m_h^2-m_W^2}\log\left(\frac{m_h}{m_W}\right)$$

$$+ \frac{4\sqrt{2}g_s m_u}{v}\frac{c_{F,3}}{N_c}\,\mathrm{Im}\left[C_{\underset{11}{dG}}\right]\left\{3 + 2\log\left(\frac{\Lambda}{m_Z}\right) + 2\log\left(\frac{\Lambda}{m_h}\right)\right\} \tag{B.65}$$

$$+ \left(C_{\underset{11}{dW}} \to -C_{\underset{11}{uW}}, d \leftrightarrow u\right) \tag{B.66}$$

$$\mathrm{Im}\left[c^{(\mathrm{S8,RR})}_{duud\,1111}\right] \times (4\pi\Lambda)^2 \supset \frac{\sqrt{2}e\,m_u}{v}\,\mathrm{Im}\left[c_w C_{\underset{11}{dB}} - s_w C_{\underset{11}{dW}}\right]\Big\{24Q_u \tag{B.67}$$

$$+16Q_u \log\left(\frac{\Lambda}{m_Z}\right) + 16Q_u \log\left(\frac{\Lambda}{m_h}\right)\Big\}$$

$$+ \frac{\sqrt{2}e\,m_u}{v\,c_w s_w}\,\mathrm{Im}\left[s_w C_{\underset{11}{dB}} + c_w C_{\underset{11}{dW}}\right]\Bigg\{8(2Q_u s_w^2 - T_u^3) \tag{B.68}$$

$$+ 8(2Q_u s_w^2 - T_u^3)\left[\log\left(\frac{\Lambda}{m_Z}\right) + \log\left(\frac{\Lambda}{m_h}\right)\right]$$

$$- \,8(2Q_u s_w^2 - T_u^3)\frac{m_Z^2}{m_h^2 - m_Z^2}\log\left(\frac{m_h}{m_Z}\right)\Bigg\}$$

$$- \frac{4\sqrt{2}e\,m_u}{v\,s_w}\,\mathrm{Im}\left[C_{\underset{11}{dW}}\right]\left\{1 + 4\log\left(\frac{\Lambda}{m_W}\right)\right\} \tag{B.69}$$

$$- \frac{2\sqrt{2}g_s m_u}{v}\,\mathrm{Im}\left[C_{\underset{11}{dG}}\right]\left\{\frac{3(2+N_c)}{N_c} + 4\log\left(\frac{\Lambda}{m_W}\right)\right. \tag{B.70}$$

$$\left. + \,\frac{4}{N_c}\log\left(\frac{\Lambda}{m_Z}\right) + \frac{4}{N_c}\log\left(\frac{\Lambda}{m_h}\right)\right\}$$

$$+ \left(C_{\underset{11}{dW}} \to -C_{\underset{11}{uW}}, d \leftrightarrow u\right) \tag{B.71}$$

B.8 O_{Hud}

Contributions from $\psi\bar{\psi}H^2D$ operators

$$\begin{aligned}
\mathrm{Im}\left[C_{\substack{Hud\\11}}\right]\times(4\pi\Lambda)^2 \supset \Bigg\{ & (4\pi)^2 + \text{Eq. (B.2a)} + \text{Eq. (B.2b)} + \text{Eq. (B.3)} \\
& - \pi^2 e^2 - \frac{2\pi^2}{3} e^2 \frac{m_Z^2}{m_W^2}\left[\frac{Q_d - Q_d\, t_w^2}{4} - Q_d Q_u\, t_w^2 \frac{m_Z^2}{m_W^2}\right] \\
& - 4e^2 - 4g^2 - 2g^2 c_{2\theta} - \frac{g^2}{2c_w^2} + e^2 Q_d \frac{c_{2\theta}}{c_w^2} + \frac{g^2}{12_\theta^4} + 2e^2 t_w^2 \\
& - g^2 t_w^2 - 2e^2 Q_d Q_u \frac{t_w^2}{c_w^2} + 2\frac{m_h^2}{v^2} - \frac{m_h^4}{3m_W^2 v^2} \\
& + 2\left[c_{F,3} g_s^2 + e^2 Q_d Q_u\right]\log\left(\frac{\Lambda}{m_n}\right) - 2e^2 \log\left(\frac{\Lambda}{m_W}\right) \\
& - \left[2e^2 + \frac{7}{3}g^2 + 2g^2(c_w^2 - 2s_w^2) - 2e^2(1 + Q_d Q_u)t_w^2\right]\log\left(\frac{\Lambda}{m_Z}\right) \\
& - \frac{5g^2}{3}\log\left(\frac{\Lambda}{m_h}\right) - 4e^2 t_w^2 Q_d Q_u \frac{m_Z^4}{m_W^4}\log^2\left(\frac{m_Z}{m_W}\right) \\
& + g^2\left[\frac{1}{3} + \frac{3m_h^2}{v^2} - \frac{2m_h^4}{m_W^2 v^2} + \frac{m_h^6}{3m_W^4 v^2}\right]\log\left(\frac{m_h}{m_W}\right) - \frac{g^2}{3}\log\left(\frac{m_h}{m_Z}\right) \\
& + 2e^2\left[Q_u(3 - t_w^2 + Q_d\, t_w^2) + \frac{c_{2\theta}}{c_w^2} - (3 - Q_d Q_u t_w^2)\frac{m_Z^2}{m_W^2}\right]\log\left(\frac{m_Z}{m_W}\right) \\
& - g^2\left[\frac{13}{3} + 2c_{2\theta^2} + \frac{1}{2c_w^2} - \left(1 + c_{2\theta} + \frac{1}{2c_w^2}\right)\frac{m_Z^2}{m_W^2} + \frac{1}{12c_w^2}\frac{m_Z^2}{m_W^2}\right]\log\left(\frac{m_Z}{m_W}\right) \\
& - \frac{e^2 Q_d}{c_w^2}\frac{m_Z^2}{m_W^2}\left[c_{2\theta} - 2Q_d Q_u s_w^2 \frac{m_Z^2}{m_W^2}\right]\mathrm{Li}_2\left(1 + \frac{m_Z^2}{m_W^2}\right) \\
& - \left[g^2 + \frac{4m_h^2}{3v^2} - \frac{m_h^4}{3m_W^2 v^2}\right] F(m_W^2, m_h, m_W) \\
& + \left[4e^2 - 2g^2 c_w - \frac{g^2}{3c_w^2} + g^2 \frac{m_Z^2}{12m_W^2}\left(\frac{1}{c_w^2} - 12\right)\right] F(m_W^2, m_W, m_Z) \\
& + e^2\left[2 - \frac{1}{c_w^2}\right] C_0(m_W^2, m_Z, m_W)\Bigg\}\,\mathrm{Im}\left[C_{\substack{Hud\\11}}\right],
\end{aligned} \tag{B.72}$$

where we defined

$$F(x,y,z) = \frac{\sqrt{\lambda(x,y^2,z^2)}}{x}\,\log\left(\frac{y^2+z^2-x+\sqrt{\lambda(x,y^2,z^2)}}{2yz}\right), \tag{B.73}$$

$$\begin{aligned} C_0(x,y,\sqrt{x}) =& \frac{\pi^2}{6} + \frac{1}{2}\log\left(\frac{\sqrt{y^4-4xy^2}-y^2}{2x+\sqrt{y^4-4xy^2}-y^2}\right) \\ &- \mathrm{Li}_2\left(\frac{2x}{y^2-\sqrt{y^4-4xy^2}}\right) + \mathrm{Li}_2\left(-\frac{2x}{2x+\sqrt{y^4-4xy^2}-y^2}\right), \end{aligned} \tag{B.74}$$

with the usual Kallen λ-function and $\mathrm{Li}_2\,(x)$ denotes the dilogarithm.

Contributions from $\psi^2 HF$ operators

$$\mathrm{Im}\left[C_{\substack{Hud\\11}}\right]\times(4\pi\Lambda)^2 \supset -\frac{5c_{F,3}g_s m_u}{\sqrt{2}v}\mathrm{Im}\left[C_{\substack{dG\\11}}\right] \tag{B.75}$$

$$-\frac{em_u}{\sqrt{2}v}\mathrm{Im}\left[-s_w C_{\substack{dW\\11}} + c_w C_{\substack{dB\\11}}\right]\left[-1+9Q_u+4Q_u m_h^2 C_0(m_h^2,m_W^2,m_h^2+m_W^2,0,0,0)\right] \tag{B.76}$$

$$+\frac{em_u}{\sqrt{2}s_w c_w v}\mathrm{Im}\left[-s_w C_{\substack{dB\\11}} - c_w C_{\substack{dW\\11}}\right]\Bigg\{-4+\frac{9}{2}Q_u+8T_u^3 \tag{B.77}$$

$$\begin{aligned} &+c_{2w}\left(\frac{1}{2}(1-9Q_u) - 4\frac{m_Z^2}{m_W^2} + \pi^2\frac{2m_Z^4}{3m_W^4}\right) + 2Q_u s_w^2\log\left(\frac{m_Z^2}{m_h^2}\right) \\ &+2Q_u s_w^2\left[\frac{m_h^4-m_W^4+m_h^2m_Z^2+3m_W^2m_Z^2-2m_Z^4}{m_h^2(m_h^2+m_W^2)}\log\left(\frac{m_Z^2}{m_h^2+m_W^2-m_Z^2}\right)\right. \\ &\left.+\frac{(m_W^2-m_Z^2)(m_W^2-2m_Z^2-4m_h^2)}{m_h^2m_W^2}\log\left(\frac{m_Z^2}{m_Z^2-m_W^2}\right)\right] \\ &+2c_{2w}\frac{(m_W^2+2m_Z^2)}{m_W^2}\log\left(\frac{m_Z^2}{m_W^2}\right) - 4c_{2w}\frac{m_Z^4}{m_W^4}\mathrm{Li}_2\left(1-\frac{m_W^2}{m_Z^2}\right) \\ &+2Q_u s_w^2\left(2m_h^2+m_Z^2\right)C_0(m_h^2,m_W^2,m_h^2+m_W^2,0,0,m_Z)\Big\} \end{aligned} \tag{B.78}$$

$$+\frac{em_u}{\sqrt{2}s_w v}C_{\substack{dW\\11}}\Bigg\{4\left(-3+4Q_u s_w^2(3-\pi^2+3s_w t_w^2)+\frac{m_h^2+m_Z^2}{m_W^2}\right) \tag{B.79}$$

$$-\frac{12m_W^4+9m_h^2m_W^2-4m_h^4}{2m_W^2(M_h^2+m_W^2)}\log\left(\frac{m_W^2}{m_h^2}\right)+\frac{2(m_Z^2-4m_W^2)}{m_W^2}\log\left(\frac{m_W^2}{m_Z^2}\right)$$

$$-\frac{4m_h^4-12m_h^2m_W^2+8m_W^4}{m_W^4}\log\left(\frac{m_h^2}{m_h^2-m_W^2}\right)-\frac{8m_W^4-12m_W^2m_Z^2+4m_Z^4}{m_W^4}\log\left(\frac{m_Z^2}{m_Z^2-m_W^2}\right)$$

$$-\frac{5m_W^4-4m_h^2m_W^2+m_h^4}{m_W^4}\log^2\left(\frac{m_W^2}{m_h^2-m_W^2}\right)-\frac{5m_W^4-4m_W^2m_Z^2+m_Z^4}{m_W^4}\log^2\left(\frac{m_W^2}{m_Z^2-m_W^2}\right)$$

$$+\frac{2\sqrt{m_h^4-4m_h^2m_W^2}}{m_h^2}\log\left(\frac{2m_W^2-m_h^2+\sqrt{m_h^4-4m_h^2m_W^2}}{2m_W^2}\right)+4Q_u s_w^2\Bigg[\log\left(\frac{m_Z^2}{m_h^2}\right)$$

$$+\frac{m_h^4-m_W^4+m_h^2m_Z^2+3m_W^2m_Z^2-2m_Z^4}{m_h^2(m_h^2+m_W^2)}\log\left(\frac{m_Z^2}{m_h^2+m_W^2-m_Z^2}\right)$$

$$+\frac{(m_W^2-2m_H^2-2m_Z^2)(m_W^2-m_Z^2)}{m_h^2m_W^2}\log\left(\frac{m_Z^2}{m_Z^2-m_W^2}\right)-3s_w^2t_w\left(\frac{2m_Z^2-4m_W^2}{m_W^3-m_Wm_Z^2}\log\left(\frac{m_W^2}{m_Z^2}\right)\right.$$

$$\left.+\frac{4m_Z(m_Z^2-m_W^2)}{m_W^3}\log\left(\frac{m_Z^2}{m_Z^2-m_W^2}\right)+\frac{m_Z(m_Z^2-2m_W^2)}{m_W^3}\log^2\left(\frac{m_W^2}{m_Z^2-m_W^2}\right)\right)\Bigg]$$

$$+48Q_u s_w^2\mathrm{Li}_2\left(2\right)-2\frac{m_h^4-4m_h^2m_W^2+5m_W^4}{m_W^4}\left(\mathrm{Li}_2\left(1-\frac{m_h^2}{m_W^2}\right)+\mathrm{Li}_2\left(\frac{m_h^2-2m_W^2}{m_h^2-m_W^2}\right)\right)$$

$$-2\frac{m_Z^4-4m_W^2m_Z^2+5m_W^4}{m_W^4}\left(\mathrm{Li}_2\left(1-\frac{m_Z^2}{m_W^2}\right)+\mathrm{Li}_2\left(\frac{m_Z^2-2m_W^2}{m_Z^2-m_W^2}\right)\right)$$

$$-24Q_u s_w^4t_w\frac{m_Z(m_Z^2-2m_W^2)}{m_W^3}\left(\mathrm{Li}_2\left(1-\frac{m_Z^2}{m_W^2}\right)+\mathrm{Li}_2\left(\frac{m_Z^2-2m_W^2}{m_Z^2-m_W^2}\right)\right)$$

$$+\left(2m_W^2-\frac{5}{2}m_h^2\right)C_0\left(m_h^2,m_W^2,m_h^2+m_W^2,m_W,m_W,0\right)+4Q_u s_w^2\Big(\left(2m_h^2+m_Z^2\right)\times$$

$$\times C_0\left(m_h^2,m_W^2,m_h^2+m_W^2,0,0,m_Z\right)-2m_h^2C_0\left(m_h^2,m_W^2,m_h^2+m_W^2,0,0,0\right)\Big)\Bigg\}$$

$$+\left(C_{\substack{dG\\11}}\to C_{\substack{uG\\11}}^\dagger,C_{\substack{dW\\11}}\to -C_{\substack{uW\\11}}^\dagger,C_{\substack{dB\\11}}\to C_{\substack{uB\\11}}^\dagger,d\leftrightarrow u\right) \tag{B.80}$$

where $C_0(s_1,s_{12},s_2,m_0,m_1,m_2)$ is the scalar Passarino-Veltman three-point function with kinematic invariants s_1,s_{12},s_2 and masses m_0,m_1,m_2 which can be evaluated numerically with computer programs like Package-X [100].

Contributions from $\psi^2\bar{\psi}^2$ operators

$$\mathrm{Im}\left[C_{\substack{Hud\\11}}\right]\times(4\pi\Lambda)^2\supset 4\sum_{i,j\in\{1,2,3\}}\frac{m_i m_j}{v^2}\mathrm{Im}\left[C^{(1)}_{\substack{ud\\1ji1}}+c_{F,3}C^{(8)}_{\substack{ud\\1ji1}}\right]\left\{1+2\log\left(\frac{2\Lambda}{m_i+m_j-(m_i-m_j)\mathrm{sgn}_{ij}}\right)\right.$$
$$\left.+\frac{1}{4}\left[2\,\mathrm{sgn}_{ij}+\frac{m_j^2}{m_W^2}\right]\log\left(\frac{m_i^2}{m_j^2}\right)+F(2m_W^2,m_i,m_j)\right\} \tag{B.81}$$

Here we defined

$$\mathrm{sgn}_{ij}=\mathrm{sgn}(m_i-m_j). \tag{B.82}$$

Contributions from ψ^2H^3 operators

$$\mathrm{Im}\left[C_{\substack{Hud\\11}}\right]\times(4\pi\Lambda)^2\supset\frac{m_u}{\sqrt{2}\,v}\left\{2\pi^2-2-2\pi^2\left[\frac{m_h^2}{m_W^2}+\frac{m_h^4}{2m_W^2}\right]\right. \tag{B.83}$$
$$+\frac{2\pi^2}{3}\left[\frac{m_Z^2}{m_W^2}+\frac{m_Z^4}{2m_W^4}\right]+\frac{3\,m_h^2-m_Z^2}{m_W^2}+$$
$$+6\left[2+\frac{m_H^2}{m_W^2}\right]\log\left(\frac{m_h}{m_W}\right)$$
$$-2\left[2+\frac{m_Z^2}{m_W^2}\right]\log\left(\frac{m_Z}{m_W}\right)-8\,\mathrm{Li}_2(2)$$
$$+3\left[1+2\frac{m_h^2}{m_W^2}+\frac{m_h^4}{m_W^4}\right]\left[\mathrm{Li}_2\left(1+\frac{m_h^2}{m_W^2}\right)+\frac{1}{2}\log^2\left(\frac{m_h^2}{m_W^2}\right)\right]$$
$$\left.-1\left[1+2\frac{m_Z^2}{m_W^2}+\frac{m_Z^4}{m_W^4}\right]\left[\mathrm{Li}_2\left(1+\frac{m_Z^2}{m_W^2}\right)+\frac{1}{2}\log^2\left(\frac{m_Z^2}{m_W^2}\right)\right]\right\}\mathrm{Im}\left[C_{\substack{dH\\11}}\right]$$
$$+\frac{m_d}{\sqrt{2}\,v}\times\{B.83\}\times\mathrm{Im}\left[C^{\dagger}_{\substack{uH\\11}}\right] \tag{B.84}$$

C Spurionic Expansion of the Wilson Coefficients and Form of Spurions

In this appendix we show the spurionic expansion of the Wilson coefficients with the different flavor symmetries, to introduce the notation we use to present the bounds. In addition we give expressions of the spurions in terms of Standard Model parameters which is fairly straightforward for the $U(3)$ flavor group and a bit more involved for the $U(2)$ group. We start with MFV, where we consider the biggest flavor group that is allowed by the gauge symmetry group of the Standard Model. As mentioned above we can simply identify the spurions with the Yukawa couplings since the full Yukawa matrices are the only source of flavor symmetry breaking. We work in the up-quark gauge basis where we explicitly have

$$y_u = \text{diag}\,(\lambda_u, \lambda_c, \lambda_t) \qquad y_d = V_{\text{CKM}}\text{diag}\,(\lambda_d, \lambda_s, \lambda_b) \qquad y_u = \text{diag}\,(\lambda_e, \lambda_\mu, \lambda_\tau)\ . \tag{C.1}$$

We find the following expansions for the Wilson coefficients appearing in the neutron EDM expression, in the up-basis defined above, keeping terms up to $\mathcal{O}(y^2_{u,d,e})$

$$C'_{\substack{uB\\pr}}\mathcal{O}'_{\substack{uB\\pr}} = C'_{\substack{uB\\pr}}\left(\bar{q}'_p\sigma^{\mu\nu}u'_r\right)\widetilde{H}B_{\mu\nu} \longrightarrow F_{uB}\left(\bar{q}'_p\sigma^{\mu\nu}u'_r\right)\widetilde{H}B_{\mu\nu}\left(\left(y_u\right)_{pr} + \mathcal{O}(y_i^3)\right) \tag{C.2}$$

$$C'_{\substack{Hud\\pr}}\mathcal{O}'_{\substack{Hud\\pr}} = C'_{\substack{Hud\\pr}}\left(\tilde{H}^\dagger iD_\mu H\right)\left(\bar{u}'_p\gamma^\mu d'_r\right) \longrightarrow F_{Hud}\left(\tilde{H}^\dagger iD_\mu H\right)\left(\bar{u}'_p\gamma^\mu d'_r\right)\left(\left(y_u^\dagger y_d\right)_{pr} + \mathcal{O}(y_i^4)\right) \tag{C.3}$$

$$C'_{\substack{uH\\pr}}\mathcal{O}'_{\substack{uH\\pr}} = C'_{\substack{uH\\pr}}|H|^2\left(\bar{q}'_p\widetilde{H}u'_r\right) \longrightarrow F_{uH}|H|^2\left(\bar{q}'_p\widetilde{H}u'_r\right)\left(\left(y_u\right)_{pr} + \mathcal{O}(y_i^3)\right) \tag{C.4}$$

$$\begin{aligned} C'^{(3)}_{\substack{lequ\\prst}}\mathcal{O}'^{(3)}_{\substack{lequ\\prst}} = C'^{(3)}_{\substack{lequ\\prst}}\left(\bar{l}'^i_p\sigma_{\mu\nu}e'_r\right)\epsilon_{ij}\left(\bar{q}'^j_s\sigma^{\mu\nu}u'_t\right) \longrightarrow F^{(3)}_{lequ}\left(\bar{l}'^i_p\sigma_{\mu\nu}e'_r\right)\epsilon_{ij}\left(\bar{q}'^j_s\sigma^{\mu\nu}u'_t\right)\times \\ \times\left[\left(y_e\right)_{pr}\left(y_u\right)_{st} + \mathcal{O}(y_i^4)\right] \end{aligned} \tag{C.5}$$

$$C'^{(1)}_{\substack{quqd\\prst}}\mathcal{O}'^{(1)}_{\substack{quqd\\prst}} = C'^{(1)}_{\substack{quqd\\prst}}\left(\bar{q}'^i_p u'_r\right)\epsilon_{ij}\left(\bar{q}'^j_s d'_t\right) \longrightarrow F^{(1)}_{quqd}\left(\bar{q}'^i_p u'_r\right)\epsilon_{ij}\left(\bar{q}'^j_s d'_t\right)\left[\left(y_u\right)_{pr}\left(y_d\right)_{st} + \mathcal{O}(y_i^4)\right] \tag{C.6}$$

$$\begin{aligned} C'^{(1)}_{\substack{qu\\prst}}\mathcal{O}'^{(1)}_{\substack{qu\\prst}} = C'^{(1)}_{\substack{qu\\prst}}\left(\bar{q}'_p\gamma_\mu q'_r\right)\left(\bar{u}'_s\gamma^\mu u'_t\right) \longrightarrow F^{(1)}_{qu}\left(\bar{q}'_p\gamma_\mu q'_r\right)\left(\bar{u}'_s\gamma^\mu u'_t\right)\times \\ \times\left[x_1\delta_{pr}\delta_{st} + x_2\left(\left(y_d y_d^\dagger\right)_{pr} + \left(y_u y_u^\dagger\right)_{pr}\right)\delta_{st} + x_3\delta_{pr}\left(y_u y_u^\dagger\right)_{st} + x_4\left(y_u\right)_{pt}\left(y_u^\dagger\right)_{sr} + \mathcal{O}(y_i^4)\right] \end{aligned} \tag{C.7}$$

$$C'^{(1)}_{\substack{ud\\prst}}\mathcal{O}'^{(1)}_{\substack{ud\\prst}} = C'^{(1)}_{\substack{ud\\prst}}\left(\bar{u}'_p\gamma_\mu u'_r\right)\left(\bar{d}'_s\gamma^\mu d'_t\right) \longrightarrow F^{(1)}_{ud}\left(\bar{u}'_p\gamma_\mu u'_r\right)\left(\bar{d}'_s\gamma^\mu d'_t\right)\left[0 + \mathcal{O}(y_i^4)\right]\ . \tag{C.8}$$

We noticed above that for the last operator to be CP violating, we have to take off-diagonal currents in flavor space. At the considered order those are not present and all the components of this Wilson coefficient are CP even. The expansions of all other Wilson coefficients which are not shown can be trivially obtained from those presented here.

Assuming the smaller symmetry group $U(2)^5$ we have to consider more spurions to make all Yukawa interactions invariant. The Yukawa matrices can then be parametrized in terms of the spurions as follows

$$Y_u = \lambda_t\begin{pmatrix}\Delta_u & x_t V_q\\ 0 & 1\end{pmatrix} \qquad Y_d = \lambda_b\begin{pmatrix}\Delta_d & x_b V_q\\ 0 & 1\end{pmatrix} \qquad Y_e = \lambda_\tau\begin{pmatrix}\Delta_e & x_\tau V_l\\ 0 & 1\end{pmatrix}. \tag{C.9}$$

In the up-quark basis this leaves us with the following expressions for the spurions in terms of Standard Model parameters

$$\begin{gathered}\Delta_e = \text{diag}(\delta'_e,\delta_e) \qquad \Delta_u = \text{diag}(\delta'_u,\delta_u) \qquad \Delta_d = O_d^T \text{diag}(\delta'_d,\delta_d) \\ V_q = \lambda_t \begin{pmatrix} V_{ub} \\ V_{cb} \end{pmatrix} \qquad V_l \in \mathbb{C}^2 \text{ unconstrained}\end{gathered} \tag{C.10}$$

with

$$\begin{gathered}(\delta'_u,\delta'_d,\delta'_e) \approx \left(\frac{\lambda_u}{\lambda_t},\frac{\lambda_d}{\lambda_b},\frac{\lambda_e}{\lambda_\tau}\right) \qquad (\delta_u,\delta_d,\delta_e) \approx \left(\frac{\lambda_c}{\lambda_t},\frac{\lambda_s}{\lambda_b},\frac{\lambda_\mu}{\lambda_\tau}\right) \\ O_d = \begin{pmatrix} c_d & s_d \\ -s_d & c_d \end{pmatrix} \qquad \frac{s_d}{c_d} = \frac{|V_{td}^*|}{|V_{ts}^*|} \qquad \alpha_d = \arg\left(\frac{V_{td}^*}{V_{ts}^*}\right).\end{gathered} \tag{C.11}$$

With these definitions we can once again construct all terms appearing in the expression of the neutron EDM. Since we have a consistent power counting now, we choose to work at an accuracy of $\mathcal{O}(10^{-2})$ which means that we have to keep terms up to $\mathcal{O}(V^2,\Delta)$. Following the notation in Ref. [81], we find, showing only the terms that can contribute the neutron EDM,

$$C'_{\substack{uB \\ pr}} \mathcal{O}'_{\substack{uB \\ pr}} \supset f_{uB} \left[\alpha_1 \bar{q}'_3 \sigma^{\mu\nu} u'_3 \widetilde{H} B_{\mu\nu} + \beta_1 \bar{Q}'^p V_q^p \sigma^{\mu\nu} u'_3 \widetilde{H} B_{\mu\nu} + \rho_1 \bar{Q}'_p \sigma^{\mu\nu} (\Delta_u)_{pr} U'_r \widetilde{H} B_{\mu\nu}\right] \tag{C.12}$$

$$C'_{\substack{Hud \\ pr}} \mathcal{O}'_{\substack{Hud \\ pr}} \supset f_{Hud} \left(\tilde{H}^\dagger i D_\mu H\right) \left(\alpha_1 \bar{u}'_3 \gamma^\mu d'_3\right) \tag{C.13}$$

$$C'_{\substack{uH \\ prst}} \mathcal{O}'_{\substack{uH \\ prst}} \supset f_{uH} |H|^2 \left[\rho_1 \bar{Q}'_p \widetilde{H} (\Delta_u)_{pr} U'_r + \beta_1 \bar{Q}'^p V_q^p \widetilde{H} d'_3 + \alpha_1 \bar{q}'_3 \widetilde{H} u'_3\right] \tag{C.14}$$

$$C'^{(3)}_{\substack{lequ \\ prst}} \mathcal{O}'^{(3)}_{\substack{lequ \\ prst}} \supset f^{(3)}_{lequ} \rho_1 \left(\bar{l}'^i_3 \sigma_{\mu\nu} e'_3\right) \epsilon_{ij} \left(\bar{Q}'^j_s \sigma^{\mu\nu} (\Delta_u)_{st} U'_t\right) \tag{C.15}$$

$$C'^{(1)}_{\substack{quqd \\ prst}} \mathcal{O}'^{(1)}_{\substack{quqd \\ prst}} \supset f^{(1)}_{quqd} \left[\rho_1 \left(\bar{q}'^i_3 (\Delta_u)_{pr} U'_r\right) \epsilon_{ij} \left(\bar{Q}'^j_p d'_3\right) + \rho_2 \left(\bar{Q}'^i_p (\Delta_d)_{pr} u'_3\right) \epsilon_{ij} \left(\bar{q}'^j_3 D'_r\right)\right] \tag{C.16}$$

$$C'^{(1)}_{\substack{qu \\ prst}} \mathcal{O}'^{(1)}_{\substack{qu \\ prst}} \supset f^{(1)}_{qu} \rho_1 \left(\bar{Q}'_p \gamma_\mu q'_3\right) (\Delta_u)_{pr} \left(\bar{u}'_3 \gamma^\mu U'_r\right) \tag{C.17}$$

$$\begin{aligned}C'^{(1)}_{\substack{qd \\ prst}} \mathcal{O}'^{(1)}_{\substack{qd \\ prst}} \supset f^{(1)}_{qd} \Big[&\rho_1 \left(\bar{Q}'_p \gamma_\mu q'_3\right) (\Delta_d)_{pr} \left(\bar{d}'_3 \gamma^\mu D'_r\right) + \beta_1 \left(\bar{Q}'^p V_q^p \gamma_\mu q'_3\right) \left(\bar{D}'_r \gamma^\mu D'_r\right) \\ &+ c_1 \left(\bar{Q}'^p V_q^p \gamma_\mu V_q^{\dagger r} Q'^r\right) \left(\bar{D}'_s \gamma^\mu D'_s\right)\Big].\end{aligned} \tag{C.18}$$

$$C'^{(1)}_{\substack{ud \\ prst}} \mathcal{O}'^{(1)}_{\substack{ud \\ prst}} \supset f^{(1)}_{ud} \left(\alpha_1 \bar{u}'_3 \gamma^\mu u'_3 \bar{d}'_3 \gamma^\mu d'_3\right) \tag{C.19}$$

For simplicity we will adopt the notation from Ref. [81] and write $C_X(Y) = f_X Y$, i.e. for example $C_{uG}(\rho_1) = f_{uG}\rho_1$.

D Bounds on Wilson coefficients and UV scale Λ

In this appendix we present the bounds on all Wilson coefficients that appear in the expression of the electron and neutron EDM. To give more meaningful bounds we factor out their naturally expected scaling in the Standard Model couplings. We also obtained bounds on the scale of new physics Λ by rescaling the Wilson coefficients by their natural scaling and demanding the remaining Wilson coefficient to be of order 1.

D.1 Electron EDM

Operator	Tree	Tree+Loop
$\mathrm{Im}\, C_{\substack{eB \\ 11}}$	$1.37 \cdot 10^{-5} \lambda_e g^{'}$	$1.70 \cdot 10^{-5} \lambda_e g^{'}$
$\mathrm{Im}\, C_{\substack{eW \\ 11}}$	$1.37 \cdot 10^{-5} \lambda_e g$	$1.68 \cdot 10^{-5} \lambda_e g$

Operator	RGE only	RGE + finite
$C_{H\widetilde{B}}$	$5.27 \cdot 10^{-3} g^{'2}$	$3.08 \cdot 10^{-3} g^{'2}$
$C_{H\widetilde{W}}$	$1.95 \cdot 10^{-3} g^2$	$1.18 \cdot 10^{-3} g^2$
$C_{HW\widetilde{B}}$	$1.52 \cdot 10^{-3} g g^{'}$	$2.12 \cdot 10^{-3} g g^{'}$
$C_{\widetilde{W}}$	—	$1.59 \cdot 10^{-2} g^3$

Operator	RGE only	RGE + finite
$\mathrm{Im}\, C^{(3)}_{\substack{lequ \\ 1111}}$	$5.43 \cdot 10^{4} \lambda_e \lambda_u$	—
$\mathrm{Im}\, C^{(3)}_{\substack{lequ \\ 1122}}$	$1.57 \cdot 10^{-1} \lambda_e \lambda_c$	—
$\mathrm{Im}\, C^{(3)}_{\substack{lequ \\ 1133}}$	$4.33 \cdot 10^{-5} \lambda_e \lambda_t$	—
$\mathrm{Im}\, C_{\substack{le \\ 1221}}$	—	$8.15 \cdot 10^{-5} g^{'2}$
$\mathrm{Im}\, C_{\substack{le \\ 1331}}$	—	$4.85 \cdot 10^{-6} g^{'2}$

Table 4: Upper bounds on the Wilson coefficients contributing to the EDM of the electron assuming $\Lambda = 5$ TeV and no further assumptions. In the upper left table the Wilson coefficients which can enter at tree level are presented. The column 'Tree+Loop' presents bounds including the tree level contribution, the RG running and all finite terms. In the other tables one can find all other Wilson coefficients which cannot enter at tree level. The left column shows only RG running, while the right column shows both RG running and finite terms. Above, the parameter λ_i is the i^{th} diagonal entry of the lepton Yukawa matrix.

Operator	Tree	Tree+Loop
$\mathrm{Im}\, C_{\substack{eB \\ 11}}$	$1.35 \cdot 10^3$	$1.11 \cdot 10^3$
$\mathrm{Im}\, C_{\substack{eW \\ 11}}$	$1.35 \cdot 10^3$	$1.13 \cdot 10^3$

Operator	RGE only	RGE + finite
$C_{H\widetilde{B}}$	$1.03 \cdot 10^2$	$1.2 \cdot 10^2$
$C_{H\widetilde{W}}$	$1.1 \cdot 10^2$	$1.27 \cdot 10^2$
$C_{HW\widetilde{B}}$	$1.62 \cdot 10^2$	$1.46 \cdot 10^2$
$C_{\widetilde{W}}$	—	$3.96 \cdot 10^1$

Operator	RGE only	RGE + finite
$\mathrm{Im}\, C^{(3)}_{\substack{lequ \\ 1111}}$	$1.73 \cdot 10^{-2}$	—
$\mathrm{Im}\, C^{(3)}_{\substack{lequ \\ 1122}}$	$1.30 \cdot 10^1$	—
$\mathrm{Im}\, C^{(3)}_{\substack{lequ \\ 1133}}$	$1.16 \cdot 10^3$	—
$\mathrm{Im}\, C_{\substack{le \\ 1221}}$	—	$5.54 \cdot 10^2$

Table 5: Lower bounds on the UV scale Λ in TeV assuming the natural scaling for all Wilson coefficients as given in the previous table and no further assumptions. The labeling of the tables is the same as for the bounds on the Wilson coefficients.

D.2 Neutron EDM

D.2.1 Bounds without Flavor Symmetries

Operator	Tree	Tree+Loop
$\mathrm{Im}\, C_{\substack{uG \\ 11}}$	$1.61 \cdot 10^{-2} \lambda_u g_s$	$3.91 \cdot 10^{-3} \lambda_u g_s$
$\mathrm{Im}\, C_{\substack{uB \\ 11}}$	$2.59 \cdot 10^{-2} \lambda_u g'$	$5.12 \cdot 10^{-2} \lambda_u g'$
$\mathrm{Im}\, C_{\substack{uW \\ 11}}$	$2.59 \cdot 10^{-2} \lambda_u g$	$4.19 \cdot 10^{-2} \lambda_u g$
$\mathrm{Im}\, C_{\substack{dG \\ 11}}$	$3.73 \cdot 10^{-3} \lambda_d g_s$	$1.11 \cdot 10^{-3} \lambda_d g_s$
$\mathrm{Im}\, C_{\substack{dB \\ 11}}$	$3.11 \cdot 10^{-3} \lambda_d g'$	$6.48 \cdot 10^{-3} \lambda_d g'$
$\mathrm{Im}\, C_{\substack{dW \\ 11}}$	$3.11 \cdot 10^{-3} \lambda_d g$	$5.44 \cdot 10^{-3} \lambda_d g$
$\mathrm{Im}\, C_{\substack{dB \\ 22}}$	$4.54 \cdot 10^{-2} \lambda_s g'$	$9.62 \cdot 10^{-2} \lambda_s g'$
$\mathrm{Im}\, C_{\substack{dW \\ 22}}$	$4.54 \cdot 10^{-2} \lambda_s g$	$8.95 \cdot 10^{-2} \lambda_s g$

Operator	RGE only	RGE + finite
$\mathrm{Im}\, C_{\substack{dG \\ 22}}$	$7.42 \cdot 10^{-2} \lambda_s g_s$	$2.19 \cdot 10^{-2} \lambda_s g_s$
$\mathrm{Im}\, C_{\substack{uG \\ 22}}$	—	$1.65 \cdot 10^{-2} \lambda_c g_s$
$\mathrm{Im}\, C_{\substack{dG \\ 33}}$	—	$1.65 \cdot 10^{-2} \lambda_b g_s$
$\mathrm{Im}\, C_{\substack{uG \\ 33}}$	—	$1.65 \cdot 10^{-2} \lambda_t g_s$

Table 6: Upper bounds on the Wilson coefficients of the dipole operators assuming $\Lambda = 5$ TeV and no further assumptions. On the left-hand side the coefficients are presented which can enter at tree level. The column 'Tree+Loop' presents bounds including the tree level contribution, the RG running and all finite terms. On the right-hand side one can find all elements which cannot enter at tree level. The left column shows only RG running, while the right column shows both RG running and finite terms. Above, the parameter λ_i is the i^{th} diagonal entry of the corresponding diagonalized quark Yukawa matrix here and in all tables that follow.

Operator	RGE only	RGE + finite
$C_{H\widetilde{G}}$	$9.40 \cdot 10^{-3} g_s^2$	$7.81 \cdot 10^{-3} g_s^2$
$C_{H\widetilde{B}}$	$2.04 \cdot 10^{0} g'^2$	$1.53 \cdot 10^{0} g'^2$
$C_{H\widetilde{W}}$	$2.99 \cdot 10^{-1} g^2$	$2.62 \cdot 10^{-1} g^2$
$C_{HW\widetilde{B}}$	$1.76 \cdot 10^{-1} g g'$	$1.61 \cdot 10^{-1} g g'$
$C_{\widetilde{W}}$	—	$3.46 \cdot 10^{0} g^3$
$C_{\widetilde{G}}$	$4.74 \cdot 10^{-5} g_s^3$	$6.91 \cdot 10^{-5} g_s^3$

Operator	RGE only	RGE + finite
$\mathrm{Im}\, C_{\substack{Hud \\ 11}}$	$1.87 \cdot 10^{-2} g'^2$	$2.03 \cdot 10^{-2} g'^2$
$\mathrm{Im}\, C_{\substack{Hud \\ 31}}$	—	$1.03 \cdot 10^{-2} g'^2$
$\mathrm{Re}\, C_{\substack{Hud \\ 31}}$	—	$3.53 \cdot 10^{-3} g'^2$
$\mathrm{Im}\, C_{\substack{uH \\ 11}}$	—	$1.33 \cdot 10^{9} \lambda_u$
$\mathrm{Im}\, C_{\substack{dH \\ 11}}$	—	$1.33 \cdot 10^{9} \lambda_d$

Table 7: Upper bounds on the Wilson coefficients of the bosonic operators on the left and the $\psi\bar{\psi}H^2D$ and ψ^2H^3 type operators on the right assuming $\Lambda = 5$ TeV and no further assumptions. The 'RGE + finite' column for $C_{\substack{Hud \\ 11}}$ also includes the tree level contribution.

Operator	RGE only	RGE + finite
$\mathrm{Im}\, C'^{(3)}_{lequ\,1111}$	$7.54 \cdot 10^{9} \lambda_e \lambda_u$	—
$\mathrm{Im}\, C'^{(3)}_{lequ\,2211}$	$1.76 \cdot 10^{5} \lambda_\mu \lambda_u$	—
$\mathrm{Im}\, C'^{(3)}_{lequ\,2211}$	$6.21 \cdot 10^{2} \lambda_\tau \lambda_u$	—
$\mathrm{Im}\, V^\dagger_{1i} C'^{(1)}_{quqd\,i111}$	$1.88 \cdot 10^{7} \lambda_u \lambda_d$	$1.84 \cdot 10^{7} \lambda_u \lambda_d$
$\mathrm{Im}\, V^\dagger_{1i} C'^{(8)}_{quqd\,i111}$	$3.82 \cdot 10^{7} \lambda_u \lambda_d$	$3.73 \cdot 10^{7} \lambda_u \lambda_d$
$\mathrm{Im}\, V^\dagger_{1i} C'^{(1)}_{quqd\,i221}$	$7.79 \cdot 10^{2} \lambda_c \lambda_d$	—
$\mathrm{Im}\, V^\dagger_{1i} C'^{(8)}_{quqd\,i221}$	$1.56 \cdot 10^{3} \lambda_c \lambda_d$	—
$\mathrm{Im}\, V^\dagger_{1i} C'^{(1)}_{quqd\,i331}$	$9.86 \cdot 10^{-2} \lambda_t \lambda_d$	—
$\mathrm{Im}\, V^\dagger_{1i} C'^{(8)}_{quqd\,i331}$	$1.98 \cdot 10^{-1} \lambda_t \lambda_d$	—
$\mathrm{Im}\, V^\dagger_{2i} C'^{(1)}_{quqd\,i112}$	$9.35 \cdot 10^{5} \lambda_u \lambda_s$	—
$\mathrm{Im}\, V^\dagger_{2i} C'^{(8)}_{quqd\,i111}$	$1.03 \cdot 10^{7} \lambda_u \lambda_s$	—
$\mathrm{Im}\, V^\dagger_{2i} C'^{(1)}_{quqd\,i222}$	$2.56 \cdot 10^{4} \lambda_c \lambda_s$	—
$\mathrm{Im}\, V^\dagger_{2i} C'^{(8)}_{quqd\,i222}$	$1.92 \cdot 10^{4} \lambda_c \lambda_s$	—
$\mathrm{Im}\, V^\dagger_{2i} C'^{(1)}_{quqd\,i332}$	$3.24 \cdot 10^{0} \lambda_t \lambda_s$	—
$\mathrm{Im}\, V^\dagger_{2i} C'^{(8)}_{quqd\,i332}$	$2.43 \cdot 10^{0} \lambda_t \lambda_s$	—
$\mathrm{Im}\, V^\dagger_{3i} C'^{(1)}_{quqd\,i113}$	$5.15 \cdot 10^{2} \lambda_u \lambda_b$	—
$\mathrm{Im}\, V^\dagger_{3i} C'^{(8)}_{quqd\,i113}$	$5.65 \cdot 10^{3} \lambda_u \lambda_b$	—
$\mathrm{Im}\, C'^{(1)}_{qu\,1221}$	—	$5.79 \cdot 10^{-2} g'^2$
$\mathrm{Im}\, C'^{(8)}_{qu\,1221}$	—	$4.70 \cdot 10^{-2} g'^2$
$\mathrm{Im}\, C'^{(1)}_{qu\,1331}$	—	$3.76 \cdot 10^{-4} g'^2$
$\mathrm{Im}\, C'^{(8)}_{qu\,1331}$	—	$4.03 \cdot 10^{-4} g'^2$
$\mathrm{Im}\, V^\dagger_{1i} V_{j1} C'^{(1)}_{qd\,ij11}$	—	$7.66 \cdot 10^{-1} g'^2$
$\mathrm{Im}\, V^\dagger_{1i} V_{j1} C'^{(8)}_{qd\,ij11}$	—	$6.60 \cdot 10^{-1} g'^2$
$\mathrm{Im}\, V^\dagger_{1i} V_{j2} C'^{(1)}_{qd\,ij21}$	—	$3.85 \cdot 10^{-1} g'^2$
$\mathrm{Im}\, V^\dagger_{1i} V_{j2} C'^{(8)}_{qd\,ij21}$	—	$3.31 \cdot 10^{-1} g'^2$
$\mathrm{Im}\, V^\dagger_{1i} V_{j3} C'^{(1)}_{qd\,ij31}$	—	$8.56 \cdot 10^{-2} g'^2$
$\mathrm{Im}\, V^\dagger_{1i} V_{j3} C'^{(8)}_{qd\,ij31}$	—	$7.37 \cdot 10^{-3} g'^2$
$\mathrm{Im}\, V^\dagger_{2i} V_{j1} C'^{(1)}_{qd\,ij12}$	—	$3.35 \cdot 10^{3} g'^2$
$\mathrm{Im}\, V^\dagger_{2i} V_{j1} C'^{(8)}_{qd\,ij12}$	—	$2.52 \cdot 10^{3} g'^2$
$\mathrm{Im}\, V^\dagger_{2i} V_{j2} C'^{(1)}_{qd\,ij22}$	—	$1.68 \cdot 10^{2} g'^2$
$\mathrm{Im}\, V^\dagger_{2i} V_{j2} C'^{(8)}_{qd\,ij22}$	—	$1.26 \cdot 10^{2} g'^2$
$\mathrm{Im}\, V^\dagger_{2i} V_{j3} C'^{(1)}_{qd\,ij32}$	—	$3.75 \cdot 10^{0} g'^2$
$\mathrm{Im}\, V^\dagger_{2i} V_{j3} C'^{(8)}_{qd\,ij32}$	—	$2.81 \cdot 10^{0} g'^2$
$\mathrm{Im}\, C'^{(1)}_{ud\,1331}$	$9.30 \cdot 10^{0} g'^2$	$7.17 \cdot 10^{0} g'^2$
$\mathrm{Im}\, C'^{(8)}_{ud\,1321}$	$6.98 \cdot 10^{0} g'^2$	$5.38 \cdot 10^{0} g'^2$

Table 8: Upper bounds on the Wilson coefficients of the 4-fermion operators assuming $\Lambda = 5$ TeV and no further assumptions. Notice that each entry of the table corresponds to one the mass-basis Wilson coefficients that enter the expression of the neutron EDM. For all of them, however, the corresponding C' Wilson coefficients in the up-quark gauge basis are indicated, together with the CKM transformations needed to the change of basis. Wherever the phase of the CKM matrix enters in the bound, the bound is given on the real instead of the imaginary part. If the summation over the CKM elements gives a symmetric contribution for the operator $O^{(1,8)}_{qd}$, they have to be ignored because they are CP even and cannot give rise to an EDM. Note also, that the 'RGE + finite' column for $V^\dagger_{1i} C'^{(1,8)}_{quqd\,i111}$ includes the tree level contribution.

Operator	Tree	Tree+Loop
$\mathrm{Im}\, C_{\substack{uG \\ 11}}$	$3.93 \cdot 10^1$	$8.55 \cdot 10^1$
$\mathrm{Im}\, C_{\substack{uB \\ 11}}$	$3.11 \cdot 10^1$	$1.98 \cdot 10^1$
$\mathrm{Im}\, C_{\substack{uW \\ 11}}$	$3.11 \cdot 10^1$	$2.30 \cdot 10^1$
$\mathrm{Im}\, C_{\substack{dG \\ 11}}$	$8.19 \cdot 10^1$	$1.65 \cdot 10^2$
$\mathrm{Im}\, C_{\substack{dB \\ 11}}$	$8.96 \cdot 10^1$	$4.97 \cdot 10^1$
$\mathrm{Im}\, C_{\substack{dW \\ 11}}$	$8.96 \cdot 10^1$	$5.94 \cdot 10^1$
$\mathrm{Im}\, C_{\substack{dB \\ 22}}$	$2.35 \cdot 10^1$	$1.47 \cdot 10^1$
$\mathrm{Im}\, C_{\substack{dW \\ 22}}$	$2.35 \cdot 10^1$	$1.54 \cdot 10^1$

Operator	RGE only	RGE + finite
$\mathrm{Im}\, C_{\substack{dG \\ 22}}$	$3.26 \cdot 10^1$	$1.99 \cdot 10^1$
$\mathrm{Im}\, C_{\substack{uG \\ 22}}$	—	$3.89 \cdot 10^1$
$\mathrm{Im}\, C_{\substack{dG \\ 33}}$	—	$3.89 \cdot 10^1$
$\mathrm{Im}\, C_{\substack{uG \\ 33}}$	—	$3.89 \cdot 10^1$

Table 9: Lower bounds on the UV scale Λ in TeV assuming natural scaling of the dipole Wilson coefficients and no further assumptions. On the left-hand side the coefficients are presented which can enter at tree level. The column 'Tree+Loop' presents bounds including the tree level contribution, the RG running and all finite terms. On the right-hand side one can find all elements which cannot enter at tree level. The left column shows only RG running, while the right column shows both RG running and finite terms.

Operator	RGE only	RGE + finite
$C_{H\widetilde{G}}$	$6.73 \cdot 10^1$	$7.16 \cdot 10^1$
$C_{H\widetilde{B}}$	$3.29 \cdot 10^0$	$3.94 \cdot 10^0$
$C_{H\widetilde{W}}$	$9.97 \cdot 10^0$	$1.06 \cdot 10^1$
$C_{HW\widetilde{B}}$	$1.33 \cdot 10^1$	$1.38 \cdot 10^1$
$C_{\widetilde{W}}$	—	$2.69 \cdot 10^0$
$C_{\widetilde{G}}$	$1.09 \cdot 10^3$	$1.01 \cdot 10^3$

Operator	RGE only	RGE + finite
$\mathrm{Im}\, C_{\substack{Hud \\ 11}}$	$3.67 \cdot 10^1$	$3.53 \cdot 10^1$
$\mathrm{Im}\, C_{\substack{Hud \\ 31}}$	—	$4.93 \cdot 10^1$
$\mathrm{Re}\, C_{\substack{Hud \\ 31}}$	—	$8.42 \cdot 10^1$
$\mathrm{Im}\, C_{\substack{uH \\ 11}}$	—	$1.37 \cdot 10^{-4}$
$\mathrm{Im}\, C_{\substack{dH \\ 11}}$	—	$1.37 \cdot 10^{-4}$

Table 10: Lower bounds on the UV scale Λ in TeV assuming natural scaling for the Wilson coefficients of the bosonic operators and no further assumptions. The 'RGE + finite' column for $C_{\substack{Hud \\ 11}}$ also includes the tree level contribution.

Operator	RGE only	RGE + finite
$\mathrm{Im}\, C'^{(3)}_{lequ\,1111}$	$4.02 \cdot 10^{-5}$	—
$\mathrm{Im}\, C'^{(3)}_{lequ\,2211}$	$1.62 \cdot 10^{-3}$	—
$\mathrm{Im}\, C'^{(3)}_{lequ\,3311}$	$1.49 \cdot 10^{-1}$	—
$\mathrm{Im}\, V^\dagger_{1i} C'^{(1)}_{quqd\,i111}$	$5.85 \cdot 10^{-4}$	$6.14 \cdot 10^{-4}$
$\mathrm{Im}\, V^\dagger_{1i} C'^{(8)}_{quqd\,i111}$	$6.42 \cdot 10^{-4}$	$6.55 \cdot 10^{-4}$
$\mathrm{Im}\, V^\dagger_{1i} C'^{(1)}_{quqd\,i221}$	$1.32 \cdot 10^{-1}$	—
$\mathrm{Im}\, V^\dagger_{1i} C'^{(8)}_{quqd\,i221}$	$8.84 \cdot 10^{-2}$	—
$\mathrm{Im}\, V^\dagger_{1i} C'^{(1)}_{quqd\,i331}$	$1.88 \cdot 10^{1}$	—
$\mathrm{Im}\, V^\dagger_{1i} C'^{(8)}_{quqd\,i331}$	$1.27 \cdot 10^{1}$	—
$\mathrm{Im}\, V^\dagger_{2i} C'^{(1)}_{quqd\,i112}$	$1.22 \cdot 10^{-3}$	—
$\mathrm{Im}\, V^\dagger_{2i} C'^{(8)}_{quqd\,i112}$	$5.96 \cdot 10^{-4}$	—
$\mathrm{Im}\, V^\dagger_{2i} C'^{(1)}_{quqd\,i222}$	$1.64 \cdot 10^{-2}$	—
$\mathrm{Im}\, V^\dagger_{2i} C'^{(8)}_{quqd\,i222}$	$1.97 \cdot 10^{-2}$	—
$\mathrm{Im}\, V^\dagger_{2i} C'^{(1)}_{quqd\,i332}$	$2.47 \cdot 10^{0}$	—
$\mathrm{Im}\, V^\dagger_{2i} C'^{(8)}_{quqd\,i332}$	$2.94 \cdot 10^{0}$	—
$\mathrm{Im}\, V^\dagger_{3i} C'^{(1)}_{quqd\,i113}$	$1.58 \cdot 10^{-1}$	—
$\mathrm{Im}\, V^\dagger_{3i} C'^{(8)}_{quqd\,i113}$	$3.69 \cdot 10^{-2}$	—

Operator	RGE only	RGE + finite
$\mathrm{Im}\, C'^{(1)}_{qu\,1221}$	—	$2.08 \cdot 10^{1}$
$\mathrm{Im}\, C'^{(8)}_{qu\,1221}$	—	$2.31 \cdot 10^{1}$
$\mathrm{Im}\, C'^{(1)}_{qu\,1331}$	—	$2.50 \cdot 10^{2}$
$\mathrm{Im}\, C'^{(8)}_{qu\,1331}$	—	$2.59 \cdot 10^{2}$
$\mathrm{Im}\, V^\dagger_{1i} V_{j1} C'^{(1)}_{qd\,ij11}$	—	$1.81 \cdot 10^{0}$
$\mathrm{Im}\, V^\dagger_{1i} V_{j1} C'^{(8)}_{qd\,ij11}$	—	$1.95 \cdot 10^{0}$
$\mathrm{Im}\, V^\dagger_{1i} V_{j2} C'^{(1)}_{qd\,ij21}$	—	$8.06 \cdot 10^{0}$
$\mathrm{Im}\, V^\dagger_{1i} V_{j2} C'^{(8)}_{qd\,ij21}$	—	$8.69 \cdot 10^{0}$
$\mathrm{Im}\, V^\dagger_{1i} V_{j3} C'^{(1)}_{qd\,ij31}$	—	$5.40 \cdot 10^{1}$
$\mathrm{Im}\, V^\dagger_{1i} V_{j3} C'^{(8)}_{qd\,ij31}$	—	$5.82 \cdot 10^{1}$
$\mathrm{Im}\, V^\dagger_{2i} V_{j1} C'^{(1)}_{qd\,ij12}$	—	$8.63 \cdot 10^{-2}$
$\mathrm{Im}\, V^\dagger_{2i} V_{j1} C'^{(8)}_{qd\,ij12}$	—	$9.97 \cdot 10^{-2}$
$\mathrm{Im}\, V^\dagger_{2i} V_{j2} C'^{(1)}_{qd\,ij22}$	—	$3.85 \cdot 10^{-1}$
$\mathrm{Im}\, V^\dagger_{2i} V_{j2} C'^{(8)}_{qd\,ij22}$	—	$4.45 \cdot 10^{-1}$
$\mathrm{Im}\, V^\dagger_{2i} V_{j3} C'^{(1)}_{qd\,ij32}$	—	$2.58 \cdot 10^{0}$
$\mathrm{Im}\, V^\dagger_{2i} V_{j3} C'^{(8)}_{qd\,ij32}$	—	$2.98 \cdot 10^{0}$
$\mathrm{Im}\, C'^{(1)}_{ud\,1331}$	$1.26 \cdot 10^{0}$	$1.61 \cdot 10^{0}$
$\mathrm{Im}\, C'^{(8)}_{ud\,1321}$	$1.52 \cdot 10^{0}$	$1.90 \cdot 10^{0}$

Table 11: Lower bounds on the UV scale Λ in TeV assuming natural scaling of the Wilson coefficients of the 4-fermion operators. Notice that each entry of the table corresponds to one the mass-basis Wilson coefficients that enter the expression of the neutron EDM. For all of them, however, the corresponding C' Wilson coefficients in the up-quark gauge basis are indicated, together with the CKM transformations needed to the change of basis. Wherever the phase of the CKM matrix enters in the bound, the bound is given from the real instead of the imaginary part of the Wilson coefficient. If the summation over the CKM elements gives a symmetric contribution for the operator $O^{(1,8)}_{qd}$, they have to be ignored because they are CP even and cannot give rise to an EDM. Note also, that the 'RGE + finite' column for $V^\dagger_{1i} C'^{(1,8)}_{quqd\,i111}$ includes the tree level contribution.

D.2.2 Bounds with Flavor Symmetries

We present here the bounds obtained when a $U(3)^5$ or $U(2)^5$ flavor symmetry is imposed in the SMEFT. The results for the purely bosonic operators are not presented, since they are left unchanged with respect the flavor generic scenario discussed previously.

Operator	Tree	Tree+Loop
Im F_{uG}	$2.99 \cdot 10^{-2}$	$4.93 \cdot 10^{-3}$
Im F_{uB}	$9.25 \cdot 10^{-3}$	$1.83 \cdot 10^{-2}$
Im F_{uW}	$1.69 \cdot 10^{-2}$	$2.73 \cdot 10^{-2}$
Im F_{dG}	$7.10 \cdot 10^{-3}$	$1.89 \cdot 10^{-3}$
Im F_{dB}	$1.23 \cdot 10^{-3}$	$2.55 \cdot 10^{-3}$
Im F_{dW}	$2.24 \cdot 10^{-3}$	$3.88 \cdot 10^{-3}$
Im $F^{(1)}_{quqd}$	$5.90 \cdot 10^{7}$	$3.40 \cdot 10^{3}$
Im $F^{(8)}_{quqd}$	$5.90 \cdot 10^{7}$	$2.93 \cdot 10^{3}$
Im F_{Hud}	—	—

Operator	RGE only	RGE + finite
Im $F^{(3)}_{lequ}$	$6.19 \cdot 10^{2}$	—
Im $F^{(1,8)}_{qu}$	—	—
Im $F^{(1,8)}_{qd}$	—	—
Im $F^{(1,8)}_{ud}$	—	—
Im F_{uH}	—	$1.33 \cdot 10^{9}$
Im F_{dH}	—	$1.33 \cdot 10^{9}$

Table 12: Upper bounds on the Wilson coefficients assuming $\Lambda = 5$ TeV and a $U(3)^5$ flavor symmetry, keeping terms up to $\mathcal{O}(y^2_{u,d,e})$. The dipoles can again enter at tree level while the 4-fermion operators all only contribute via RG running. The operators $O^{(1,8)}_{qu}, O^{(1,8)}_{qd}, O^{(1,8)}_{ud}$ and O_{Hud} are forbidden at the considered order in the spurions. The bounds on all bosonic operators are obviously the same as above.

Operator	Tree	Tree+Loop
Im F_{uG}	$2.89 \cdot 10^{1}$	$7.45 \cdot 10^{1}$
Im F_{uB}	$5.20 \cdot 10^{1}$	$3.16 \cdot 10^{1}$
Im F_{uW}	$3.85 \cdot 10^{1}$	$2.82 \cdot 10^{1}$
Im F_{dG}	$5.93 \cdot 10^{1}$	$1.24 \cdot 10^{2}$
Im F_{dB}	$1.43 \cdot 10^{2}$	$7.51 \cdot 10^{1}$
Im F_{dW}	$1.06 \cdot 10^{2}$	$7.00 \cdot 10^{1}$
Im $F^{(1)}_{quqd}$	$6.51 \cdot 10^{-4}$	$4.76 \cdot 10^{-2}$
Im $F^{(8)}_{quqd}$	$6.51 \cdot 10^{-4}$	$5.21 \cdot 10^{-2}$
Im F_{Hud}	—	—

Operator	RGE only	RGE + finite
Im $F^{(3)}_{lequ}$	$1.50 \cdot 10^{-1}$	—
Im $F^{(1,8)}_{qu}$	—	—
Im $F^{(1,8)}_{qd}$	—	—
Im $F^{(1,8)}_{ud}$	—	—
Im F_{uH}	—	$1.37 \cdot 10^{-4}$
Im F_{dH}	—	$1.37 \cdot 10^{-4}$

Table 13: Lower bounds on the UV scale Λ in TeV, assuming $F_i = 1$ for all the coefficients of the operators, under a $U(3)^5$ flavor symmetry, keeping terms up to $\mathcal{O}(y^2_{u,d,e})$.

Operator	Tree	Tree+Loop
$\mathrm{Im}\, C_{uG}(\alpha_1)$	—	$3.05 \cdot 10^{-2}$
$\mathrm{Im}\, C_{uG}(\rho_1)$	$2.97 \cdot 10^{-2}$	$5.83 \cdot 10^{-3}$
$\mathrm{Im}\, C_{uB}(\rho_1)$	$9.19 \cdot 10^{-3}$	$1.82 \cdot 10^{-2}$
$\mathrm{Im}\, C_{uW}(\rho_1)$	$1.68 \cdot 10^{-2}$	$2.71 \cdot 10^{-2}$
$\mathrm{Im}\, C_{dG}(\alpha_1)$	—	$7.38 \cdot 10^{-4}$
$\mathrm{Im}\, C_{dG}(\rho_1)$	$1.83 \cdot 10^{-4}$	$5.22 \cdot 10^{-5}$
$\mathrm{Im}\, C_{dG}(\beta_1)$	—	$4.23 \cdot 10^{-1}$
$\mathrm{Re}\, C_{dG}(\beta_1)$	—	$3.09 \cdot 10^{1}$
$\mathrm{Im}\, C_{dB}(\rho_1)$	$3.17 \cdot 10^{-5}$	$6.59 \cdot 10^{-5}$
$\mathrm{Im}\, C_{dW}(\rho_1)$	$5.78 \cdot 10^{-5}$	$1.00 \cdot 10^{-4}$
$\mathrm{Im}\, C^{(1)}_{quqd}(\rho_1)$	—	$1.23 \cdot 10^{1}$
$\mathrm{Im}\, C^{(1)}_{quqd}(\rho_2)$	—	$2.68 \cdot 10^{-3}$
$\mathrm{Im}\, C^{(8)}_{quqd}(\rho_1)$	—	$1.35 \cdot 10^{2}$
$\mathrm{Im}\, C^{(8)}_{quqd}(\rho_2)$	—	$5.66 \cdot 10^{-3}$

Operator	RGE only	RGE + finite
$\mathrm{Im}\, C^{(3)}_{lequ}(\rho_1)$	$6.30 \cdot 10^{0}$	—
$\mathrm{Im}\, C^{(1)}_{qu}(\rho_1)$	—	$3.85 \cdot 10^{0}$
$\mathrm{Im}\, C^{(8)}_{qu}(\rho_1)$	—	$4.12 \cdot 10^{0}$
$\mathrm{Im}\, C^{(1)}_{qd}(\rho_1)$	—	$1.03 \cdot 10^{0}$
$\mathrm{Im}\, C^{(1)}_{qd}(\beta_1)$	—	$2.35 \cdot 10^{3}$
$\mathrm{Re}\, C^{(1)}_{qd}(c_1)$	—	$6.78 \cdot 10^{3}$
$\mathrm{Im}\, C^{(8)}_{qd}(\rho_1)$	—	$9.80 \cdot 10^{-1}$
$\mathrm{Im}\, C^{(8)}_{qd}(\beta_1)$	—	$8.73 \cdot 10^{3}$
$\mathrm{Re}\, C^{(8)}_{qd}(c_1)$	—	$5.30 \cdot 10^{3}$
$\mathrm{Im}\, C_{uH}(\rho_1)$	—	$1.32 \cdot 10^{9}$
$\mathrm{Im}\, C_{dH}(\rho_1)$	—	$3.53 \cdot 10^{7}$

Table 14: Upper bounds on the Wilson coefficients assuming $\Lambda = 5$ TeV and a $U(2)^5$ flavor symmetry, keeping terms up to $\mathcal{O}(\Delta, V^2)$. We use the notation of Ref. [82] for the Wilson coefficients (see also App. C). The operators O_{Hud} and $O^{(1,8)}_{ud}$ don't contribute at the considered order.

Operator	Tree	Tree+Loop
$\mathrm{Im}\, C_{uG}(\alpha_1)$	—	$2.86 \cdot 10^{1}$
$\mathrm{Im}\, C_{uG}(\rho_1)$	$2.90 \cdot 10^{1}$	$6.89 \cdot 10^{1}$
$\mathrm{Im}\, C_{uB}(\rho_1)$	$5.22 \cdot 10^{1}$	$3.17 \cdot 10^{1}$
$\mathrm{Im}\, C_{uW}(\rho_1)$	$3.86 \cdot 10^{1}$	$2.83 \cdot 10^{1}$
$\mathrm{Im}\, C_{dG}(\alpha_1)$	—	$1.84 \cdot 10^{2}$
$\mathrm{Im}\, C_{dG}(\rho_1)$	$3.69 \cdot 10^{2}$	$7.85 \cdot 10^{2}$
$\mathrm{Im}\, C_{dG}(\beta_1)$	—	$7.69 \cdot 10^{0}$
$\mathrm{Re}\, C_{dG}(\beta_1)$	—	$8.99 \cdot 10^{-1}$
$\mathrm{Im}\, C_{dB}(\rho_1)$	$8.88 \cdot 10^{2}$	$3.55 \cdot 10^{2}$
$\mathrm{Im}\, C_{dW}(\rho_1)$	$6.58 \cdot 10^{2}$	$3.88 \cdot 10^{2}$
$\mathrm{Im}\, C^{(1)}_{quqd}(\rho_1)$	—	$1.28 \cdot 10^{0}$
$\mathrm{Im}\, C^{(1)}_{quqd}(\rho_2)$	—	$1.36 \cdot 10^{2}$
$\mathrm{Im}\, C^{(8)}_{quqd}(\rho_1)$	—	$3.39 \cdot 10^{-1}$
$\mathrm{Im}\, C^{(8)}_{quqd}(\rho_2)$	—	$9.06 \cdot 10^{1}$

Operator	RGE only	RGE + finite
$\mathrm{Im}\, C^{(3)}_{lequ}(\rho_1)$	$1.86 \cdot 10^{0}$	—
$\mathrm{Im}\, C^{(1)}_{qu}(\rho_1)$	—	$2.58 \cdot 10^{0}$
$\mathrm{Im}\, C^{(8)}_{qu}(\rho_1)$	—	$2.42 \cdot 10^{0}$
$\mathrm{Im}\, C^{(1)}_{qd}(\rho_1)$	—	$4.92 \cdot 10^{0}$
$\mathrm{Im}\, C^{(1)}_{qd}(\beta_1)$	—	$1.03 \cdot 10^{-1}$
$\mathrm{Re}\, C^{(1)}_{qd}(c_1)$	—	$6.07 \cdot 10^{-2}$
$\mathrm{Im}\, C^{(8)}_{qd}(\rho_1)$	—	$5.05 \cdot 10^{0}$
$\mathrm{Im}\, C^{(8)}_{qd}(\beta_1)$	—	$5.35 \cdot 10^{-2}$
$\mathrm{Re}\, C^{(8)}_{qd}(c_1)$	—	$6.87 \cdot 10^{-2}$
$\mathrm{Im}\, C_{uH}(\rho_1)$	—	$1.37 \cdot 10^{-4}$
$\mathrm{Im}\, C_{dH}(\rho_1)$	—	$8.41 \cdot 10^{-4}$

Table 15: Lower bounds on the UV scale Λ in TeV assuming $C_X(Y) = 1$ for all the coefficients of the operators, under a $U(2)^5$ flavor symmetry, keeping terms up to $\mathcal{O}(\Delta, V^2)$.

References

[1] V. Andreev, *Improved limit on the electric dipole moment of the electron*, *Nature* **562** (oct, 2018) 355–360.

[2] Muon (g-2) collaboration, G. W. Bennett et al., *An Improved Limit on the Muon Electric Dipole Moment*, *Phys. Rev. D* **80** (2009) 052008, [0811.1207].

[3] A. G. Grozin, I. B. Khriplovich and A. S. Rudenko, *Electric dipole moments, from e to tau*, *Phys. Atom. Nucl.* **72** (2009) 1203–1205, [0811.1641].

[4] C. Abel, S. Afach, N. J. Ayres, C. A. Baker, G. Ban, G. Bison et al., *Measurement of the permanent electric dipole moment of the neutron*, *Phys. Rev. Lett.* **124** (Feb, 2020) 081803.

[5] D. Buttazzo and P. Paradisi, *Probing the muon g-2 anomaly at a Muon Collider*, 2012.02769.

[6] J. Doyle, "*Search for the Electric Dipole Moment of the Electron with Thorium Monoxide – The ACME Experiment.*" Talk at the KITP, September 2016.

[7] n2EDM collaboration, N. J. Ayres et al., *The design of the n2EDM experiment*, 2101.08730.

[8] M. Pospelov and A. Ritz, *CKM benchmarks for electron electric dipole moment experiments*, *Phys. Rev. D* **89** (2014) 056006, [1311.5537].

[9] I. Khriplovich and A. Zhitnitsky, *What is the value of the neutron electric dipole moment in the kobayashi-maskawa model?*, *Physics Letters B* **109** (1982) 490–492.

[10] C. Jarlskog, *Commutator of the quark mass matrices in the standard electroweak model and a measure of maximal* CP *nonconservation*, *Phys. Rev. Lett.* **55** (Sep, 1985) 1039–1042.

[11] C. Smith and S. Touati, *Edm with and beyond flavor invariants*, 1707.06805.

[12] R. D. Peccei and H. R. Quinn, *Constraints imposed by* CP *conservation in the presence of pseudoparticles*, *Phys. Rev. D* **16** (Sep, 1977) 1791–1797.

[13] UTfit collaboration, M. Bona et al., *Model-independent constraints on $\Delta F = 2$ operators and the scale of new physics*, *JHEP* **03** (2008) 049, [0707.0636].

[14] UTfit collaboration, *Latest results from UTfit* , 2016.

[15] G. F. Giudice and A. Romanino, *Electric dipole moments in split supersymmetry*, *Phys. Lett. B* **634** (2006) 307–314, [hep-ph/0510197].

[16] Y. Nakai and M. Reece, *Electric Dipole Moments in Natural Supersymmetry*, *JHEP* **08** (2017) 031, [1612.08090].

[17] C. Cesarotti, Q. Lu, Y. Nakai, A. Parikh and M. Reece, *Interpreting the Electron EDM Constraint*, *JHEP* **05** (2019) 059, [1810.07736].

[18] D. Aloni, P. Asadi, Y. Nakai, M. Reece and M. Suzuki, *Spontaneous CP Violation and Horizontal Symmetry in the MSSM: Toward Lepton Flavor Naturalness*, 2104.02679.

[19] B. Keren-Zur, P. Lodone, M. Nardecchia, D. Pappadopulo, R. Rattazzi and L. Vecchi, *On Partial Compositeness and the CP asymmetry in charm decays*, *Nucl. Phys. B* **867** (2013) 394–428, [1205.5803].

[20] M. König, M. Neubert and D. M. Straub, *Dipole operator constraints on composite Higgs models*, *Eur. Phys. J. C* **74** (2014) 2945, [1403.2756].

[21] G. Panico and A. Wulzer, *The Composite Nambu-Goldstone Higgs*, vol. 913. Springer, 2016, 10.1007/978-3-319-22617-0.

[22] I. Doršner, S. Fajfer, A. Greljo, J. F. Kamenik and N. Košnik, *Physics of leptoquarks in precision experiments and at particle colliders*, *Phys. Rept.* **641** (2016) 1–68, [1603.04993].

[23] K. Fuyuto, M. Ramsey-Musolf and T. Shen, *Electric Dipole Moments from CP-Violating Scalar Leptoquark Interactions*, *Phys. Lett. B* **788** (2019) 52–57, [1804.01137].

[24] W. Dekens, J. de Vries, M. Jung and K. K. Vos, *The phenomenology of electric dipole moments in models of scalar leptoquarks*, *JHEP* **01** (2019) 069, [1809.09114].

[25] W. Altmannshofer, S. Gori, H. H. Patel, S. Profumo and D. Tuckler, *Electric dipole moments in a leptoquark scenario for the B-physics anomalies*, *JHEP* **05** (2020) 069, [2002.01400].

[26] W. Altmannshofer, S. Gori, N. Hamer and H. H. Patel, *Electron EDM in the complex two-Higgs doublet model*, *Phys. Rev. D* **102** (2020) 115042, [2009.01258].

[27] W.-S. Hou, G. Kumar and S. Teunissen, *Charged Lepton EDM with Extra Yukawa Couplings*, 2109.08936.

[28] H. E. Logan, S. Moretti, D. Rojas-Ciofalo and M. Song, *CP violation from charged Higgs bosons in the three Higgs doublet model*, *JHEP* **07** (2021) 158, [2012.08846].

[29] K. Cheung, A. Jueid, Y.-N. Mao and S. Moretti, *Two-Higgs-doublet model with soft CP violation confronting electric dipole moments and colliders*, *Phys. Rev. D* **102** (2020) 075029, [2003.04178].

[30] E. J. Chun, J. Kim and T. Mondal, *Electron EDM and Muon anomalous magnetic moment in Two-Higgs-Doublet Models*, *JHEP* **12** (2019) 068, [1906.00612].

[31] H. Davoudiasl, I. M. Lewis and M. Sullivan, *Higgs Troika for Baryon Asymmetry*, *Phys. Rev. D* **101** (2020) 055010, [1909.02044].

[32] H. Davoudiasl, I. M. Lewis and M. Sullivan, *Multi-TeV signals of baryogenesis in a Higgs troika model*, *Phys. Rev. D* **104** (2021) 015024, [2103.12089].

[33] A. Abada and T. Toma, *Electric dipole moments in the minimal scotogenic model*, *JHEP* **04** (2018) 030, [1802.00007].

[34] P. Fileviez Perez and A. D. Plascencia, *Electric dipole moments, new forces and dark matter*, *JHEP* **03** (2021) 185, [2008.09116].

[35] G. Panico, A. Pomarol and M. Riembau, *Eft approach to the electron electric dipole moment at the two-loop level*, 1810.09413.

[36] J. Aebischer, W. Dekens, E. E. Jenkins, A. V. Manohar, D. Sengupta and P. Stoffer, *Effective field theory interpretation of lepton magnetic and electric dipole moments*, *JHEP* **07** (2021) 107, [2102.08954].

[37] U. Haisch and A. Hala, *Bounds on cp-violating higgs-gluon interactions: the case of vanishing light-quark yukawa couplings*, 1909.09373.

[38] U. Haisch and G. Koole, *Beautiful and charming chromodipole moments*, *JHEP* **09** (2021) 133, [2106.01289].

[39] J. Brod and E. Stamou, *Electric dipole moment constraints on CP-violating heavy-quark Yukawas at next-to-leading order*, *JHEP* **07** (2021) 080, [1810.12303].

[40] E. Fuchs, M. Losada, Y. Nir and Y. Viernik, *CP violation from τ, t and b dimension-6 Yukawa couplings - interplay of baryogenesis, EDM and Higgs physics*, *JHEP* **05** (2020) 056, [2003.00099].

[41] K. Fuyuto and M. Ramsey-Musolf, *Top Down Electroweak Dipole Operators*, *Phys. Lett. B* **781** (2018) 492–498, [1706.08548].

[42] V. Cirigliano, A. Crivellin, W. Dekens, J. de Vries, M. Hoferichter and E. Mereghetti, *CP Violation in Higgs-Gauge Interactions: From Tabletop Experiments to the LHC*, *Phys. Rev. Lett.* **123** (2019) 051801, [1903.03625].

[43] V. Cirigliano, W. Dekens, J. de Vries and E. Mereghetti, *Constraining the top-Higgs sector of the Standard Model Effective Field Theory*, *Phys. Rev. D* **94** (2016) 034031, [1605.04311].

[44] Y. T. Chien, V. Cirigliano, W. Dekens, J. de Vries and E. Mereghetti, *Direct and indirect constraints on CP-violating Higgs-quark and Higgs-gluon interactions*, *JHEP* **02** (2016) 011, [1510.00725].

[45] B. Sekhar Chivukula and H. Georgi, *Composite-technicolor standard model*, *Physics Letters B* **188** (1987) 99–104.

[46] G. D'Ambrosio, G. F. Giudice, G. Isidori and A. Strumia, *Minimal flavour violation: an*

effective field theory approach, *Nucl.Phys.B645:155-187,2002* (July, 2002) , [hep-ph/0207036].

[47] G. Isidori and D. M. Straub, *Minimal flavour violation and beyond*, 1202.0464.

[48] T. Cohen, N. Craig, X. Lu and D. Sutherland, *Is smeft enough?*, 2008.08597.

[49] B. Grzadkowski, M. Iskrzynski, M. Misiak and J. Rosiek, *Dimension-six terms in the standard model lagrangian*, 1008.4884.

[50] M. Jiang, N. Craig, Y.-Y. Li and D. Sutherland, *Complete one-loop matching for a singlet scalar in the Standard Model EFT*, *JHEP* **02** (2019) 031, [1811.08878].

[51] V. Gherardi, D. Marzocca and E. Venturini, *Matching scalar leptoquarks to the SMEFT at one loop*, *JHEP* **07** (2020) 225, [2003.12525].

[52] E. E. Jenkins, A. V. Manohar and P. Stoffer, *Low-energy effective field theory below the electroweak scale: Operators and matching*, *JHEP 1803 (2018) 016* (Sept., 2017) , [http://arxiv.org/abs/1709.04486v2].

[53] W. Dekens and P. Stoffer, *Low-energy effective field theory below the electroweak scale: matching at one loop*, *JHEP 1910 (2019) 197* (Aug., 2019) , [1908.05295].

[54] E. E. Jenkins, A. V. Manohar and M. Trott, *Renormalization group evolution of the standard model dimension six operators i: Formalism and lambda dependence*, http://arxiv.org/abs/1308.2627v4.

[55] E. E. Jenkins, A. V. Manohar and M. Trott, *Renormalization group evolution of the standard model dimension six operators ii: Yukawa dependence*, http://arxiv.org/abs/1310.4838v3.

[56] R. Alonso, E. E. Jenkins, A. V. Manohar and M. Trott, *Renormalization group evolution of the standard model dimension six operators iii: Gauge coupling dependence and phenomenology*, http://arxiv.org/abs/1312.2014v4.

[57] E. E. Jenkins, A. V. Manohar and P. Stoffer, *Low-energy effective field theory below the electroweak scale: Anomalous dimensions*, http://arxiv.org/abs/1711.05270v2.

[58] Q. Bonnefoy, E. Gendy, C. Grojean and J. T. Ruderman, *Beyond Jarlskog: 699 invariants for CP violation in SMEFT*, 2112.03889.

[59] M. Pospelov and A. Ritz, *Electric dipole moments as probes of new physics*, *Annals Phys.* **318** (2005) 119–169, [hep-ph/0504231].

[60] R. Gupta, B. Yoon, T. Bhattacharya, V. Cirigliano, Y.-C. Jang and H.-W. Lin, *Flavor diagonal tensor charges of the nucleon from 2+1+1 flavor lattice qcd*, *Phys. Rev. D 98, 091501 (2018)* (Aug., 2018) , [1808.07597].

[61] J. Engel, M. J. Ramsey-Musolf and U. van Kolck, *Electric dipole moments of nucleons, nuclei, and atoms: The standard model and beyond*, 1303.2371.

[62] J. Hisano, J. Y. Lee, N. Nagata and Y. Shimizu, *Reevaluation of neutron electric dipole moment with qcd sum rules*, *Phys.Rev.D85:114044,2012* (Apr., 2012) , [1204.2653].

[63] J. de Vries, E. Mereghetti, R. G. E. Timmermans and U. van Kolck, *The Effective Chiral Lagrangian From Dimension-Six Parity and Time-Reversal Violation*, *Annals Phys.* **338** (2013) 50–96, [1212.0990].

[64] JLQCD collaboration, N. Yamanaka, S. Hashimoto, T. Kaneko and H. Ohki, *Nucleon charges with dynamical overlap fermions*, *Phys. Rev. D* **98** (2018) 054516, [1805.10507].

[65] N. Yamanaka and E. Hiyama, *Weinberg operator contribution to the nucleon electric dipole moment in the quark model*, *Phys. Rev. D* **103** (2021) 035023, [2011.02531].

[66] S. Weinberg, *Larger higgs-boson-exchange terms in the neutron electric dipole moment*, *Physical Review Letters* **63** (nov, 1989) 2333–2336.

[67] A. Hook, *TASI Lectures on the Strong CP Problem and Axions*, *PoS* **TASI2018** (2019) 004, [1812.02669].

[68] M. Pospelov and A. Ritz, *Hadron electric dipole moments from cp-odd operators of dimension five via qcd sum rules: The vector meson*, *Phys.Lett. B471 (2000) 388-395* (Oct., 1999) , [hep-ph/9910273].

[69] M. Pospelov and A. Ritz, *Neutron edm from electric and chromoelectric dipole moments of quarks*, *Phys.Rev. D63 (2001) 073015* (Oct., 2000) , [hep-ph/0010037].

[70] C. Cheung and C.-H. Shen, *Non-renormalization theorems without supersymmetry*, *Phys. Rev. Lett. 115, 071601 (2015)* (May, 2015) , [1505.01844].

[71] A. Azatov, R. Contino, C. S. Machado and F. Riva, *Helicity selection rules and non-interference for bsm amplitudes*, *Phys. Rev. D 95, 065014 (2017)* (July, 2016) , [1607.05236].

[72] N. Craig, M. Jiang, Y.-Y. Li and D. Sutherland, *Loops and trees in generic efts*, http://arxiv.org/abs/2001.00017v1.

[73] M. Jiang, J. Shu, M.-L. Xiao and Y.-H. Zheng, *New selection rules from angular momentum conservation*, *Phys. Rev. Lett. 126, 011601 (2021)* (Jan., 2020) , [2001.04481].

[74] C. Anastasiou, R. Britto, B. Feng, Z. Kunszt and P. Mastrolia, *Unitarity cuts and Reduction to master integrals in d dimensions for one-loop amplitudes*, *JHEP* **03** (2007) 111, [hep-ph/0612277].

[75] S. D. Badger, *Direct Extraction Of One Loop Rational Terms*, *JHEP* **01** (2009) 049, [0806.4600].

[76] N. Arkani-Hamed, T.-C. Huang and Y.-t. Huang, *Scattering Amplitudes For All Masses and Spins*, 1709.04891.

[77] F. Boudjema, K. Hagiwara, C. Hamzaoui and K. Numata, *Anomalous moments of quarks and leptons from nonstandard$WW\gamma$couplings*, *Physical Review D* **43** (apr, 1991) 2223–2232.

[78] B. Gripaios and D. Sutherland, *On lhc searches for cp-violating, dimension-6 electroweak gauge boson operators*, *Phys. Rev. D 89, 076004 (2014)* (Sept., 2013) , [1309.7822].

[79] P. Baratella, C. Fernandez and A. Pomarol, *Renormalization of higher-dimensional operators from on-shell amplitudes*, 2005.07129.

[80] S. M. Barr, E. M. Freire and A. Zee, *Mechanism for large neutrino magnetic moments*, *Physical Review Letters* **65** (nov, 1990) 2626–2629.

[81] D. A. Faroughy, G. Isidori, F. Wilsch and K. Yamamoto, *Flavour symmetries in the SMEFT*, *JHEP* **08** (2020) 166, [2005.05366].

[82] J. Fuentes-Martín, G. Isidori, J. Pagès and K. Yamamoto, *With or without U(2)? Probing non-standard flavor and helicity structures in semileptonic B decays*, *Phys. Lett. B* **800** (2020) 135080, [1909.02519].

[83] R. Barbieri, D. Buttazzo, F. Sala and D. M. Straub, *Flavour physics from an approximate $U(2)^3$ symmetry*, *JHEP* **07** (2012) 181, [1203.4218].

[84] C. Hartmann and M. Trott, *On one-loop corrections in the standard model effective field theory; the $\Gamma(h \to \gamma\,\gamma)$ case*, *JHEP* **07** (2015) 151, [1505.02646].

[85] F. Jegerlehner, *Facts of life with gamma(5)*, *Eur.Phys.J.C18:673-679,2001* (May, 2000) , [hep-th/0005255].

[86] G. t Hooft and M. Veltman, *Regularization and renormalization of gauge fields*, *Nuclear Physics B* **44** (jul, 1972) 189–213.

[87] P. Breitenlohner and D. Maison, *Dimensional renormalization and the action principle*, *Communications in Mathematical Physics* **52** (feb, 1977) 11–38.

[88] G. Bonneau, *Trace and axial anomalies in dimensional renormalization through zimmermann-like identities*, *Nuclear Physics B* **171** (1980) 477–508.

[89] C. Becchi, A. Rouet and R. Stora, *The abelian higgs kibble model, unitarity of the s-operator*, *Physics Letters B* **52** (1974) 344–346.

[90] C. Becchi, A. Rouet and R. Stora, *Renormalization of the abelian higgs-kibble model*, *Communications in Mathematical Physics* **42** (1975) 127–162.

[91] C. Becchi, A. Rouet and R. Stora, *Renormalization of gauge theories*, *Annals of Physics* **98** (1976) 287–321.

[92] T. Bhattacharya, V. Cirigliano, R. Gupta, E. Mereghetti and B. Yoon, *Dimension-5 cp-odd operators: Qcd mixing and renormalization*, 1502.07325.

[93] L. Abbott, *The background field method beyond one loop*, *Nuclear Physics B* **185** (jul, 1981) 189–203.

[94] L. Abbott, M. Grisaru and R. Schaefer, *The background field method and the s-matrix*, *Nuclear Physics B* **229** (dec, 1983) 372–380.

[95] A. Denner, S. Dittmaier and G. Weiglein, *Application of the background-field method to the electroweak standard model*, *Nucl.Phys. B440 (1995) 95-128* (Oct., 1994) , [hep-ph/9410338].

[96] A. Denner, S. Dittmaier and G. Weiglein, *The background-field formulation of the electroweak standard model*, *Acta Phys.Polon.B27:3645-3660,1996* (Sept., 1996) , [hep-ph/9609422].

[97] A. Helset, M. Paraskevas and M. Trott, *Gauge fixing the standard model effective field theory*, *Phys. Rev. Lett. 120, 251801 (2018)* (Mar., 2018) , [1803.08001].

[98] T. Corbett, *The feynman rules for the smeft in the background field gauge*, 2010.15852.

[99] T. Corbett and M. Trott, *One loop verification of smeft ward identities*, 2010.08451.

[100] H. H. Patel, *Package-x: A mathematica package for the analytic calculation of one-loop integrals*, http://arxiv.org/abs/1503.01469v2.

[101] A. Alloul, N. D. Christensen, C. Degrande, C. Duhr and B. Fuks, *Feynrules 2.0 - a complete toolbox for tree-level phenomenology*, *Comput.Phys.Commun. 185 (2014) 2250-2300* (Oct., 2013) , [1310.1921].

[102] T. Hahn, *Generating feynman diagrams and amplitudes with feynarts 3*, *Comput.Phys.Commun. 140 (2001) 418-431* (Dec., 2000) , [hep-ph/0012260].

[103] T. Hahn and M. Perez-Victoria, *Automatized one-loop calculations in 4 and d dimensions*, http://arxiv.org/abs/hep-ph/9807565v1.